

2019

Mitochondria-Dependent Cellular Toxicity of α -synuclein Modeled in Yeast

Rajalakshmi Santhanakrishnan
Wright State University

Follow this and additional works at: https://corescholar.libraries.wright.edu/etd_all



Part of the [Biomedical Engineering and Bioengineering Commons](#)

Repository Citation

Santhanakrishnan, Rajalakshmi, "Mitochondria-Dependent Cellular Toxicity of α -synuclein Modeled in Yeast" (2019). *Browse all Theses and Dissertations*. 2272.
https://corescholar.libraries.wright.edu/etd_all/2272

This Dissertation is brought to you for free and open access by the Theses and Dissertations at CORE Scholar. It has been accepted for inclusion in Browse all Theses and Dissertations by an authorized administrator of CORE Scholar. For more information, please contact library-corescholar@wright.edu.

**MITOCHONDRIA-DEPENDENT CELLULAR TOXICITY OF
 α -SYNUCLEIN MODELED IN YEAST**

A dissertation submitted in partial fulfillment of the
requirements for the degree of
Doctor of Philosophy

By:

RAJALAKSHMI SANTHANAKRISHNAN
M.B.B.S., Madras Medical College, Chennai, India, 2010

2019
Wright State University

COPYRIGHT BY
RAJALAKSHMI SANTHANAKRISHNAN
2019

WRIGHT STATE UNIVERSITY
GRADUATE SCHOOL

April 24, 2019

I HEREBY RECOMMEND THAT THE DISSERTATION PREPARED UNDER MY SUPERVISION BY Rajalakshmi Santhanakrishnan ENTITLED Mitochondria-dependent cellular toxicity of α -synuclein modeled in yeast BE ACCEPTED IN PARTIAL FULFILLMENT OF THE REQUIREMENTS FOR THE DEGREE OF Doctor of Philosophy.

Quan Zhong, Ph.D.
Dissertation Director

Mill W. Miller, Ph.D.
Director, Biomedical Sciences Ph.D. Program

Barry Milligan, Ph.D.
Interim Dean of the Graduate School

Committee on Final Exam

David R. Cool, Ph.D.

Paula Ann Bubulya, Ph.D.

David R. Ladle, Ph.D.

Weiwen Long, Ph.D.

ABSTRACT

Santhanakrishnan, Rajalakshmi. Ph.D., Biomedical Sciences Ph.D. Program, Wright State University, 2019. Mitochondria-Dependent Cellular Toxicity of α -synuclein Modeled in Yeast.

Parkinson's disease is the second most common neurodegenerative disease. This disease is caused by the degeneration of dopaminergic neurons, leading to debilitating motor symptoms and early mortality. The protein α -synuclein (α -syn), encoded by *SNCA*, misfolds and forms inclusions in Parkinson's disease brains. When α -syn is overexpressed in yeast, it causes cellular toxicity and an increased number of aggregates, recapitulating the toxic phenotypes observed in humans and animal models. Yeast models are a powerful tool to perform high-throughput overexpression screening to identify modifiers of α -syn toxicity. α -syn causes mitochondrial dysfunction by inhibiting complex I and inducing mitochondrial fragmentation. Prior screening of α -syn were limited to only the galactose condition, where mitochondrial function is dispensable. Previous screening was performed exclusively with the *GALI* promoter, restricting the genes to only those induced by galactose. We have validated an overexpression system using *GAL3* alleles that can induce genes under mitochondrial-dependent glycerol-ethanol condition and other non-galactose conditions (calorie restriction, nitrogen starvation and raffinose). α -syn showed discrepancy in the correlation of toxicity and aggregation in non-galactose conditions. Compared to galactose, under glycerol-ethanol condition, α -syn

exhibited higher toxicity, formed more aggregates, and decreased viability and respiratory competency despite having similar expression under the two conditions. We screened 14,827 human gene clones and identified 87 that can suppress α -syn toxicity in glycerol-ethanol. Genes involved in RNA polymerase II function, anterior-posterior axis and nucleoplasm were overrepresented. Among the suppressor hits, we identified four 14-3-3 protein isotypes (β , γ , θ , and ζ). None of the four suppressors suppressed the toxicity under galactose. However, the 14-3-3 suppressors did not reduce aggregates under glycerol-ethanol. No increase in respiratory competency was observed; however, 14-3-3 β was seen to effectively reduce the number of cells that accumulate ROS. Overall, we have created an overexpression system that describes a new path for performing screening in non-galactose conditions. Our results based on novel phenotypes of α -syn show that screening in these conditions is indeed important. We have identified previously unknown suppressors of α -syn toxicity and ruled out underlying mechanisms of action.

TABLE OF CONTENTS

	Page
Abbreviations	xii
Acknowledgments	xiv
I. INTRODUCTION.....	1
Parkinson's disease and α -synuclein.....	1
Misfolding and aggregates of α -synuclein cause Parkinson's disease.....	3
ER-associated misfolded protein degradation in yeast.....	4
α -synuclein and mitochondrial dysfunction.....	6
Yeast screening models identified functions of α -synuclein.....	7
Drawback of prior yeast screening models.....	8
Constitutive <i>GAL3</i> alleles induce <i>GAL1</i> promoter in glycerol condition.....	9
II. MATERIALS AND METHODS.....	12
Yeast strains, media, and plasmids.....	12
Gateway cloning.....	12
Site-directed mutagenesis.....	13
One-step yeast transformation.....	13
Yeast mating.....	14
β -Galactosidase assay.....	14
Serial dilution growth assays.....	15
Western blotting.....	15

	Page
Fluorescence microscopy.....	16
Quantification of α -synuclein aggregates.....	17
Examination of mitochondria.....	17
Quantification of viable and respiratory-competent cells.....	18
Reactive oxygen species quantification.....	19
Split green fluorescent protein system and oligomer engineering.....	20
Human gene plasmid library and transformation into yeast.....	21
High-throughput screening.....	22
Confirmation of genetic hits.....	22
Gene ontology analysis.....	23
Statistical analyses.....	24
III. AIM 1: TO DEVELOP A METHOD OF GENE OVEREXPRESSION UNDER NON-GALACTOSE CONDITIONS USING <i>GAL3</i> ALLELES.....	30
Rationale.....	30
Experimental design.....	31
<i>GAL1</i> promoter and <i>GAL3</i> alleles.....	31
β -galactosidase assay.....	31
Mating strategy to perform β -galactosidase assays.....	31
Results.....	33
1.1: To develop and test a method for gene overexpression under non-galactose conditions.....	33

	Page
1.2: To test a gene overexpression method using neurodegenerative disease gene models and <i>GAL3</i> alleles.....	35
1.3: To assess the toxicity, aggregate formation and expression level of IntTox and HiTox α -synuclein under non-galactose conditions using integrated <i>GAL3</i> _{A368V} allele.....	41
IV. AIM 2: TO EXAMINE THE ROLE OF MITOCHONDRIA IN α -SYNUCLEIN TOXICITY UNDER GLYCEROL-ETHANOL.....	53
Rationale.....	53
Experimental design.....	53
Spotting assay.....	53
Measurement of aggregates and examination of mitochondria.....	54
Measurement of ROS.....	54
Mitochondrial targeting of α -synuclein.....	54
Results.....	54
2.1: To test the toxicity and aggregation of IntTox α -synuclein under glycerol-ethanol.....	54
2.2: To determine the mechanisms of IntTox α -synuclein toxicity under glycerol-ethanol.....	60
V. AIM 3: TO SCREEN AND CHARACTERIZE THE SUPPRESSORS OF INTTOX α -SYNUCLEIN TOXICITY UNDER GLYCEROL-ETHANOL.....	79
Rationale.....	79
Experimental design.....	79

	Page
Human gene library and genetic screening by mating.....	79
Confirmation of genetic hits.....	80
Results.....	80
3.1: To identify human gene suppressors of IntTox α -synuclein toxicity under glycerol-ethanol.....	80
3.2 To characterize the 14-3-3 isotype suppressors of IntTox α -synuclein toxicity	87
VI. DISCUSSION.....	102
VII CONCLUSION.....	114
VIII REFERENCES.....	116

LIST OF FIGURES

Figure	Page
1. Glycerol metabolism in yeast.....	10
2. Schematic representation of the mating strategy used in this study.....	32
3. <i>GAL3_{F237Y}</i> , <i>GAL3_{A368V}</i> and <i>GAL3_{S509P}</i> induce <i>GAL1</i> promoter under glycerol-ethanol.....	34
4. Combinations of <i>GAL3_{F237Y}</i> , <i>GAL3_{A368V}</i> and <i>GAL3_{S509P}</i> do not induce <i>GAL1</i> promoter in non-galactose conditions.....	36
5. Combination of <i>GAL3_{F237Y}</i> and <i>GAL3_{S509P}</i> fails to enable transition to ‘closed active’ Gal3p conformation.....	37
6. <i>GAL3_{A368V}</i> and <i>GAL3_{F237Y}</i> induce toxicity of IntTox α -synuclein under glycerol-ethanol.....	39
7. <i>GAL3_{A368V}</i> does not induce toxicity of neurodegenerative disease-related genes in the presence of glucose.....	42
8. <i>GAL3_{A368V}</i> induces the <i>GAL1</i> promoter under calorie restriction and nitrogen starvation conditions.....	44
9. IntTox and HiTox α -synuclein overexpression cause toxicity under non-galactose conditions.....	45
10. IntTox α -synuclein does not form aggregates under non-galactose conditions.....	49
11. HiTox α -synuclein forms aggregates under non-galactose conditions.....	50

Figure	Page
12. HiTox α -synuclein expression increases while IntTox α -syn expression is unaffected under non-galactose conditions.....	51
13. IntTox α -synuclein is toxic under glycerol-ethanol but not under galactose.....	56
14. IntTox α -synuclein is toxic under galactose in haploid condition.....	57
15. IntTox α -synuclein is toxic under glycerol-ethanol but not under galactose in diploid yeast strains.....	58
16. Protein expression levels of IntTox α -syn do not differ between galactose and glycerol-ethanol conditions.....	61
17. Aggregates of IntTox α -synuclein are elevated under glycerol-ethanol compared to galactose.....	63
18. Aggregates of IntTox α -synuclein are elevated in haploid galactose and diploid glycerol-ethanol yeast strains	65
19. IntTox α -synuclein reduces the number of viable and respiratory-competent cells only under glycerol-ethanol.....	68
20. Mitochondria show dense morphology under glycerol-ethanol and disrupted membrane potential signal under both galactose and glycerol-ethanol in the presence of α -synuclein.	71
21. Quantitative assessment of reactive oxygen species under galactose and glycerol-ethanol conditions in the presence of α -synuclein.....	73
22. Number of cells that accumulate ROS are elevated under galactose and glycerol-ethanol conditions in the presence of α -synuclein.....	76
23. Targeting of α -synuclein to mitochondria was not successful	78

Figure	Page
24. Schematic representation of the yeast overexpression screening to identify suppressors of IntTox α -synuclein toxicity under glycerol-ethanol	81
25. Sample image of spotting showing a suppressor of IntTox α -synuclein in glycerol-ethanol agar plate.....	82
26. Four 14-3-3 isotypes suppress the toxicity of IntTox α -synuclein in glycerol-ethanol.....	88
27. Four 14-3-3 isotypes do not suppress the toxicity of IntTox α -synuclein in galactose.....	89
28. 14-3-3 β increases IntTox α -synuclein aggregates in glycerol-ethanol.....	90
29. 14-3-3 suppressor isotypes do not reduce IntTox α -synuclein protein expression in glycerol-ethanol.....	92
30. 14-3-3 suppressor isotypes do not increase viability or respiratory competency in glycerol-ethanol.....	94
31. 14-3-3 isotypes do not modify the mitochondrial structure or the disrupted membrane potential signal.....	97
32. 14-3-3 isotypes do not decrease ROS production.....	99
33. 14-3-3 β decreases the percentage of cells that accumulate ROS.....	101

LIST OF TABLES

Table	Page
1. Yeast strains.....	25
2. Plasmids.....	26
3. Primers.....	28
4. Gene Ontology enrichment analysis of IntTox α -synuclein suppressor hits.....	84
5. 14-3-3 protein isotypes that suppressed the IntTox α -synuclein toxicity under glycerol-ethanol condition.....	86

ABBREVIATIONS

ALS	Amyotrophic lateral sclerosis
ANOVA	Analysis of variance
ATP	Adenosine triphosphate
BF	Bright field
CFP	Cyan fluorescent protein
COX4	Cytochrome C oxidase 4
DHE	Dihydroethidium
DNA	Deoxy-ribonucleic acid
ER	Endoplasmic reticulum
ERAD	Endoplasmic reticulum-associated degradation
GFP	Green fluorescent protein
GO	Gene ontology
HiTox α -syn	> 6 copies of α -syn
IntTox α -syn	4–5 copies of α -syn
LRRK2	Leucine-rich repeat kinase 2
MPTP	1-methyl-4-phenyl-1,2,3,6-tetrahydropyridine
NADH	Nicotinamide adenine dinucleotide hydrogen
NoTox α -syn	1 copy of α -syn
OD	Optical density
ORF	Open reading frame
PCR	Polymerase chain reaction
PGC1 α	Peroxisome proliferator-activated receptor γ coactivator 1 α
PGK1	Phosphoglycerate kinase 1
PINK1	Phosphatase and tensin homolog-induced kinase 1
RNA	Ribonucleic acid

ROS	Reactive oxygen species
rpm	Rotations per minute
SE	Standard error
<i>SNCA</i>	α -Synuclein gene
Su9	Subunit 9
TFP	Teal fluorescent protein
Tx Red	Texas Red
UPR	Ubiquitin protein response
WT	Wild-type
YFP	Yellow fluorescent protein
YPD	Yeast peptone dextrose
YPGE	Yeast peptone glycerol-ethanol
α -syn	α -Synuclein protein

Acknowledgments

I would like to thank my advisor, Dr. Quan Zhong for giving me an opportunity to work in her lab. I am grateful for her immense help, support and guidance throughout my graduate studies. I would like to thank my committee members Dr. David Cool, Dr. Paula Bubulya, Dr. David Ladle and Dr. Weiwen Long for their kindness and invaluable suggestions during the committee meetings. Thank you to Dr. Mill Miller for his advice and support during my graduate training. Thank you to Karen Luchin for her tremendous work and for knowing the answer to every question I had. I would like to extend my gratitude to past and present members of JuZhong lab especially, Shuzhen Chen, Andy Koesters and Elliott Hayden for training me when I was new in the lab. Thank you Ishita Haider for synthesizing NoTox *SNCA* strain and engineering pMitoLoc plasmids, Roselle Almazan for generating the integrated *GAL3_{A368V}* allele strains, Dr. Dali Liu for providing the structural analysis of *GAL3* alleles and Shuzhen Chen for preparing the human gene clones and transforming human gene library in *SNCA* yeast model. I am also thankful to Dr. Shulin Ju for his thoughts and comments during the lab meetings. Thank you, Annabel Almazan, Sara Seibert, Krushangi Shah, Jimmy Readler, Andrew Stacy, and Pavani Beesetty for your help with my preliminary exam and preparing me for the presentations. I was blessed to be surrounded by incredibly supportive friends, Soham Parikh, Alan Cone and Aicha Kebe who encouraged me a lot. I am grateful to my husband and my parents for their fullest support during PhD training.

I. INTRODUCTION

Parkinson's disease and α -synuclein

Parkinson's disease is the second most common neurodegenerative disease worldwide.¹ Parkinson's disease is a motor disorder that presents with three cardinal symptoms: bradykinesia (slow movement), rigidity, and tremors. Nonmotor symptoms, including cognitive impairment, autonomic dysfunction, sleep disorders, and depression also affect the patient's quality of life. Parkinson's disease is an aging disease with the prevalence increasing from 0.3% in the general population, to greater than 4% among individuals over 85 years of age.^{2,3} The disease is difficult to treat because once the first symptoms appear, 60% of motor neurons have already degenerated. As such, the prevalence of Parkinson's disease is expected to double by the year 2030,⁴ adding tremendously to the ever-increasing medical economic burden associated with the disease. Furthermore, the mortality rate is double that of the healthy general population,⁵ with available treatment strategies neither modifying the progression of the disease nor delaying the onset of disability. Hence, there is an incredible impetus for further research in this field.⁶

Neurologically, Parkinson's disease is characterized by the degeneration of pigmented dopaminergic neurons in the *substantia nigra pars compacta* of the midbrain and histologically, by the presence of Lewy bodies which are intracellular α -synuclein (α -syn) aggregates.⁷ Although the specific underlying cause of Parkinson's disease is unknown, a combination of genetic mutations and environmental factors appear to play a

role. Further, over 90% of the disease incidence is sporadic, meaning there is no family history of disease; while approximately 10% of the disease incidence is familial, meaning there is a family member who has the disease. There are six genes whose mutations have been linked to Parkinson's disease,⁸ although mutations are responsible for less than 5% of the overall incidence. Mutations in *SNCA* and leucine-rich repeat kinase 2 (*LRRK2*) genes cause autosomal dominance, whereas those in *ATP13A2*, *Parkin*, phosphatase and tensin homolog-induced kinase 1 (*PINK1*), and *DJ-1* cause autosomal recessive disease. Autosomal dominant disease is a pattern of inheritance in which an affected individual has one copy of a mutant gene and one normal gene on a pair of autosomal chromosomes. Autosomal recessive diseases are caused by two copies of the mutant gene on a pair of autosomal chromosomes. Individuals with autosomal dominant diseases have a 50% chance of passing the mutant gene on to each of their children.

SNCA was the first gene identified whose mutations, duplications and triplications were found to cause Parkinson's disease.⁹ *SNCA* mutations cause early onset (< 50 years of age) Parkinson's disease and are associated with high mortality.¹⁰ Patients with triplication of the *SNCA* have much earlier disease onset and rapid progression compared with patients with duplication of *SNCA*.¹¹ The widely studied missense mutations of *SNCA* include A30P, E46K, A53T, G51D, and H50Q.¹² α -syn protein, encoded by *SNCA*, is a small 140-amino acid cytoplasmic protein that belongs to the synuclein family and is primarily expressed in the brain.¹³ Mutations, duplications and triplications of *SNCA* accelerate aggregation of the α -syn resulting in intracytoplasmic neuronal inclusions which constitute the Lewy bodies.^{14,15} Lewy bodies are present in 95% of Parkinson's disease brains even in the absence of *SNCA* mutations.¹⁶ Although the precise mechanism

responsible for initiating the misfolding and aggregation of α -syn remains uncharacterized, environmental and stress factors such as higher pH and temperature, as well as oxidative stress appear to play a role.

Misfolding and aggregates of α -synuclein cause Parkinson's disease

α -syn consists of three domains: an amphipathic N-terminal domain, a hydrophobic center, and a hydrophilic C-terminal domain. This composition results in an α -helical, random loop formation that facilitates the interactions of α -syn with phospholipid-containing membranes including those of the mitochondria, endoplasmic reticulum (ER)/Golgi and the nucleus.^{17,18} The ability to interact with organelle membranes makes α -syn a molecular chaperone, enabling docking of synaptic vesicles to the cell membrane and facilitating intracellular protein trafficking.^{17,19} Through these mechanisms, α -syn regulates cellular functions such as neuronal differentiation,²⁰ apoptotic inhibition,²¹ regulation of synaptic plasticity,²² and regulation of dopamine release.²³

Further, α -syn is an unfolded protein in its native form; however, mutations in *SNCA* together with environmental factors (e.g., oxidative stress, pesticide or metal exposure) cause misfolding of α -syn which then becomes tightly configured in long filamentous protofibrils and fibrils.²⁴ The distinctive feature of the α -syn aggregation is the slow primary nucleation process that becomes accelerated when in contact with the lipid membranes.²⁵ Nucleation involves the formation of a β -sheet core that folds into itself and aggregates with others to form protofilaments; from the protofilaments, mature fibrils are formed.²⁶ Under normal conditions, α -syn exists as monomers, which form soluble oligomers on contact with cellular membranes and then assemble into insoluble

fibrils when triggered by several stressors (e.g. *SNCA* mutations, duplications, and triplications, oxidative stress, metal exposure, etc.). The cells protective systems, including the lysosome autophagy system and ubiquitin proteasome system, prevent the toxic forms from spreading across the neurons resulting in Lewy body formation.²⁷ α -syn, in its aggregate state, contains five β -sheet cores of amyloid fibrils, each comprised of 35 – 96 amino acid residues (N-terminal amphipathic region). The point-mutations are primarily located within this core region.²⁶ Missense *SNCA* mutations can increase the rates of fibril formation initiation and their proliferation, however, does not affect fibril elongation.²⁸

ER-associated misfolded protein degradation in yeast

Under normal conditions, the misfolded proteins are processed by the ubiquitin proteasome system or the autophagy-lysosome pathway.²⁹ The ER plays a major role in protein quality control. In the ER, once the protein undergoes post-translational modifications, it must become properly folded before transport to the Golgi apparatus. Consequently, if the protein becomes misfolded, it will not enter the Golgi but will instead be redirected to the ER-associated degradation (ERAD) pathway.^{30,31} There are four major proteins that make up the ERAD pathway namely, Yos9, Der1, Hrd3, and Usa1. These four proteins, along with the Hrd1/Der3 (E3 ubiquitin ligase) complex, recognize the substrate (misfolded protein) at the ER.³² Once recognized, it is ubiquitinated and Hrd1 mediates the retro-translocation to the Cdc48 complex.^{33,34} Substrate delivery cofactors Rad23 and Dsk2 aid in further recognition of the substrate by the 26S proteasome where the deubiquitinating enzymes (Rpn11 and Ubp6) remove the polyubiquitin chain and are then degraded.³⁵ Perturbations in the ER quality control lead

to the accumulation of misfolded proteins and cause ER stress. The unfolded protein response (UPR) pathway is the cell's protective mechanism against ER stress. UPR is associated with an increase in ER chaperones, glycosylases and ERAD proteins (increasing the protein folding capacity) and degradation of messenger ribonucleic acid (mRNA) (decreasing the protein influx).³⁶ If a large amount of misfolded proteins accumulate, uncontrolled UPR results in increased production of reactive oxygen species (ROS) from the ER and mitochondria, which in turn induces caspase-mediated apoptosis.³⁷

ER stress has been reported in Parkinson's disease patient brains³⁸ as well as in genetic models of α -syn overexpression.^{39,40} In fact, levodopa, a Parkinson's disease therapeutic drug, attenuated ER stress in neuronal cell cultures.⁴¹ α -syn is not a resident ER protein; however, it has been shown to consistently interact with the ER, thereby inhibiting the ER-Golgi transport system in yeast.^{39,42} Although, the overexpression of α -syn alone did not induce UPR and ER stress, the association between α -syn and the ER membrane did.⁴⁰

Additionally, deletion of *YCA1*, a yeast orthologue of mammalian caspase, leads to accumulation of damaged cells due to an absence of apoptosis.⁴³ Disruption of UPR or the deletion of *YCA1* did not prevent α -syn mediated apoptosis in yeast; however, yeast lacking mitochondria (ρ^0 cells) prevented apoptosis.⁴⁴ Taken together, these studies suggest that α -syn may interact with biological membranes and/or synaptic vesicles, permitting it to transform into an aggregated form which then causes ER stress and disrupts protein trafficking. The resulting accumulation of misfolded proteins activates

UPR, increases ROS production and causes caspase-mediated apoptosis that is primarily dependent on mitochondrial function.

α -synuclein and mitochondrial dysfunction

Mitochondria and α -syn have been independently shown to cause both familial and idiopathic Parkinson's disease.⁴⁵⁻⁴⁷ Several studies have shown that α -syn increases fragmentation of the mitochondria, independent of the mitochondrial fission protein Dynamin-related protein 1 (Drp1).⁴⁸ Furthermore, α -syn can localize to the nucleus under oxidative stress, where it binds to the peroxisome proliferator-activated receptor γ coactivator 1 α (*PGC1 α*) promoter, thereby decreasing *PGC1 α* -regulated genes and indirectly affecting mitochondrial function.⁴⁹ *PGC1 α* is a member of a family of transcription coactivators that plays a central role in mitochondrial biogenesis. In human dopaminergic neuron cultures, cell lines and transgenic mouse models, α -syn has been shown to reduce complex I activity, and increase mitophagy.⁵⁰⁻⁵³ Both wild-type (WT) and mutant α -syn increase ROS production.⁵⁴⁻⁵⁶ Additionally, fluorescence resonance energy transfer analysis showed that α -syn preferentially interacts with mitochondria over the ER and other synaptic vesicles.⁵⁷ Overall, α -syn reduces mitochondrial function via several mechanisms including, reducing complex I activity, increasing mitochondrial fragmentation and mitophagy, and accelerating ROS production.

The association of Parkinson's disease and mitochondria was first reported in the 1980s, when the use of the mitochondrial toxin 1-methyl-4-phenyl-1,2,3,6-tetrahydropyridine (MPTP) as an illegal drug was found to lead to the development of Parkinson's disease-like symptoms.⁵⁸ Further, systemic infusion of rotenone (electron transport chain inhibitor) in animal models⁵⁹ and mutations in *DJ-1*, a mitochondrial ROS

scavenger, have been shown to cause Parkinson's disease;⁶⁰ while mutations in *PINK1*⁶¹ and *Parkin*,⁶² associated with Parkinson's disease, cause reduced complex I activity and adenosine triphosphate (ATP) synthesis. Lastly, a conditional knockout of mitochondrial transcription factor A in dopaminergic neurons causes respiratory chain deficiency and a Parkinson's disease-like phenotype including motor dysfunction.⁶³ It is, therefore, apparent that mitochondria play a central role in the development and progression of Parkinson's disease.

Yeast screening models identified functions of α -synuclein

Researchers have used the yeast *Saccharomyces cerevisiae* to understand the mechanisms of α -syn induced cellular toxicity.⁶⁴ Specifically, when the human *SNCA* is overexpressed in yeast under a *GALI* promoter, the toxicity has been found to increase with increasing copy number.⁶⁵ Concordantly, the increasing copy number is associated with increase in the number of intracellular inclusions.⁶⁶ Moreover, in yeast, mutations or overexpression of *SNCA* triggers aggregate formation, inhibit vesicular trafficking, cause mitochondrial dysfunction, and reduce proteasome degradation, recapitulating the cellular phenotypes of Parkinson's disease present in humans.⁶⁷ In addition, overexpression screening in yeast has led to the improved understanding of the cellular functions of α -syn that were previously unknown.⁶⁸ Results of α -syn overexpression screening have been validated in both *in vitro* and *in vivo* neuronal models.⁶⁹

Two major yeast genetic overexpression screening studies^{39,42} were performed, which identified 77 previously unknown genetic modifiers of α -syn toxicity. In these screens, the transmembrane ATPase Yor291w (yeast homolog of *ATP13A2*) was identified as a suppressor of α -syn toxicity; while mutations in *ATP13A2* induced

juvenile onset Parkinson's disease. Interestingly, yeast were employed to identify the connections between these two unrelated genes (*ATP13A2* and *SNCA*).⁴² Indeed, *Caenorhabditis elegans* and rat midbrain cultures were used to verify that *ATP13A2* antagonized α -syn-mediated dopaminergic neuronal degeneration.⁴² Further, we now know that vesicular transport plays a key role in Parkinson's disease pathology because of yeast modifier screening. In fact, *YPT1*, a guanine triphosphatase (GTPase) that enhances ER-Golgi trafficking, suppressed α -syn toxicity while *GYP8*, which converts *YPT1* to its inactive state, enhanced α -syn toxicity.³⁹ Yeast screening assays have not only been used to identify critical cellular perturbations in Parkinson's disease, but also to assess the efficacy of therapeutic agents (N-aryl benzimidazole) for the suppression of α -syn mediated toxicity.⁶⁹

Drawback of prior yeast screening models

All screening studies mentioned above were performed exclusively under galactose growth conditions. Since, *SNCA* and the yeast genes that were screened were under the *GALI* promoter, galactose is essential to induce overexpression of these genes. Galactose is a fermentable carbon source and undergoes glycolysis. Hence, under galactose conditions, yeast do not require mitochondrial oxidative phosphorylation for metabolism.⁷⁰ Given that α -syn affects mitochondria in multiple ways, screening for modifiers in only galactose conditions would likely cause modifiers of α -syn toxicity related to mitochondria and the respiratory function of the cell to be overlooked. Luckily, the ability of yeast to grow on non-fermentable carbon sources (where mitochondrial function is essential for survival) will allow us to perform screening under a mitochondrial-dependent growth condition. We sought to develop an overexpression

system with the capacity to induce gene expression under non-galactose conditions, specifically those containing glycerol. Glycerol metabolizes to one molecule of pyruvate and two nicotinamide adenine dinucleotide hydrogen (NADH). Only one of the NADH molecules is used to ferment pyruvate to ethanol (**Figure 1**); while the other NADH causes a redox imbalance, forcing the NADH to enter the mitochondria for oxidative phosphorylation,⁷¹ making glycerol a mitochondrial-dependent growth condition. We hypothesized that performing the screening under glycerol-rich conditions will permit the identification of novel modifiers of α -syn toxicity. This hypothesis was supported by a yeast screening study examining differences between fermentable and non-fermentable conditions, which revealed 794 genes to be differentially expressed.⁷² When cells were transferred from glucose to glycerol conditions, the transcriptome levels of as many as 1284 RNAs increased. Further, under glycerol conditions, genes involved in mitochondrial metabolism including those associated with electron transport chain, oxidative phosphorylation, and tricyclic acid cycle, had increased expression. Thus, metabolism, gene and protein expression all vary widely between fermentable and non-fermentable carbon source. Since α -syn affects mitochondria, inducing overexpression of α -syn in glycerol will allow for identification of previously overlooked and interesting results.

Constitutive *GAL3* alleles induce *GALI* promoter in glycerol condition

The *GALI* promoter has an upstream activating sequence that is bound by Gal4p, the transcriptional activator, which in turn is repressed by Gal80p, the transcriptional repressor. Under galactose, Gal3p, the protein encoded by *GAL3*, undergoes conformational changes whereby it changes from its native ‘open inactive’ conformation

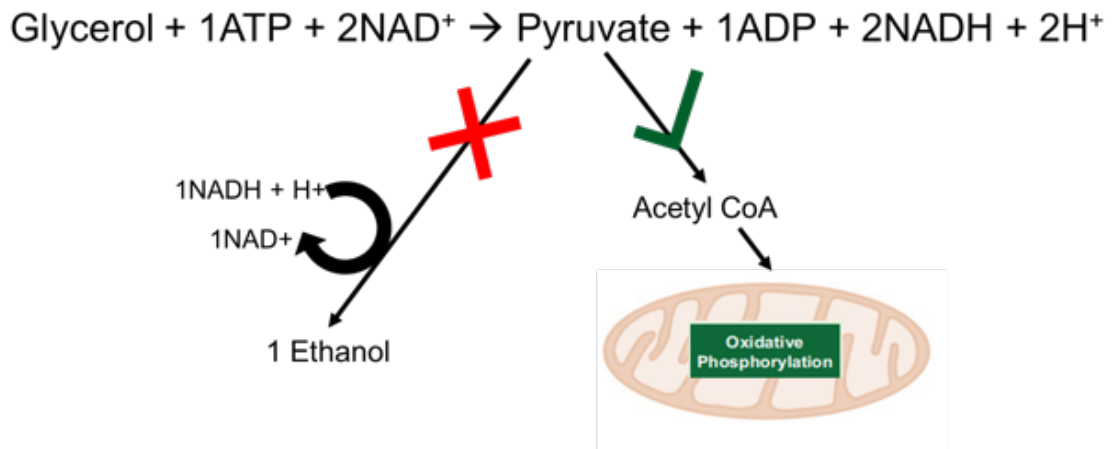


Figure 1. Glycerol metabolism in yeast

Metabolism of glycerol results in one molecule of pyruvate and two molecules of NADH.

Only one of the two released NADH molecules can be used to ferment pyruvate to ethanol. The additional NADH causes redox imbalance, forcing the NADH to become converted to acetyl CoA and enter the mitochondria for oxidative phosphorylation.

to one that is 'closed active'. The closed conformation allows Gal3p to bind and remove Gal80p from Gal4p, resulting in expression of the target gene.^{73,74} *GAL3* alleles had previously been shown to constitutively induce the *GALI* promoter in glycerol condition in the absence of galactose by inducing the 'closed' conformation of Gal3p.⁷⁵ We wanted to test if these alleles can be utilized to induce the *GALI* promoter not just in galactose but also in other non-galactose growth conditions. *GALI* promoter was preserved because it provides a simple switch in gene regulation as growth on galactose medium induces expression, whereas growth on glucose represses expression.^{76,77} Glucose repression would help eliminate the problem of cellular toxicity in expressing α -syn. Thus, we chose three *GAL3* alleles (*GAL3_{F237Y}*, *GAL3_{A368V}* and *GAL3_{S509P}*)⁷⁵ from the previous publication to test gene induction in non-galactose conditions.

II. MATERIALS AND METHODS

Yeast strains, media, and plasmids

Yeast strains, plasmids, and polymerase chain reaction (PCR) primers used in this study are listed in **Tables 1–3**, respectively. Yeast cells were grown using standard methods. Briefly, for integrated strains, including NoTox, IntTox and HiTox α -syn, fused in sarcoma (FUS), TAR DNA-binding protein 43 (TDP-43), and mutant huntingtin (HTT103Q), yeast cells were precultured in yeast peptone dextrose (YPD) medium. Yeast containing free plasmids were precultured in selective medium containing 2% glucose. Precultures with optical densities between 8–14 at 600 nm (OD_{600}) were washed with double distilled water and transferred to selective medium containing specific carbon sources. Mating of yeast strains was performed either in YPD liquid medium or YPD agar plates. The carbon sources used in this study include 2% glucose, 2% raffinose, 2% galactose, 0.5% glucose, 0.1% glucose, and 3% glycerol with 1% ethanol. The nitrogen starvation conditions lacked ammonium sulfate, whereas the other conditions contained ammonium sulfate (5 g/L). Yeast were incubated at 30 °C either in a shaker or a stationary incubator for 3 h to 5 d, depending on the experimental specifications. IntTox α -syn yeast strain was a gift from the Susan Lindquist Lab.

Gateway cloning

The LR reaction is a technique used to transfer entry clone plasmids to yeast expression vectors, enabling expression of the target gene in yeast cells.⁷⁸ This reaction

included a 10 μ L mixture containing 100 ng of entry clone plasmid deoxy-ribonucleic acid (DNA), 150 ng of destination vector plasmid, 3 μ L LR clonase, and Tris EDTA (TE) buffer. The contents were mixed thoroughly and incubated at 25 $^{\circ}$ C overnight. Next, DH5 α competent bacterial cells were transformed with 5 μ L of the LR reaction mixture using the bacterial transformation technique. The expression clone was then extracted from the bacteria using a plasmid miniprep kit according to manufacturer's instructions (Zymo Research, California, USA) and confirmed with restriction enzyme digestion and/or Sanger sequencing.

Site-directed mutagenesis

Primers for *GAL3* alleles were designed online using the QuikChange Primer Design Program available at www.agilent.com/genomics/qcpd (**Table 2 and 3**). PCR for mutagenesis was set up by creating a 50 μ L mixture containing 5 μ L of 10 \times Pfu reaction buffer, 50 ng template DNA, 125 ng each of forward and reverse primers, 1 μ L deoxyribonucleotide triphosphate (dNTP), 1 μ L Pfu, and double distilled water. Next, parental DNA from the reaction mixture was digested with *DpnI*, and 2 μ L of the digested content was transformed into DH5 α bacterial cells. A minimum of two, and a maximum of four bacterial colonies were picked for each allele, and the mutations were confirmed by Sanger sequencing.

One-step yeast transformation

Yeast were grown overnight and washed twice with distilled water, and 1 mL of culture was mixed with transformation buffer (80 μ L of 50% polyethylene glycol (PEG) 3350, 10 μ L of 1 M dithiothreitol, and 10 μ L of 1 M lithium acetate).⁷⁹ No DNA was added to the negative control; to the remaining samples, 100–200 ng plasmid DNA was

added to the mixture and incubated in a 42 °C water bath for 1 h. The samples were then plated on selective agar plates containing glucose or YPD (with or without drugs based on the plasmid) and incubated at 30 °C for 3 days. Single colonies were isolated, and glycerol stocks were obtained and used for further experiments.

Yeast mating

Single colonies of yeast strains of opposite mating types with different auxotrophic markers were streaked on YPD agar plates in a cross pattern and incubated at 30 °C for 16 h. The center of the cross was then streaked to double dropout agar plates. Plates were incubated at 30 °C for 3 d or until individual colonies were visible. For library screening, two yeast strains of opposite mating types were freshly grown separately in selective medium in 96-well plates. Using pins, the two strains were transferred and mixed in 96-well plates containing 160 µL of YPD. The cells were allowed to grow overnight to form diploids, which were then transferred using pins into triple dropout liquid medium containing 2% glucose for selection.

β-Galactosidase assay

A microplate stopped assay protocol was used to perform β-galactosidase assays (ThermoFisher Scientific, Massachusetts, USA). Briefly, a yeast strain (W303 *MATα*) was integrated with the pRS303-LacZ plasmid (**Table 2**).⁸⁰ This strain was then mated with *GAL3* allele strains (W303 *MATa*), resulting in diploid yeast. Single colonies were grown on double selective 2% glucose medium overnight. Once an OD₆₀₀ of 0.1 was observed, cultures were shifted to many growth conditions: 0.1%, 0.5%, and 2% glucose; 2% galactose; 2% raffinose with and without ammonium sulfate; 2% glucose without ammonium sulfate; and 3% glycerol with 1% ethanol. After the cells reached log phase

with an OD₆₀₀ reading between 0.6 and 1.8, 70 μL of the working solution (35 μL β-galactosidase buffer and 35 μL Y-Per reagent) was added to 70 μL yeast culture in each well, and a timer was started. Duplicates of each culture were used to assess reproducibility. When a yellow color became visible in the wells, 56 μL of the stop solution was added to each well, the plates were vortexed for 30 s at 1,000 rpm, the timer was stopped, and the total reaction time was recorded. The plates were then centrifuged at 1,850 rpm for 5 min, and 160 μL of the supernatant was transferred to flat-bottomed 96-well plates. The absorbance at 420 nm (A₄₂₀) of each well was measured using a microplate reader (Fisher Scientific, Ontario, Canada) with the well containing water as the blank. The formula used to calculate β-galactosidase activity was:

$$\beta - \text{galactosidase activity} = \frac{1,000 \times A_{420}}{t \times V \times \text{OD}_{600}}$$

where, t is the time (in min), V is the volume of cells in mL (0.070 mL), A₄₂₀ is the absorbance at 420 nm, and OD₆₀₀ is the optical density at 600 nm.

Serial dilution growth assays

Yeast were grown overnight in YPD or selective medium containing 2% glucose. Yeast cultures were normalized to an OD₆₀₀ of 1.0. A 10-fold serial dilution was performed 4 times, and the diluted samples were spotted in a horizontal pattern on synthetic agar plates with the following carbon sources: 0.1%, 0.5%, and 2% glucose; 2% galactose with or without ammonium sulfate; 2% raffinose with or without ammonium sulfate; 2% glucose without ammonium sulfate; and 3% glycerol with 1% ethanol. Plates were incubated at 30 °C, and images were collected every 24 h between days 2 and 5.

Western blotting

Proteins were extracted from yeast cells using a post-alkaline extraction method.⁸¹ The extracts were separated by sodium dodecyl sulfate polyacrylamide gel electrophoresis and transferred to polyvinylidene difluoride membranes, which were then rinsed with water and blocked with 5% non-fat dry milk in tris-buffered saline with tween 20 (TBST) for 1 h. Incubation with primary antibodies was performed overnight at 4°C. The membrane was washed five times for 5 min each in TBST and then incubated with secondary antibodies for 1 h at room temperature. The membrane was washed again five times for 5 min each in TBST and developed with nitro blue tetrazolium (NBT)/5-bromo-4-chloro-3-indolyl-phosphate (BCIP) solution (ThermoFisher Scientific, Massachusetts, USA). The primary antibodies used were anti-green fluorescent protein (GFP; ab6556, Abcam, Cambridge, UK) and anti-phosphoglycerate kinase 1 (PGK1; PA5-28612, Invitrogen, California, USA) at a dilution of 1:10,000. PGK1 is a key enzyme in glycolysis and gluconeogenesis and localizes to the plasma membrane, mitochondria and cytoplasm. *PGK1* is an essential yeast gene and null mutants are unable to grow in glucose, galactose or glycerol carbon sources; and thus, it was chosen as the loading control. The secondary antibodies used were alkaline phosphatase-conjugated anti-rabbit and anti-mouse antibodies at a dilution of 1:10,000. The experiment was repeated thrice unless otherwise specified. Image quantification was performed using ImageJ software with *PGK1* as the reference bands.

Fluorescence microscopy

Yeast strains were grown overnight in selective medium containing 2% glucose. Cultures were centrifuged at 3,900 rpm for 5 min, washed twice with sterile water, and then resuspended in medium containing either 2% galactose or 3% glycerol with 1%

ethanol. The cultures were diluted to a starting OD₆₀₀ of 1.0 and incubated at 30 °C to induce protein expression for 3–18 h. Cultures were harvested, centrifuged, and resuspended in sterile water. Three µL of the resuspension were then placed on a microscope slide with a cover slip. An Olympus IX83 inverted fluorescent microscope and Olympus DP74 digital camera (Olympus, Japan) were used to capture images at 40× magnification using fluorescein isothiocyanate, yellow fluorescent protein (YFP), cyan fluorescent protein (CFP), and Texas Red (Tx Red) filter cubes (chroma 39002, 39003, 49001, and 39010, respectively). Brightfield images were obtained before switching to other channels.

Quantification of α -synuclein aggregates

The YFP microscopic pictures obtained were used for counting. The total number of cells and number of cells with aggregates were counted using Image J software and verified manually. A minimum of 200 cells per biological repeat were counted. The percentage of cells containing aggregates was calculated as the ratio of the number of cells with aggregates to the total number of cells.

Examination of mitochondria

The MitoLoc plasmid (pMitoLoc) was purchased from Addgene. pMitoLoc contained two fluorescently tagged proteins that both localized to the mitochondria - GFP fused to the fungal mitochondrial localization signal of the F₀-ATPase subunit 9 (preSu9), a mitochondrial membrane potential independent signal and mCherry protein fused to the N-terminal localization sequence of cytochrome C oxidase 4 (preCOX4), imported into mitochondria proportional to the membrane potential. Expression of plasmids was achieved by transforming the plasmid into yeast strains and plating on agar

plates containing the antibiotic nourseothricin.⁸² Since *SNCA*, tagged with a YFP, overlapped with the GFP signal of pMitoLoc, we re-engineered the plasmid to replace preSu9-GFP with preSu9-teal fluorescent protein (preSu9-TFP). First, we amplified the TFP sequence by PCR with an overhang sequence of the GFP upstream region in the pMitoLoc. The downstream region of GFP was also amplified by PCR with part of the overhang sequence of mTFP. The two amplified products were further merged by PCR. The pMitoLoc and the final PCR product were digested and ligated, resulting in replacement of preSu9-GFP with preSu9-TFP. This enabled us to visualize *SNCA* simultaneously with the mitochondrial structure and membrane potential - *SNCA* in yellow, all mitochondria in teal, and healthy mitochondria in red. pMitoLoc was transformed into the two strains - the vector (pRS303-GAL) and α -syn. Mating was then performed with the strain containing *GAL3_{A368V}*. Diploid yeast strains were induced in galactose and glycerol-ethanol for 6 and 18 h, at which point microscope images were captured. For Aim 3, the suppressor and vector plasmids were transformed into the α -syn containing pMitoLoc. Merging of mitochondrial images were performed using ImageJ software.

Quantification of viable and respiratory-competent cells

Diploid cells containing *GAL3_{A368V}* and α -syn or vector were precultured in medium containing 2% glucose overnight. Cultures with an OD₆₀₀ of 8–14 were washed twice with water and transferred to galactose and glycerol-ethanol conditions beginning at an OD₆₀₀ of 1.0. The cells were induced for 6 and 18 h. OD₆₀₀ was measured and recorded at the two time points, and 10⁷ cells were diluted to a total volume of 1 mL. Next, 100 μ L of the diluted culture was isolated and mixed with 900 μ L distilled water.

Of this mixture, 10 μL was diluted with 990 μL water. For strains containing $\alpha\text{-syn}$, 100 μL of the mixture was plated onto YPD and YPGE agar plates. Of the remaining mixture, 100 μL was diluted in 900 μL water. For strains with and without $\alpha\text{-syn}$, 100 μL of this final mixture was plated onto both YPD and YPGE agar plates. Thus, for all strains, we plated a 10^{-5} dilution of the original culture, and for $\alpha\text{-syn}$ strains, in addition to a 10^{-5} dilution, we also plated a 10^{-4} dilution of the original culture. The $\alpha\text{-syn}$ strain was toxic under glycerol-ethanol growth conditions; therefore, we used two dilution factors for $\alpha\text{-syn}$ strains as we expected that a single digit colony count may give erroneous results. Including a 10^{-4} dilution for $\alpha\text{-syn}$ strains enabled corroboration of the colony counts recorded at the 10^{-5} dilution. After plating, the agar plates were incubated in a stationary incubator at 30 °C for 3 d for YPD and 4 d for YPGE. Single colonies were counted by visualization, and numbers were recorded. The number of colonies in YPD plates represented cells that were viable, and the number of colonies in YPGE plates represented cells that were respiratory-competent. For $\alpha\text{-syn}$, when deciding whether to use the counts from the 10^{-4} or 10^{-5} dilutions, we chose the one nearest to 100. This colony count was then multiplied by the dilution factor, and statistical analyses was performed using the final derived number.

Reactive oxygen species quantification

Diploid yeast cells containing $\alpha\text{-syn}$ and *GAL3_{A368V}* (1×10^7 cells) were harvested and centrifuged at 3600 rpm for 5 min after induction in galactose and glycerol-ethanol at 3, 6, and 18 h. ROS was measured using dihydroethidium (DHE),⁸³ which was dissolved in 500 μL of selective medium, added to the centrifuged cells, and incubated at room temperature (23 ± 2 °C) for 20 min in the dark. Cells were then centrifuged and washed

twice with phosphate-buffered saline, and 160 μL of cells was added to black flat-bottomed CoStar plates. Using a plate reader (Fisher Scientific, Ontario, Canada), the density of the cells was measured at an OD_{600} , and the absorbance was measured at $\lambda_{\text{ex}} = 485 \text{ nm}$ and $\lambda_{\text{em}} = 620 \text{ nm}$.⁸⁴ The amount of ROS was calculated as the ratio of the measured absorbance to OD_{600} . The same volume of cell solution (3 μL) was used for microscopic imaging in the Tx Red channel for visual analysis and qualitative assessment of ROS.

Split green fluorescent protein system and oligomer engineering

DNA was prepared by digesting pRS416-GAL-ccdB-DsRed and pRS426-GAL-ccdB-DsRed with *Hind*III and *Sla*I (or *Xho*I), removing the Ds Red tag and purifying the vector. Forward and reverse primers for GFP₁₁ were diluted to 100 μM and then further to 1 μM . Next, 50 μL of forward and reverse primers were combined and placed in boiling water for 10 min. The mixture was then allowed to cool completely to room temperature for 1 h to allow annealing, 1 μL of the mixture was then diluted 10-fold, and DNA ligation was performed. The ligation mixture had a total volume of 10 μL , including 1 μL T4 ligase, 1 μL oligomer mixture (obtained previously), 1 μL T4 ligase buffer, and 100–150 ng of digested linearized pRS416-Gal-ccdB or pRS426-Gal-ccdB. This mixture was then transformed into T1K *Escherichia coli* bacteria and plated on lysogeny broth agar plates containing carbenicillin. DNA was extracted from the bacterial cells and confirmed by restriction digestion. An LR reaction was then performed to individually insert the entry clones, *SNCA*, *TOM6*, and *CIT1*, into the destination vectors of pRS416-GAL-ccdb-GFP₁₁ and pRS426-GAL-ccdb-GFP₁₁. The plasmid constructs were confirmed at each step by restriction digestion and sequencing. Subsequently, the

gateway vector was transformed into W303 *MATa* yeast integrated with p404-MTS mCherry plasmid. The W303 *MAT α* yeast strain containing *GAL3_{A368V}* was mated with the W303 *MATa* yeast strain containing p404-MTS-mCherry and *SNCA*. Since we did not observe a green color with any of the three strains, we further examined the genetic code of the plasmids. We noticed the presence of a stop codon in the reading frame of both plasmid constructs that may have prevented the transcription of GFP₁₁. We also noticed a glycine-rich coding sequence between the gene and GFP₁₁ that may have caused hairpin formation. To remove the stop codon and glycine sequences, we performed Yeast Gap Repair.⁸⁵ First, PCR was performed using primers (**Table 3**) to synthesize the gene and GFP₁₁ while removing the intervening stop codon and glycine. Second, pRS416GAL-SNCA-GFP₁₁ and pRS416GAL-CIT1-GFP₁₁ were cut using *HindIII* enzyme, whereas pRS416GAL-TOM6 GFP₁₁ was cut using *EcoRI* enzyme. The cut plasmid was then purified, and 400 ng of purified plasmids was mixed with 100 ng of PCR product; using a one-step yeast transformation, this mixture was transformed into W303 *MATa* yeast that had an integrated p404-MTS mCherry plasmid. Using the PCR product as template, the yeast repairs the gap in the cut plasmid construct. The final plasmid product contained the gene and GFP₁₁, without the intervening stop codon and glycine sequences. The construct was confirmed by restriction digestion, however, still required confirmation via sequencing.

Human gene plasmid library and transformation into yeast

The Ju and Zhong laboratory generated a human gene library containing 14,827 sequence-verified individual human gene open reading frames (ORFs) (corresponding to 12,890 human genes) cloned into the destination vector pRS416GAL-ccdB (*URA*

marker) in the W303 *MATa* yeast that contained an integrated IntTox *SNCA* (**Table 1**). Plasmid DNA in the destination vector was stored frozen at -80 °C. A high-throughput yeast transformation protocol⁸⁶ was used to transform all the plasmid DNA. Transformed yeast were saved as glycerol stocks and stored at -80 °C.

High-throughput screening

IntTox α -syn strain containing the human genes and strain containing *GAL3_{A368V}* were grown separately in selective glucose media overnight in 96-well plates. After overnight growth, we used pins to cross the two strains in YPD media and grew the yeast overnight. The grown culture was transferred using pins to a triple selective glucose media and grown for 48 h. The culture was then spotted onto triple selective glucose and glycerol-ethanol agar plates using the bench-top RoToR HDA robot (Singer Instruments, Roadwater, UK). The robot spots four times for each well; thus, in the agar plate there were a total of 384 spots. The agar plates were incubated in 30 °C for 2 d (for glucose plates) and 5 d (for glycerol-ethanol plates) when the images were taken using a Canon EOS 200D camera (Peschiera Borromeo (Mi), Italy).

Confirmation of genetic hits

Four types of scoring by visual examination of the agar plates were used: trace, mild, moderate, and strong. The original human gene plasmid of the hits was revived from the bacterial glycerol stock. The bacteria were grown in lysogeny broth with carbenicillin and isolated using a plate miniprep technique (GenScript 96-well Plasmid Miniprep Kit, New Jersey, USA). Next, 1.3 mL medium containing antibiotics was added to 96-well plates. Bacteria were inoculated in the medium using pins to transfer the glycerol stock into the new medium. The plates were covered with adhesive tape and

grown overnight at 37 °C in a shaking incubator until an OD₆₀₀ between 1–4 was reached. The cells were then harvested by centrifugation at 2500 rpm for 10 min, and 250 μL of resuspension solution with RNase A was added to each well, followed by vigorous vortexing. Next, 250 μL lysis solution was added to each well and thoroughly mixed, and 250 μL neutralization solution was then added. The plates were inverted multiple times until a clear precipitate was formed. The plates were centrifuged, the supernatants were transferred to new 96-well filter plates, and the plates were centrifuged again. Filtered lysates were then transferred to a binding plate and centrifuged at 2500 rpm for 10 min. The flow-through was then placed on a new deep-well plate, and 500 μL of wash solution with ethanol was added. The samples were then centrifuged to remove residual wash solution. The binding plate was placed on top of the collection plate and 50 μL elution solution was added. After incubation at room temperature for 2 min, the plate was centrifuged at 2500 rpm for 5 min. Each plasmid containing human gene clones was then individually transformed into the IntTox α-syn W303 *MATa* strain using a standardized yeast one-step transformation protocol and plated on double selective agar plates. After allowing cells to grow at 30 °C for 4 d, the cells were isolated, grown in double selective medium, and mated with the *GAL3_{A368V}* allele from the opposite mating type. The toxicity was confirmed after individually spotting the diploid strains.

Gene ontology analysis

Gene ontology (GO) enrichment analysis was performed using the analysis tool found at <http://geneontology.org>. The software that runs the analysis is called the PANTHER Classification System, (<http://www.pantherdb.org/>) which is maintained up to date with GO annotations. This is a comprehensive system that combines data from 82

complete genomes and their phylogenetic trees. The statistical model that is used for GO analysis is the hidden Markov models.⁸⁷ Results from this analysis will provide information on which GO terms are overrepresented or underrepresented using annotations for that gene set. The gene IDs of the IntTox α -syn toxicity suppressors along with the entire list of human gene clones from the library (reference list) were used for the analysis; duplicate genes were deleted prior to analysis. Three GO aspects - molecular function, biological process and cellular component were set for the analysis. GO terms shared by the suppressor list were compared to the background distribution of annotation. The closer the p value was to zero, the more significant the GO term associated with the group of genes was determined to be. A Fischer's exact test was used and a Bonferroni correction for multiple testing was selected. Only results that were Bonferroni-corrected for $p < 0.05$ are displayed.

Statistical analyses

The data presented in figures as bars represent means + standard errors of the means (SE). Experiments were performed independently a minimum of three times. Where necessary, a natural log transformation was performed to correct for violation of the assumption of constant variance between groups. For analysis including different time points, interactions between genes and times were assessed first before measuring differences between genes and controls. The differences between α -syn and controls were assessed by one-way analysis of variance (ANOVA), two-way ANOVA, repeated measure ANOVA, or Type III tests of fixed effects. To compare the suppressors of α -syn with the vector, Dunnett's test was performed. Results with p values < 0.05 were considered significant. Analyses were performed using SAS (v. 9.4) software.

Table 1. Yeast strains

Strain	Genotype	Reference
W303	<i>MATa can1-100 his3-11,15 leu2-3,112 trp1-1 ura3-1 ade2-1</i>	
W303	<i>MATα can1-100 his3-11,15 leu2-3,112 trp1-1 ura3-1 ade2-1</i>	
<i>NoTox</i> α-syn (1 copy of α-syn)	α-syn-WT, <i>MATa can1-100 his3-11,15 leu2-3,112 trp1-1 ura3-1 ade2-1</i> pRS303-GAL-αSynWT-YFP	This study
<i>IntTox</i> α-syn (4–5 copies of α-syn)	α-syn-WT, <i>MATa can1-100 his3-11,15 leu2-3,112 trp1-1 ura3-1 ade2-1</i> pRS303-GAL-αSynWT-YFP pRS304-GAL-αSynWT-YFP	42
<i>HiTox</i> α-syn (> 6 copies of α-syn)	α-syn-WT, <i>MATa can1-100 his3-11,15 leu2-3,112 trp1-1 ura3-1 ade2-1</i> pRS304-GAL-αSynWT-GFP pRS306-GAL-αSynWT-GFP	42
1X FUS	FUS-WT, <i>MATa can1-100 his3-11,15 leu2-3,112 trp1-1 ura3-1 ade2-1</i> pRS303-GAL-FUSWT	89
2X TDP-43	TDP-43-WT, <i>MATa can1-100 his3-11,15 leu2-3,112 trp1-1 ura3-1 pdr1::Kan, pdr3::Kan</i> pRS303-GAL-TDP-43-GFP pRS304-GAL-TDP-43-GFP	88
HTT103Q	HTT103Q, <i>MATa can1-100 his3-11,15 leu2-3,112 trp1-1 ura3-1 ade2-1</i> pRS303-GAL-FLAG-HTT103Q-EYFP	90

Table 2. Plasmids

Plasmid	Reference
pRS303-GAL1-ccdB (<i>HIS3</i>)	89
pRS415-GPD-ccdB (<i>LEU2</i>)	This study
pRS415-GPD-GAL3 (<i>LEU2</i>)	This study
pRS415-GPD-GAL4 (<i>LEU2</i>)	This study
pRS415-GPD-GAL3-A368V (<i>LEU2</i>)	This study
pRS415-GPD-GAL3-F237Y (<i>LEU2</i>)	This study
pRS415-GPD-GAL3-S509P (<i>LEU2</i>)	This study
pRS415-GPD-GAL3-A368V- F237Y (<i>LEU2</i>)	This study
pRS415-GPD-GAL3-F237Y- S509P (<i>LEU2</i>)	This study
pRS415-GPD-GAL3-S509P-A368V (<i>LEU2</i>)	This study
pRS415-GPD-GAL3-S509P-A368V-F237Y (<i>LEU2</i>)	This study
pRS303-LacZ (<i>HIS3</i>)	Addgene
pRS416-GAL1-1433 β (<i>URA3</i>)	This study
pRS416-GAL1-1433 θ (<i>URA3</i>)	This study
pRS416-GAL1-1433 γ (<i>URA3</i>)	This study
pRS416-GAL1-1433 ζ (<i>URA3</i>)	This study
pRS416-GAL1-1433 σ (<i>URA3</i>)	This study
pRS416-GAL1-1433 η (<i>URA3</i>)	This study
pRS416-GAL1-GLRX1 (<i>URA3</i>)	This study
pRS416-GAL1-TM39B (<i>URA3</i>)	This study
pMitoLoc-preCOX4-mCherry & preSU9-GFP	Addgene
pMitoLoc-preCOX4-mCherry & preSU9-TFP	This study
p404-Grx5-GFP ₁₋₁₀	99
p404-MTS-mCherry- GFP ₁₋₁₀	99
pRS416-GAL1-ccdB-DsRed (<i>URA3</i>)	This study
pRS416-GAL1-GFP ₁₁ -SNCA (<i>URA3</i>)	This study
pRS416-GAL1- GFP ₁₁ -TOM6 (<i>URA3</i>)	This study

pRS416-GAL1- GFP ₁₁ -CIT1 (<i>URA3</i>)	This study
pRS426-GAL1-ccdB-DsRed (<i>URA3</i>)	This study
pRS426-GAL1- GFP ₁₁ -SNCA (<i>URA3</i>)	This study
pRS426-GAL1- GFP ₁₁ -TOM6 (<i>URA3</i>)	This study
pRS426-GAL1- GFP ₁₁ -CIT1 (<i>URA3</i>)	This study
pRS416-GAL1-ccdB- GFP ₁₁ (<i>URA3</i>)	This study
pRS426-GAL1-ccdB- GFP ₁₁ (<i>URA3</i>)	This study
pRS416-GAL1-ccdB (<i>URA3</i>)	This study

Table 3. Primers

Name	Sequence (5' → 3')
t710a	CAA AACTAAAGGCCACACCTTTCAAGTATCCTCAATTGA AAAATCAT
t710a_antisense	ATGATTTTTCAATTGAGGATACTTGAAAGGTGTGGCCTT TAGTTTTG
a1103t	ATGATTTTTCAATTGAGGATACTTGAAAGGTGTGGCCTT TAGTTTTG
a1103t_antisense	GGAAAAGTTGTCAGGTAAACTCTAGTGAACCTCCTCAC
c1526t	GAACTAAAAGACGCAATTATAGTTTTGAAGCCTGCCTTG G
c1526t_antisense	CCAAGGCAGGCTTCAA AACTATAATTGCGTCTTTTAGTT C
Hind-GFP ₁₁ -Xho F	AGCTTAGGTGGTGGTTCTGGAGGCGGTTCTATGAGAGAT CATATGGTTTTGCATGAATATGTTAATGCTGCTGGTATTA CTTAGC
Hind- GFP ₁₁ -Xho R	TCGAGCTAAGTAATACCAGCAGCATTAAACATATTCATGC AAAACCATATGATCTCTCATAGAACCGCCTCCAGAACCA CCACCTA
M13F	TGTA A A A C G A C G G C C A G T
Trp1_OutF	GGCAGCCCCGATCTAAAAGA
Trp1_OutR	AGACCGAGAAAAGGCTAGCA
Trp1_InR	TTTTCGCCCTTTGACGTTGG
Trp1_InF	ACTGAGAGTGCACCATAGATCA
Leu2_up_F	TGTGTAGAATTGCAGATTCCCT
Leu2_dn_R	TCGCATTATCCTCGGGTTCA
Leu2_up_F	TGTGTAGAATTGCAGATTCCCT
Leu2_int_up_R	CGGTGATGACGGTGAAAACC
Leu2_int_dn_F	CAACACTCAACCCTATCTCGG
Leu2_dn_R	TCGCATTATCCTCGGGTTCA

TOM6_F	TGTTGGTGGTGGTTCTGGAG
CIT1_F	AACGGTGGTGGTTCTGGAG
SNCA_F	CTACGGTGGTGGTTCTGGAG

III AIM 1: TO DEVELOP A METHOD OF GENE OVEREXPRESSION UNDER NON-GALACTOSE CONDITIONS USING *GAL3* ALLELES

Rationale

Yeast genetic screening has identified key biological pathways of many neurodegenerative disease-related genes including *SNCA*,^{42,64,88} *FUS*,⁸⁹ and *HTT*.^{64,90} *SNCA* mutations cause Parkinson's disease, *FUS* mutations cause amyotrophic lateral sclerosis (ALS), and mutations in *HTT* cause Huntington's disease. However, all prior screening studies have been performed under galactose-enriched growth condition, exclusively. Furthermore, mutations in *SNCA*, *FUS*, and *HTT* cause mitochondrial dysfunction, which is associated with disease pathology. Additionally, calorie restriction, in yeast and animal models, has been shown to delay neurodegeneration.^{91,92} Autophagy, a mechanism of recycling obsolete cellular constituents has also been widely studied in neurodegenerative disorders. Specifically, attenuation of autophagy has been shown to initiate development of Parkinson's disease,^{93,94} while induction of autophagy delays progression of ALS.⁹⁵ As discussed previously, mitochondria can be studied under a respiratory glycerol condition, and calorie restriction, in yeast, can be induced by reducing the concentration of glucose in the growth medium. Further, autophagy can be induced by depleting the medium of nitrogen.^{96,97} We analyzed a method that would enable the study of genes under these non-galactose conditions. As such, we sought to test and validate a novel overexpression system that involved constitutive *GAL3* alleles

that can induce *GALI* promoter in non-galactose conditions.⁷⁵ These alleles were integrated into a haploid yeast strain where the WT *GAL3* was knocked down. Since our laboratory previously designed a diploid screening method,⁹⁸ here we determined if the *GAL3* alleles were capable of inducing the *GALI* promoter in diploid yeast strains without the deletion of two WT *GAL3* genes.

Experimental design

***GALI* promoter and *GAL3* alleles.** We chose one intermediate strength and two strong *GAL3* alleles from the previous publication.⁷⁵ Three mutations in the *GAL3* gene (F237Y, A368V, and S509P) were generated by site-specific mutagenesis using the pRS415-GPD vector (*LEU* marker) and transformed into the WT yeast strain W303 *MATa*. We also generated double- and triple-combination mutants (F237Y+A368V, F237+S509P, A368V+S509P, and F237+A368V+S509P).

β -galactosidase assay. We used β -galactosidase assays to quantify the induction of the *GALI* promoter under 2% glucose, 2% galactose, 3% glycerol with 1% ethanol, 2% raffinose, calorie restriction (0.5% and 0.1% glucose), and nitrogen starvation (2% raffinose and 2% glucose) conditions. β -galactosidase, a widely used reporter gene, hydrolyzes o-nitrophenyl- β -D-galactopyranoside to o-nitrophenol and galactose, resulting in a yellow color. The intensity of the yellow color was determined by measuring the A₄₂₀. An LR reaction was performed to synthesize the pRS303-LacZ plasmid. We then performed a high efficiency yeast transformation to integrate the pRS303-LacZ plasmid (*HIS* marker) into the WT yeast strain W303 *MAT α* .

Mating strategy to perform β -galactosidase assays. We grew *GAL3* alleles (*MATa*) and β -galactosidase (*MAT α*) together in YPD agar plate (**Figure 2**). We then transferred the

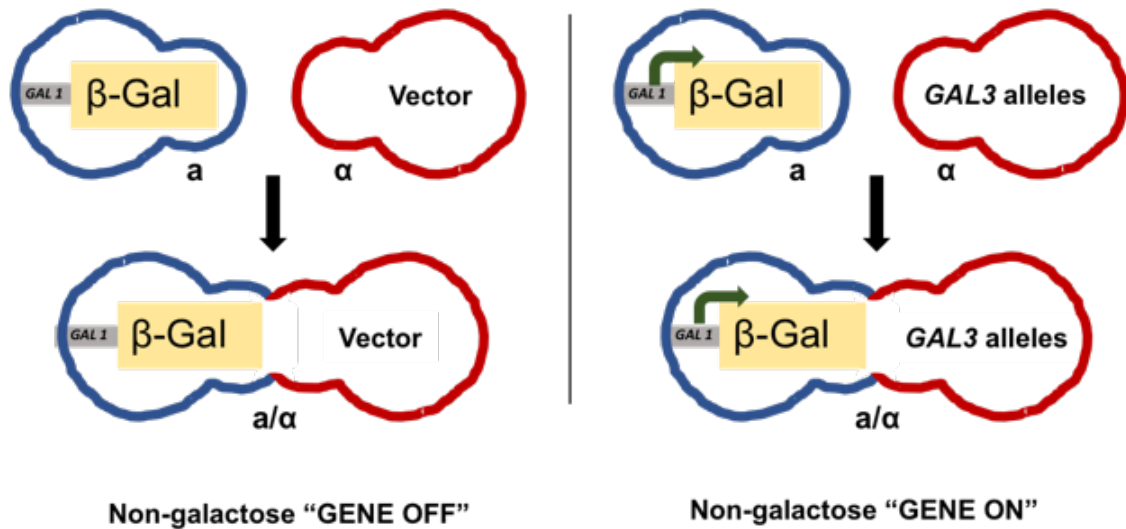


Figure 2. Schematic representation of the mating strategy used in this study.

Mating of the β -galactosidase gene under the *GAL1* promoter and the *GAL3* alleles to measure β -galactosidase activity. We used three *GAL3* alleles (*GAL3_{F237Y}*, *GAL3_{A368V}* and *GAL3_{S509P}*) or their combinations for the experiments in Aim 1. The β -galactosidase gene was integrated into the haploid *MAT α* yeast strain chromosome, whereas the *GAL3* alleles were transformed into the haploid opposite mating type *MATa* yeast strain using a constitutive promoter, pRS415-GPD (**Table 2**). Single colonies of two haploid yeast (W303 *MAT α* containing β -galactosidase enzyme and W303 *MATa* containing *GAL3* alleles) were crossed in YPD agar plates and allowed to grow overnight. The yeast patch from the crossed area was picked and streaked on double selective agar plates and incubated for 2–3 days to isolate a single colony. The resulting diploid yeast contained both the β -galactosidase gene and the *GAL3* alleles.

cells to double-selection 2% glucose medium and grew them overnight. The cells were then washed and transferred to double selective medium containing different carbon sources beginning at an OD₆₀₀ of 0.1. The diploid yeast strains were permitted to grow to mid-log phase, at which point the experiment was conducted.

Results

1.1: To develop and test a method of gene overexpression under non-galactose conditions

GAL3 alleles induce the *GAL1* promoter under non-galactose conditions in the absence of glucose. Figure 3 shows the results of β -galactosidase assays for the control, WT *GAL3*, and *GAL3* alleles - *GAL3*_{F237Y}, *GAL3*_{A368V}, and *GAL3*_{S509P}. β -galactosidase is under the control of the *GAL1* promoter; thus, higher the enzyme activity results in higher promoter induction. Glucose served as the negative control, while galactose as the positive control. *GAL3*_{F237Y}, *GAL3*_{A368V} and *GAL3*_{S509P} exhibited significantly higher induction under glycerol-ethanol compared to the vector control (all $p < 0.0001$). For the spotting assays, we initially analyzed the genes in a glycerol-rich growth condition and observed that the cells expressing α -syn exhibited growth only after five days of incubation. Hence, we supplemented the media with 1% ethanol to aid the cells in more rapid growth. Only *GAL3*_{S509P} exhibited significantly ($p = 0.008$) higher induction under nitrogen starvation compared to the vector control. However, under calorie restriction conditions, none of the alleles showed significant induction when compared to the control. Since all three alleles exhibited significant induction in the glycerol-ethanol condition, we hypothesized that the combination of allele mutants will elicit a more dramatic induction of the promoter.

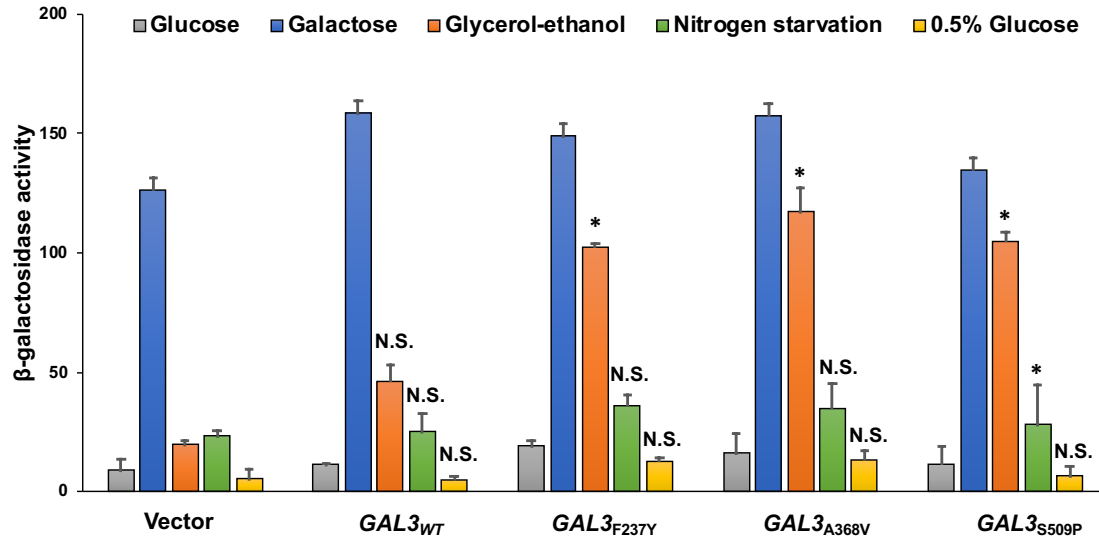


Figure 3. *GAL3^{F237Y}*, *GAL3^{A368V}* and *GAL3^{S509P}* induce *GAL1* promoter under glycerol-ethanol.

Single diploid yeast colonies containing both the β -galactosidase enzyme (W303 *MAT α* strain) and *GAL3* alleles (W303 *MAT α* strain) were grown overnight in double selective 2% glucose media. The pre-culture (OD₆₀₀ of 8–14) was washed twice with distilled water and inoculated into media lacking histidine (gene) and leucine (*GAL3* vector) beginning at an OD₆₀₀ of 0.1. Media consisted of 2% glucose (negative control), 2% galactose (positive control), 3% glycerol with 1% ethanol, nitrogen starvation containing 2% glucose, and calorie restriction containing 0.5% glucose. The culture was grown until mid-log phase when the cells were isolated. The intensity of the yellow color was measured at A₄₂₀. β -galactosidase activity of *GAL3^{WT}*, *GAL3^{F237Y}*, *GAL3^{A368V}* and *GAL3^{S509P}* was compared to the empty vector (pRS415-GPD) in each condition by two-way ANOVA. * $p < 0.05$ and hence significantly different compared to control; N.S, no significant difference compared to control; WT, wild-type.

Combining GAL3 alleles do not induce the GAL1 promoter under non-galactose conditions. Interestingly, neither the double- nor the triple-combination mutants (**Figure 4**) induced the *GAL1* promoter. Gal3p regularly transitions between the ‘open inactive’ and ‘closed active’ conformation, and the *GAL3* alleles induce the ‘closed active’ conformation even under non-galactose conditions.⁷³ However, the results of this experiment suggest that the combination of alleles fails to induce the ‘closed active’ conformation. Hence, we performed structural analysis of the position of alleles and their combinations in relation to the ‘transition site’ or the ‘switch region’ (**Figure 5**). We found that F237 formed hydrophobic bonds and was located adjacent to the ‘switch’ region; a mutation in this position enabled transition to a ‘closed active’ conformation. The combination of F237Y and S509P showed a mutual negating effect of the closed conformation, likely caused by disruption of the β -sheet formation at S509. Thus, the allele combinations likely inhibited transition to the ‘closed active’ conformation, thereby preventing its constitutive action.

1.2: To test a gene overexpression method using neurodegenerative disease gene models and *GAL3* alleles

***GAL3_{A368V}* and *GAL3_{F237Y}* induce *GAL1* promoter under glycerol-ethanol.** We sought to identify the strongest inducer among the three *GAL3* alleles using IntTox α -syn under glycerol-ethanol growth conditions. We chose the IntTox α -syn as this strain exhibits toxicity when induced in galactose under haploid conditions. Hence, a phenotypic change in glycerol-ethanol condition would be readily detectable. Here, we created a diploid strain of IntTox α -syn and all three *GAL3* alleles as our genetic screening will be

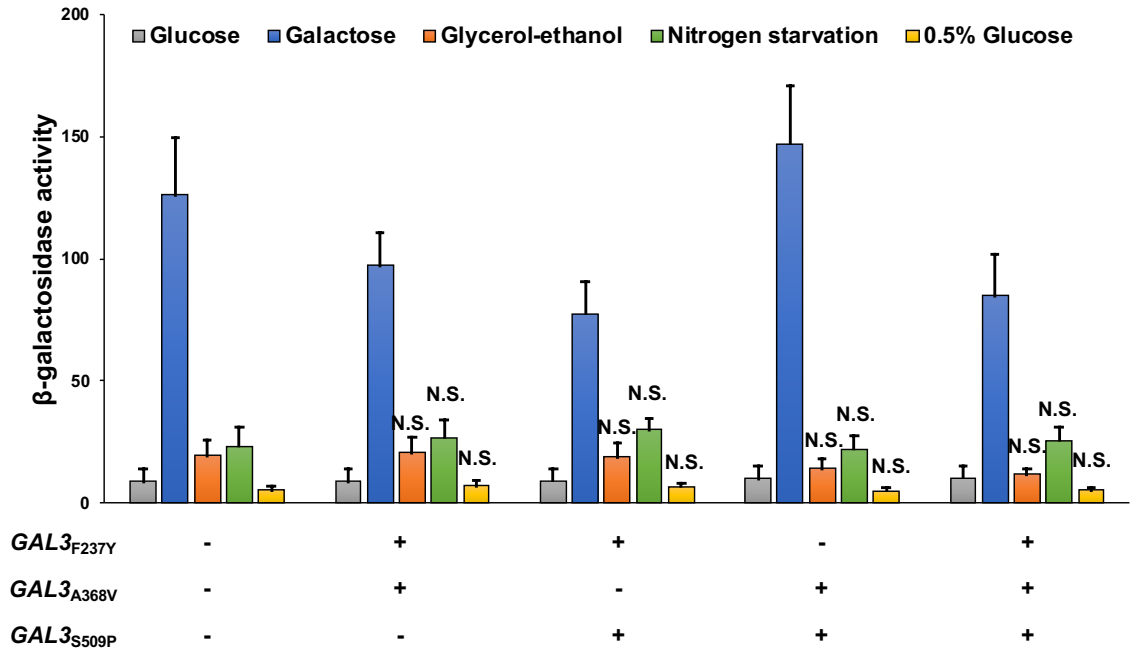


Figure 4. Combinations of *GAL3*_{F237Y}, *GAL3*_{A368V} and *GAL3*_{S509P} do not induce *GAL1* promoter in non-galactose conditions.

Double and triple mutations of the alleles were generated using PCR as described in the methods. Single diploid yeast colonies containing both β -galactosidase enzyme (W303 *MAT α* strain) and *GAL3* allele combinations (W303 *MAT α* strain) were grown overnight in double selective 2% glucose media. The pre-culture (OD₆₀₀ of 8–14) was washed twice with distilled water and inoculated into five different media lacking histidine (gene) and leucine (*GAL3* vector) starting at OD₆₀₀ of 0.1: 2% glucose (negative control), 2% galactose (positive control), 3% glycerol with 1% ethanol, nitrogen starvation containing 2% glucose, and calorie restriction containing 0.5% glucose. The culture was grown until mid-log phase when the cells were isolated, and the assay was performed. The intensity of the yellow color was measured at A₄₂₀. β -Galactosidase activity of *GAL3* allele combinations was compared to the empty vector in each condition by two-way ANOVA. N.S, no significant difference compared to control; WT, wild-type.

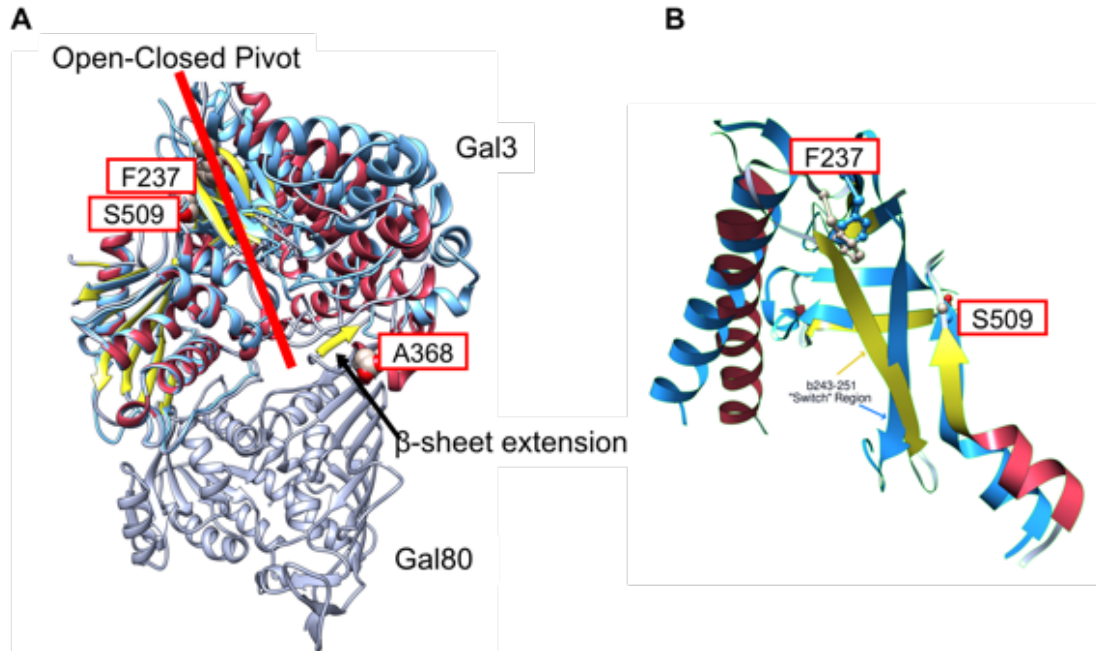


Figure 5. Combination of *GAL3*_{F237Y} and *GAL3*_{S509P} fails to enable transition to ‘closed active’ Gal3p conformation.

(A) Position of the F237, A368 and S509 in relation to the ‘Open-Closed Pivot’ in Gal3p. The structure on the top of the figure is the Gal3p which, in its closed conformation, binds to the transcriptional repressor, Gal80p (gray colored structure in the bottom of the figure). A368 is located at the transition site, which is the region where the galactose binds and the conformation switches from ‘open inactive’ to ‘closed active’. (B) F237 forms hydrophobic bonds and is located adjacent to the ‘Switch’ region; a mutation in this position causes transition to a closed conformation. A mutation in S509 disrupts the adjacent β-sheet and initiates a closed conformation. However, the combination of F237 and S509 fails to enable the transition, likely due to the mutual cancelling effect caused by disruption of the hydrophobic bonds and the β-sheet.

performed in diploid conditions. The diploid strain was plated onto double selective glucose (negative control), galactose (positive control) and glycerol-ethanol agar plates. Two primary findings were observed (**Figure 6**). First, the IntTox α -syn was no longer toxic under galactose condition. The only difference between previous IntTox α -syn studies showing toxicity in galactose and our study is that previously, IntTox α -syn was tested in haploid state while our study was performed in diploid state. Second, *GAL3_{F237Y}* and *GAL3_{A368V}* induced IntTox α -syn under glycerol-ethanol condition and elicited toxicity. Alternatively, *GAL3_{S509P}* did not cause toxicity to IntTox α -syn although we saw significant induction of the *GALI* promoter in the β -galactosidase assay (**Figure 3**). As expected, *GAL3_{WT}* and the empty vector did not induce the gene, corroborating the findings of the β -galactosidase assay. Taken together the results from the spotting and β -galactosidase assays suggest that both *GAL3_{A368V}* and *GAL3_{F237Y}* induced the *GALI* promoter in glycerol-ethanol. Among the two, we chose *GAL3_{A368V}* for the next experiments.

GAL3_{A368V} does not induce toxicity of neurodegenerative disease-genes in the presence of glucose. We next wanted to determine if *GAL3_{A368V}* effectively induces genes in non-galactose conditions other than glycerol, and if so, whether it causes toxicity. Four neurodegenerative disease-related genes, *SNCA* (IntTox and HiTox), *FUS*, *TDP-43*, and *HTT103Q* were chosen, all of which have been shown to cause cellular toxicity under galactose condition. We generated a diploid yeast containing the genes and *GAL3_{A368V}* and plated the cells under double selective nitrogen starvation and calorie restriction conditions. Nitrogen starvation conditions (activate autophagy) lacks ammonium sulfate and contains 2% glucose in the media; whereas the calorie restriction condition (delays

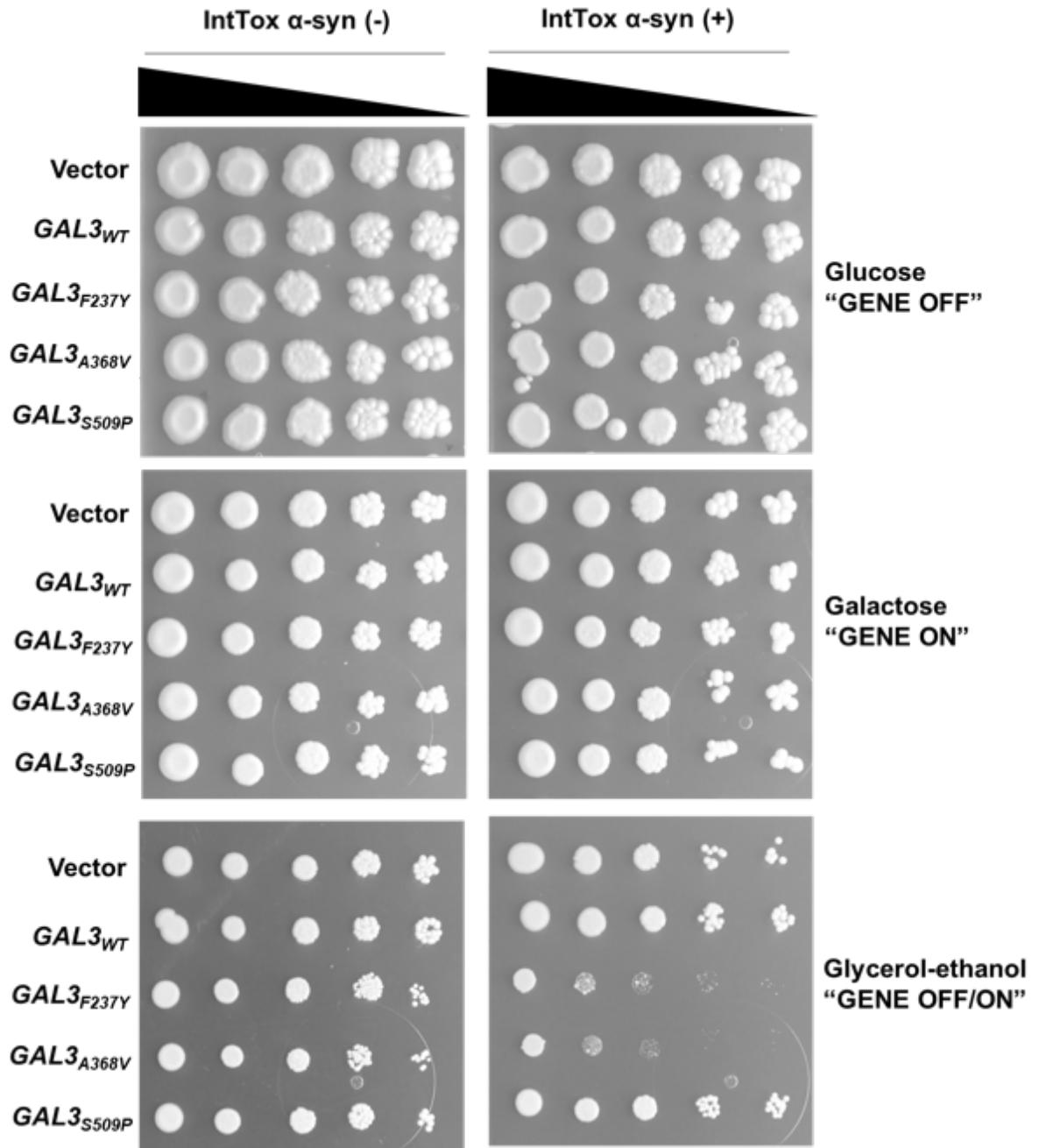


Figure 6. *GAL3_{A368V}* and *GAL3_{F237Y}* induce toxicity of IntTox α -synuclein under glycerol-ethanol.

Single diploid yeast colonies containing empty vector (pRS303-GAL) or IntTox α -syn (W303 *MAT α* strain) and empty vector or *GAL3* alleles (W303 *MAT α* strain) were grown overnight in double selective 2% glucose media lacking histidine (gene) and leucine

(*GAL3* vector). The culture was washed twice with distilled water and diluted to an OD₆₀₀ of 1.0 and was spotted (left-most column). The diluted culture was further serially diluted 10-fold and spotted four times; the dilution was repeated until the last column on the right. The dilution is indicated by the tapering triangle bar on the top. Cells were then spotted onto solid double selective agar plates containing 2% glucose (negative control), 2% galactose (positive control), or 3% glycerol and 1% ethanol, and incubated for 2–5 days.

neurodegeneration) has a reduced media glucose content of 0.5%. Under both conditions with all four genes, no toxicity was observed (**Figure 7**).

1.3: To assess the toxicity, aggregate formation and expression level of IntTox and HiTox α -synuclein under non-galactose conditions using integrated *GAL3_{A368V}* allele.

GAL3_{A368V} induces the GAL1 promoter in the presence of 0.1% glucose and raffinose.

We integrated the *GAL3_{A368V}* allele into the yeast genome and performed β -galactosidase assays. We chose conditions that had not been tested previously. In the calorie restriction condition, since 0.5% glucose did not allow for *GAL1* promoter induction, we now reduced the amount of glucose to 0.1%. In addition, we tested raffinose and nitrogen starvation. Raffinose is an alternate carbon source that undergoes partial oxidative phosphorylation. *GAL3_{A368V}* significantly increased β -galactosidase activity under calorie restriction ($p = 0.01$), raffinose ($p < 0.0001$), and nitrogen starvation ($p < 0.0001$) compared to the vector (**Figure 8**). Thus, we concluded that *GAL3_{A368V}* can induce *GAL1* promoter in non-galactose conditions provided the glucose content is relatively low.

IntTox and HiTox α -syn overexpression cause toxicity under non-galactose conditions.

Since *GAL1* promoter induction was observed in the above conditions, we next tested the IntTox and HiTox α -syn cellular phenotypes in these conditions. Glucose served as the negative control and galactose, the positive control (**Figure 9**). Neither IntTox nor HiTox α -syn induced toxicity under calorie restriction condition. We know that *GAL1* promoter is induced in this condition (**Figure 8**). Both IntTox and HiTox α -syn showed toxicity under raffinose and nitrogen starvation. The addition of nitrogen starvation to raffinose caused suppression of IntTox α -syn-induced toxicity. Of these findings, the most

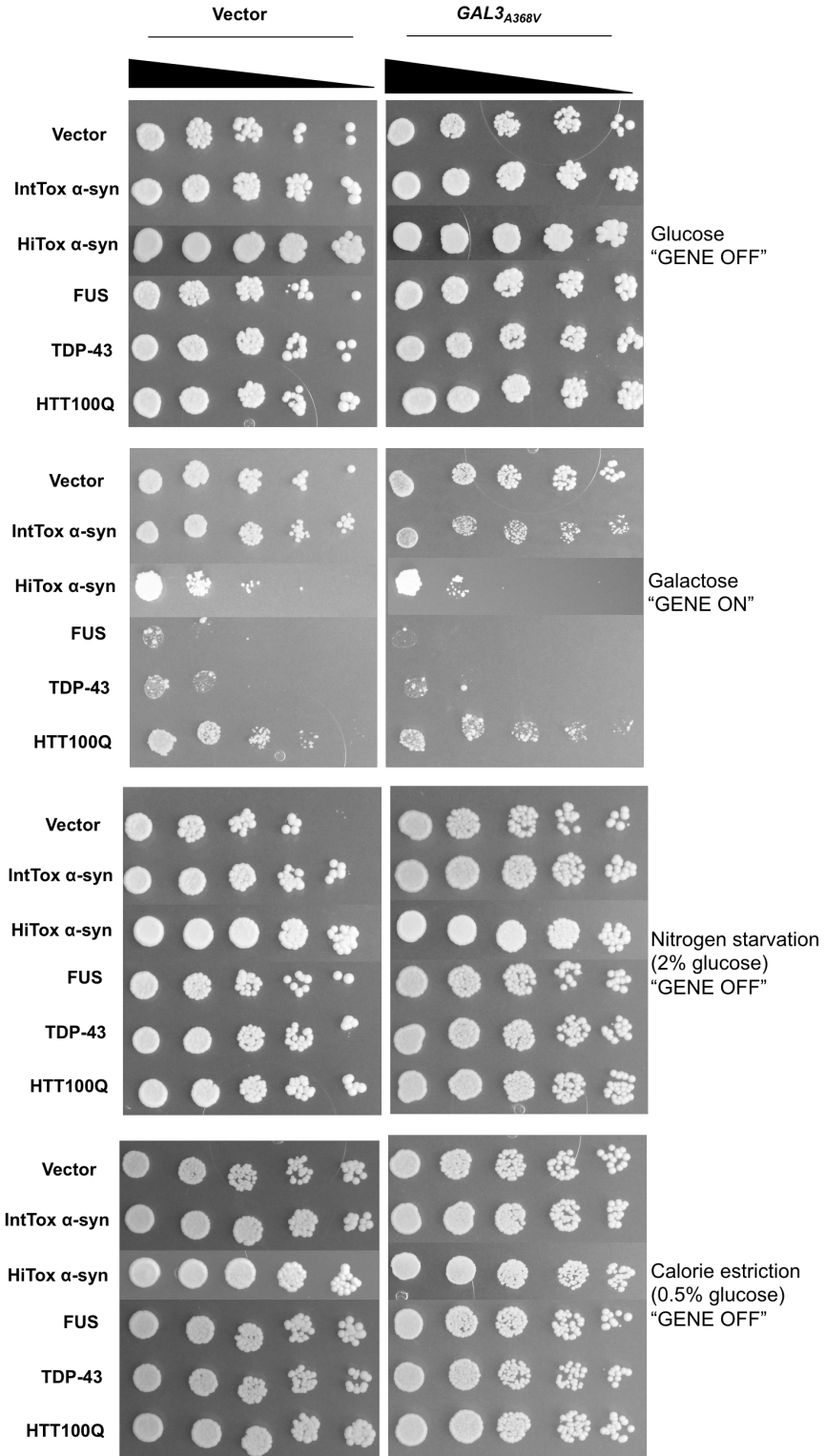


Figure 7. $GAL3_{A368V}$ does not induce toxicity of neurodegenerative disease-related genes in the presence of glucose.

Single diploid yeast colonies containing both empty vector (pRS303-GAL), IntTox and HiTox α -syn, FUS, TDP-43 or HTT103Q (W303 *MATa* strain) and empty vector (pRS415-GPD) or *GAL3* alleles (W303 *MAT α* strain) were grown overnight in double selective 2% glucose media. The culture was washed twice with distilled water and diluted to an OD₆₀₀ of 1.0 and was spotted (left-most column). The diluted culture was further serially diluted 10-fold and spotted four times; the dilution was repeated until the last column on the right. The dilution is indicated by the tapering triangle bar on the top. Cells were then spotted onto solid double selective agar plates containing 2% glucose (negative control), 2% galactose (positive control), nitrogen starvation (2% glucose) or calorie restriction (0.5% glucose) and incubated for 2–3 days.



Figure 8. *GAL3_{A368V}* induces the *GAL1* promoter under calorie restriction and nitrogen starvation conditions.

GAL3_{A368V} was integrated into the yeast genome using a high efficiency yeast transformation protocol. Single diploid yeast colonies containing both β -galactosidase enzyme (W303 *MAT α* strain) and *GAL3_{A368V}* (W303 *MAT α* strain) were grown overnight in double selective 2% glucose media. The culture was washed twice with distilled water and inoculated into five different media lacking histidine (gene) and leucine (*GAL3* vector) starting at OD₆₀₀ 0.1: 2% glucose (negative control), 2% galactose (positive control), calorie restriction (0.1% glucose), 2% raffinose, and nitrogen starvation (2% raffinose). The culture was grown until mid-log phase when the cells were isolated, at which point the assay was performed. The intensity of the yellow color was measured at A₄₂₀. β -galactosidase activity of *GAL3_{A368V}* was compared to the empty vector in each condition by two-way ANOVA. * $p < 0.05$ and, hence, significantly different compared to the control. N.S, no significant difference compared to control.

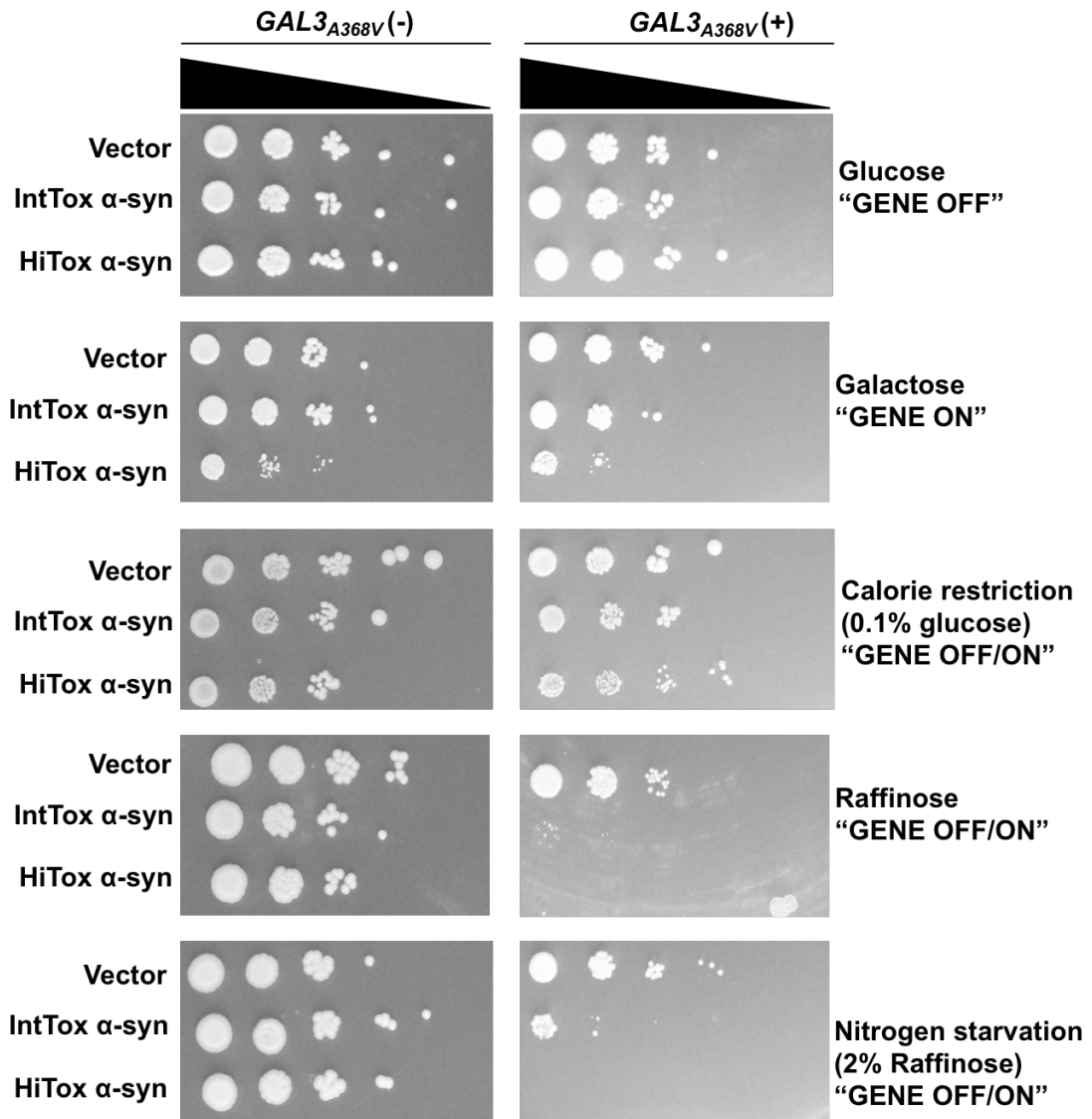


Figure 9. IntTox and HiTox α -synuclein overexpression cause toxicity under non-galactose conditions.

Single diploid yeast colonies containing both empty vector (pRS303-GAL), IntTox α -syn, or HiTox α -syn (W303 *MAT α* strain) and empty vector (pRS415-GPD) or *GAL3_{A368V}* (W303 *MAT α* strain) were grown overnight in double selective 2% glucose media. The culture was washed twice with distilled water and diluted to an OD₆₀₀ of 1.0 and was spotted (left-most column). The diluted culture was further serially diluted 10-fold and

spotted four times; the dilution was repeated until the last column on the right. The dilution is indicated by the tapering triangle bar on the top. Cells were then spotted onto solid double selective agar plates containing 2% glucose (negative control), 2% galactose (positive control), calorie restriction (0.1% glucose), 2% raffinose, and nitrogen starvation (2% raffinose), and incubated for 2–7 days.

interesting is the absence of toxicity in HiTox α -syn cultures in calorie restriction condition, while toxicity was present in IntTox α -syn cultures containing raffinose, as these findings are in stark contrast to those previously observed for galactose.⁶⁵ Hence, this study highlights the necessity of studying α -syn in non-galactose conditions and validates the use of *GAL3_{A368V}* performing the same.

IntTox and HiTox α -syn toxicity do not correlate with the presence of aggregates under non-galactose conditions. Toxicity of IntTox and HiTox α -syn often correlates with the presence of aggregates in yeast.⁶⁵ Since we observed toxicity of the two strains in the spotting assay, we next sought to examine α -syn aggregates under the same conditions. Under calorie restriction, no IntTox α -syn aggregates were observed, however, those of HiTox α -syn were evident (**Figure 10 and 11**). Under raffinose and nitrogen starvation conditions, we saw similar patterns with aggregates only being formed by HiTox α -syn, not IntTox α -syn (**Figure 10 and 11**). When comparing the results of the spotting assay and microscopic aggregates, two interesting findings become apparent. First, although IntTox α -syn was toxic under raffinose conditions, no aggregates were formed. Second, HiTox α -syn was not toxic under calorie restriction but aggregates were formed. Thus, non-galactose conditions serve to define a new paradigm shift where toxicity produced by α -syn does not necessarily correlate with the presence of aggregates. The next logical question was whether the expression levels of α -syn under non-galactose conditions are responsible for the observed differences in toxicity and aggregation.

Although verification of expression levels across growth conditions require further experimental repeats, IntTox α -syn did not seem to exhibit different expression

levels in the non-galactose growth conditions compared to that in galactose. HiTox α -syn seemed to show higher expression levels in calorie restriction, raffinose and nitrogen starvation conditions (**Figure 12**). In either situation, the results do not explain the increased toxicity of IntTox α -syn in raffinose conditions nor the reduced toxicity of HiTox α -syn in calorie restriction conditions. It, therefore, appears that the toxicity is not mediated by protein expression levels.

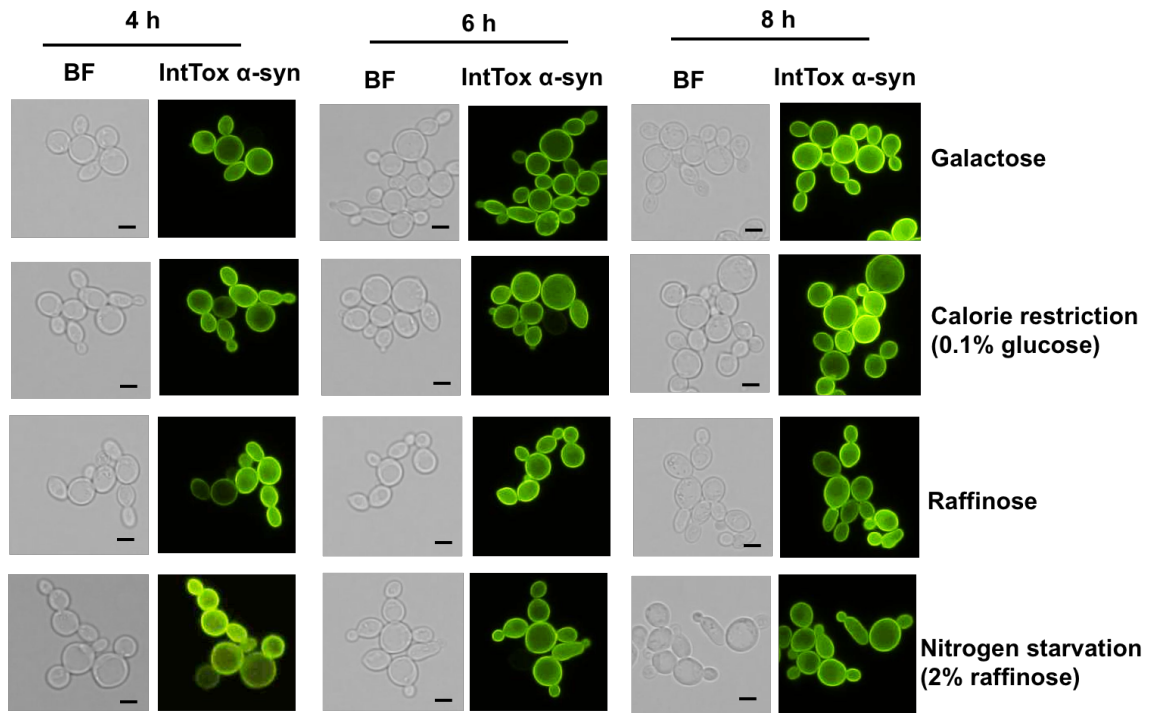


Figure 10. IntTox α -synuclein does not form aggregates under non-galactose conditions.

Single diploid yeast colonies containing both IntTox α -syn (W303 *MAT α* strain) and *GAL3_{A368V}* (W303 *MAT α* strain) were grown overnight in double selective 2% glucose media. The culture was washed twice with distilled water and diluted to an OD₆₀₀ of 1.0 and was grown in double selective media of four types: 2% galactose, calorie restriction (0.1% glucose), raffinose and nitrogen starvation (2% raffinose), and induced for 4, 6 and 8 h. At each time point, the cells were isolated and 3 μ L of suspension was placed on a glass slide and viewed under the bright field and YFP channel. Bar: 5 μ m. BF, bright field.

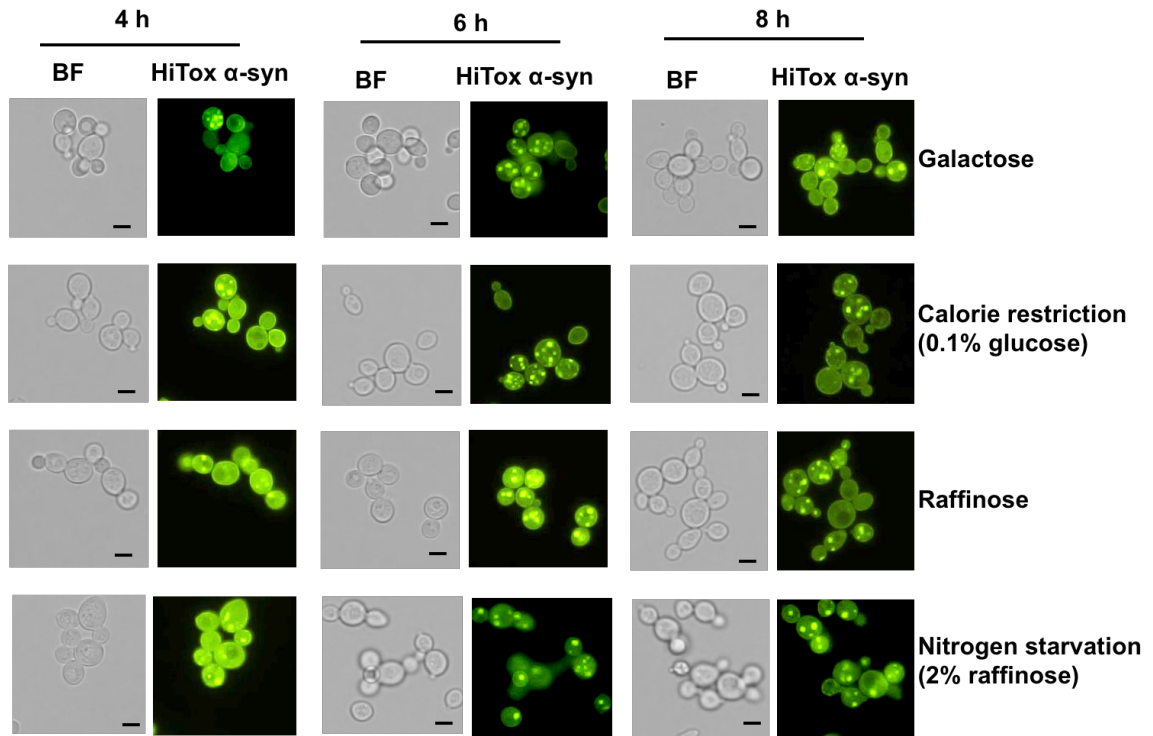


Figure 11. HiTox α -synuclein forms aggregates under non-galactose conditions.

Single diploid yeast colonies containing both HiTox α -syn (W303 *MAT α* strain) and *GAL3_{A368V}* (W303 *MAT α* strain) were grown overnight in double selective 2% glucose media. The culture was washed twice with distilled water and diluted to an OD₆₀₀ of 1.0 and was grown in four different types of double selective media: 2% galactose, calorie restriction (0.1% glucose), raffinose and nitrogen starvation (2% raffinose), and induced for 4, 6 and 8 h. At each time point, the cells were isolated and 3 μ L of suspension was placed on a glass slide and viewed under the BF and YFP channels. Scale bar: 5 μ m. BF, bright field.

Figure 12. HiTox α -synuclein expression increases while IntTox α -synuclein expression is unaffected under non-galactose conditions.

Single diploid yeast colonies containing both IntTox α -syn, or HiTox α -syn (W303 *MATa* strain) and empty vector (pRS415-GPD) or *GAL3_{A368V}* (W303 *MATa* strain) were grown overnight in double selective 2% glucose media. The culture was washed twice with distilled water and diluted to an OD₆₀₀ of 1.0 and was grown in four different types of double selective media: 2% galactose, calorie restriction (0.1% glucose), raffinose and nitrogen starvation (2% raffinose). The cultures were then induced for 6 h after which point the protein was extracted. *SNCA* encoding IntTox α -syn, or HiTox α -syn were tagged with YFP and, hence, an antibody against GFP was used. PGK1 was used as the loading control protein. (A) shows the blotting images and (B) shows quantification of the bands. Image quantification was performed using ImageJ. The experiment was repeated twice, and the bar graphs represent mean + SE. Protein expression in galactose condition served as reference values.

IV. AIM 2: TO EXAMINE THE ROLE OF MITOCHONDRIA IN α -SYNUCLEIN TOXICITY UNDER GLYCEROL-ETHANOL

Rationale

When α -syn was induced under non-galactose conditions, variations were observed in the toxicity levels, presence of aggregates and protein expression. For this study, we focused on the glycerol-ethanol condition, which is a non-fermentable carbon source for yeast and thus requires a fully functional mitochondria for survival. We know that mitochondrial dysfunction causes Parkinson's disease, and α -syn affects the mitochondria by inhibiting complex I activity and causing mitochondrial fragmentation. Since we observed higher toxicity of α -syn in glycerol-ethanol compared to galactose, we sought to better understand the underlying mechanisms related to this new phenotype. Since mitochondria appears to be vital in glycerol metabolism, we focused on studying the respiratory competency of the cells, mitochondrial structure and membrane potential, as well as ROS production.

Experimental design

Spotting assay. The strains that were used include NoTox α -syn (1 copy of *SNCA*), IntTox α -syn (4–5 copies of *SNCA*), and HiTox α -syn (> 6 copies of *SNCA*). We also assessed the toxicity of two ALS disease-associated genes: *FUS* and *TDP-43*. For this Aim, *SNCA*, *FUS*, and *TDP-43* were transformed into the W303 *MATa* of yeast (**Table 1**), and *GAL3_{A368V}* was transformed into the opposite mating type W303 *MAT α* . Without

mating, we also spotted the genes on galactose and glycerol-ethanol plates under haploid conditions (without *GAL3_{A368V}*).

Measurement of aggregates and examination of mitochondria. We used IntTox α -syn strain tagged with YFP for microscopic examination of aggregates; while pMitoLoc was used to simultaneously examine total and healthy mitochondria. For both measurements, diploid yeast strains containing IntTox α -syn and *GAL3_{A368V}* were precultured in 2% glucose medium overnight. Cultures with an OD₆₀₀ between 8–14 were then washed and resuspended in selective galactose or glycerol-ethanol medium. The starting OD₆₀₀ was 1.0 and the suspended medium was incubated for 3–18 h. Aggregates were visualized with the YFP channel and mitochondria were visualized with the CFP and Tx Red channels.

Measurement of ROS. After induction for 3, 6 and 18 h, cells were isolated and incubated with DHE for 20 min. The amount of red fluorescence was directly proportional to the amount of ROS produced. Diploid yeast strains containing IntTox α -syn and *GAL3_{A368V}* were used.

Mitochondrial targeting of α -synuclein. We used a split GFP system for this experiment.⁹⁹ *SNCA* was cloned with the 11th β -strand of GFP (GFP₁₁). If *SNCA* (cloned to GFP₁₁) reconstitutes with GFP₁₋₁₀, which contain mitochondrial targeting sequences, we would expect to see green fluorescence emitted from the reconstituted GFP.

Results

2.1: To test the toxicity and aggregation of IntTox α -synuclein under glycerol-ethanol

IntTox α -syn is toxic under glycerol-ethanol but not under galactose condition with similar expression. A single copy of *SNCA* (NoTox α -syn), 4–5 copies of *SNCA* (IntTox α -syn), and > 6 copies of *SNCA* (HiTox α -syn), *FUS* and *TDP-43* (**Table 1**) were transformed into the *MATa* yeast strain W303; while *GAL3_{A368V}*, was transformed into the *MAT α* yeast strain. The toxicity phenotypes of the α -syn diploid strains were detected by spotting assays under galactose and glycerol-ethanol agar plates. NoTox α -syn did not exhibit toxicity under either condition (**Figure 13**). Alternatively, IntTox α -syn was toxic under the glycerol-ethanol condition but not toxic under the galactose condition; while HiTox α -syn, *FUS* and *TDP-43* were toxic under both conditions.

We also tested all genes under haploid conditions without *GAL3_{A368V}* to better understand (i) if the glycerol-ethanol condition alone is toxic to the cells and (ii) if a phenotypic difference was observable for the genes, between the haploid and diploid strains. Results show that without *GAL3_{A368V}*, no induction under glycerol-ethanol conditions was observed (**Figure 14**); and no toxicity was induced by any of the genes. Further, compared to diploid strain spotting, IntTox α -syn exhibited a unique phenotype i.e. higher toxicity in the haploid strain. Given these two interesting phenotypes, we decided to employ only IntTox α -syn in subsequent experiments.

The OD₆₀₀ measurement during the induction of IntTox α -syn in liquid media over time corroborated the findings of the spotting assay. Under the glycerol-ethanol condition IntTox α -syn was found to be more toxic than galactose (**Figure 15**). As a haploid strain, IntTox α -syn showed toxicity in galactose (blue dotted line), however, no induction was observed and thus, no toxicity was present in the glycerol-ethanol (orange dotted line). To further verify our findings, we wanted to examine if the expression of

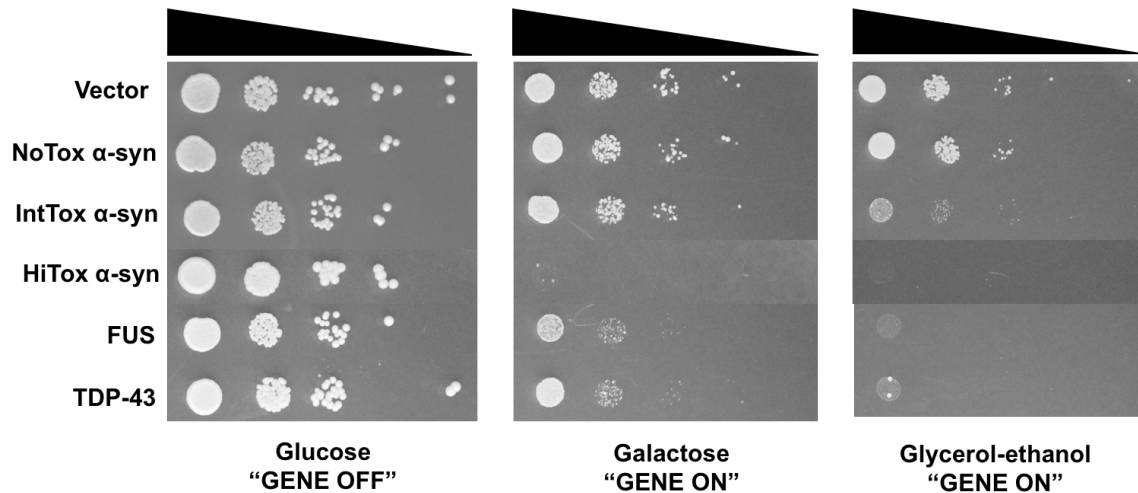


Figure 13. IntTox α -synuclein is toxic under glycerol-ethanol but not under galactose.

Single diploid yeast colonies containing both empty vector (pRS303-GAL), NoTox α -syn, IntTox α -syn, HiTox α -syn, FUS, or TDP-43 (W303 *MAT α* strain) and empty vector (pRS415-GPD) or *GAL3* alleles (W303 *MAT α* strain) were grown overnight in double selective 2% glucose media. The culture was washed twice with distilled water and diluted to an OD₆₀₀ of 1.0 and was spotted (left-most column). The diluted culture was further serially diluted 5-fold and spotted four times; the dilution was repeated until the last column on the right. The dilution is indicated by the tapering triangle bar on the top. Cells were then spotted onto solid double selective agar plates containing 2% glucose (negative control), 2% galactose (positive control), or 3% glycerol and 1% ethanol, and incubated for 2–5 days.

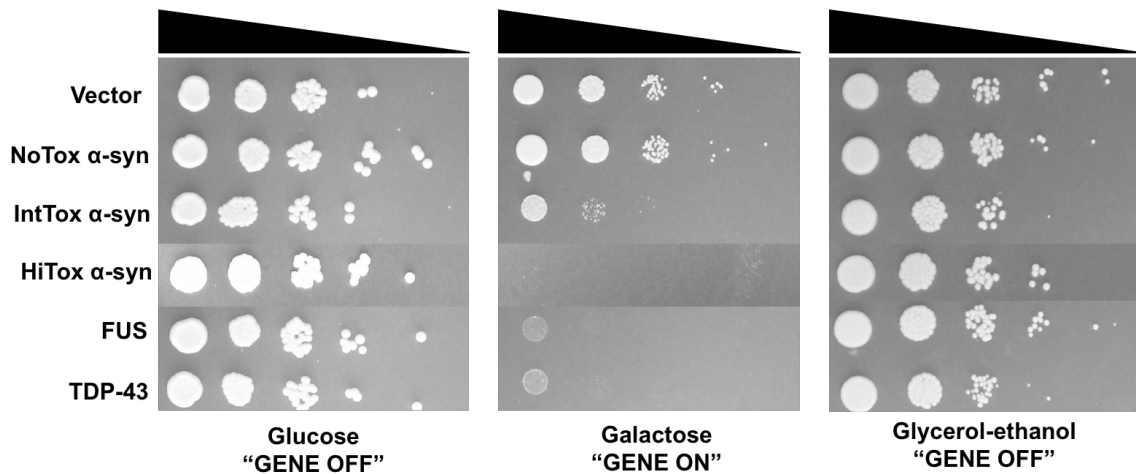


Figure 14. IntTox α -synuclein is toxic under galactose in haploid condition.

Single haploid yeast colonies containing empty vector (pRS303-GAL), NoTox α -syn, IntTox α -syn, HiTox α -syn, FUS, or TDP-43 (W303 *MATa* strain) was grown overnight in double selective 2% glucose media. The culture was washed twice with distilled water and diluted to an OD_{600} of 1.0 and was spotted (left-most column). The diluted culture was further serially diluted 5-fold and spotted four times; the dilution was repeated until the last column on the right. The dilution is indicated by the tapering triangle bar on the top. Cells were then spotted onto solid double selective agar plates containing 2% glucose (negative control), 2% galactose (positive control), or 3% glycerol and 1% ethanol, and incubated for 2 – 5 days.

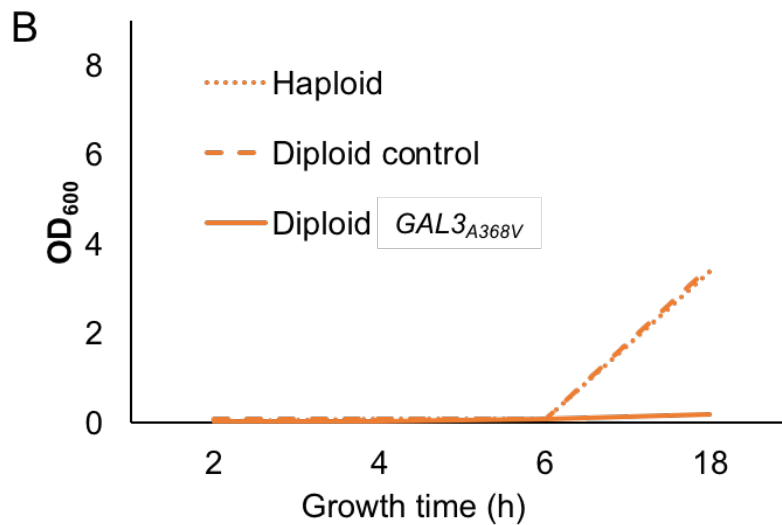
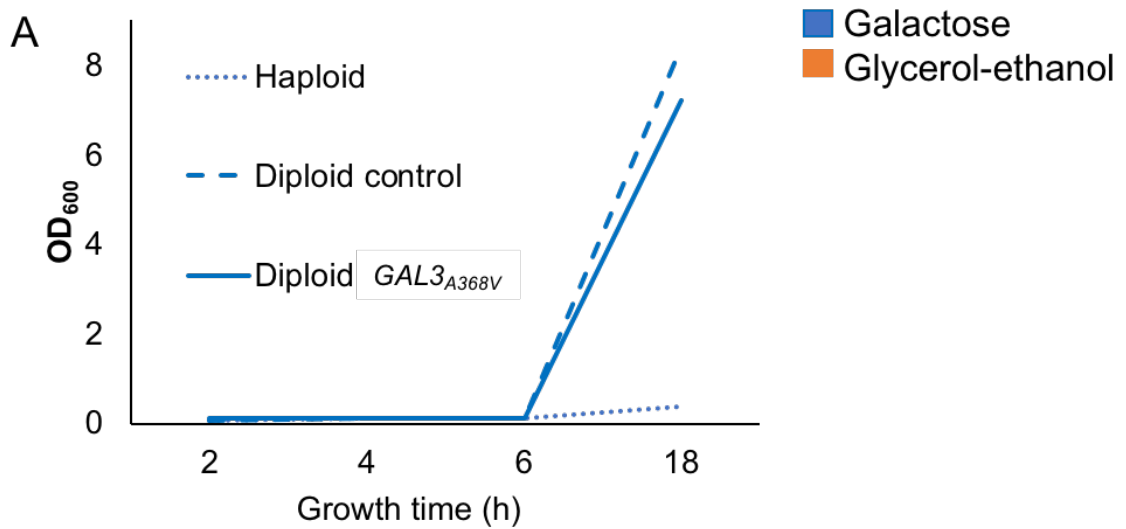


Figure 15. IntTox α -synuclein is toxic under glycerol-ethanol but not under galactose in diploid yeast strains.

Three yeast strains were used: IntTox α -syn without *GAL3_{A368V}* (haploid), IntTox α -syn with empty vector (pRS303-GAL) (diploid control) and IntTox α -syn with *GAL3_{A368V}* (diploid *GAL3_{A368V}*). Single haploid or diploid yeast colonies were grown overnight in double selective 2% glucose media. The culture was washed twice with distilled water

and diluted to an OD₆₀₀ of 0.1 and resuspended in selective 2% galactose (A) or 3% glycerol with 1% ethanol (B) liquid media. The OD₆₀₀ was measured at 2, 4, 6 and 18 h.

IntTox α -syn was higher in glycerol-ethanol. IntTox α -syn protein levels were similar under both conditions (**Figure 16A, B**). Thus, glycerol-ethanol increased the toxicity of neurodegenerative disease-associated genes. However, fluctuations in protein expression levels was not responsible for the increased toxicity of IntTox α -syn.

IntTox α -syn forms aggregates under glycerol-ethanol and not under galactose. Our next objective was to examine the aggregate formation of IntTox α -syn in both the conditions. IntTox α -syn was tagged with YFP and the diploid strain was induced for 4, 6, 8, and 18 h. Under the galactose condition, very few aggregates of IntTox α -syn were observed before 8 h (**Figure 17A**), and less than 5% of the cells (**Figure 17B**) contained aggregates at 18 h. Alternatively, under the glycerol ethanol condition, the aggregates were visible as early as 6 h and increased steadily until 18 h of induction, at which point, approximately 55% of the cells contained aggregates and this percentage was significantly higher than that in galactose ($p = 0.0001$).

We also examined the aggregates in the haploid strain and found that under galactose condition after 18 h of induction, the proportion of cells with aggregates was approximately 45% (**Figures 18 A and B**); while under the glycerol-ethanol condition, no induction of IntTox α -syn was observed. Under galactose, the diploid control and diploid *GAL3_{A368V}* had significantly lower (both $p < 0.04$) number of aggregates compared to haploid condition. There was no difference ($p = 0.16$) between diploid glycerol-ethanol and haploid galactose conditions.

2.2: To determine the mechanisms of IntTox α -synuclein toxicity under glycerol-ethanol

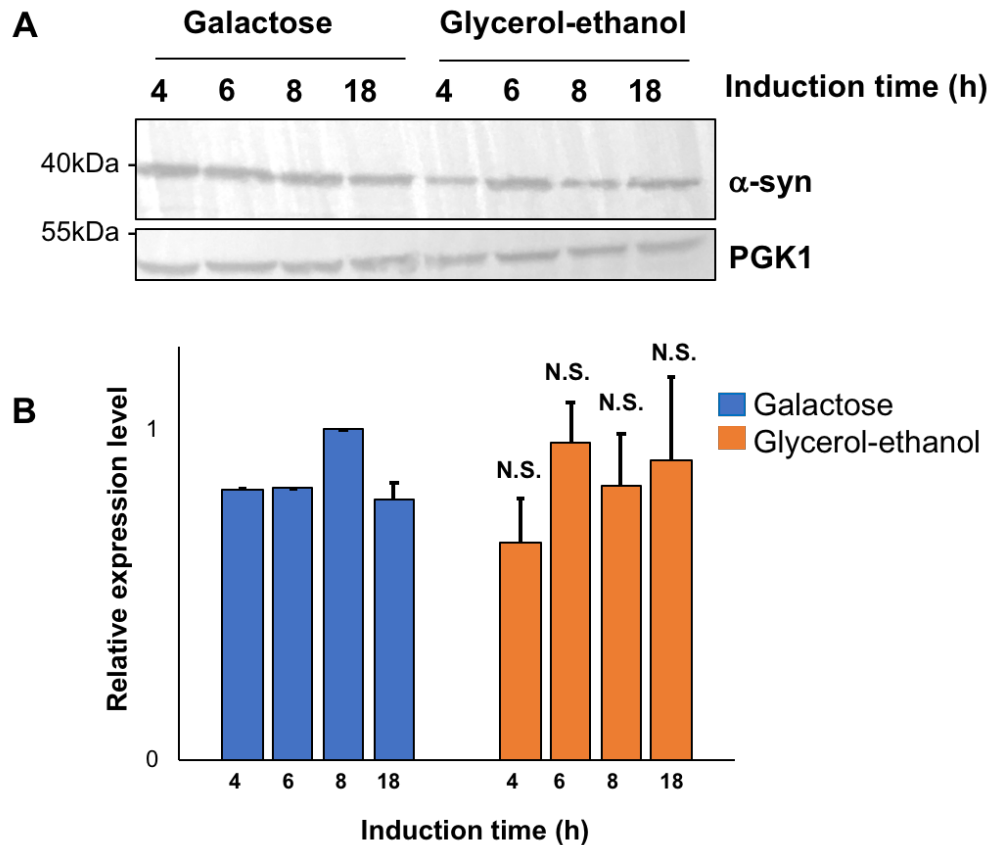


Figure 16. Protein expression levels of IntTox α -synuclein do not differ between galactose and glycerol-ethanol conditions.

Single diploid yeast colonies containing both IntTox α -syn (W303 *MATa* strain) and *GAL3_{A368V}* (W303 *MATa* strain) were grown overnight in double selective 2% glucose media. The culture was washed twice with distilled water and diluted to an OD₆₀₀ of 1.0 and was grown in double selective 2% galactose and 3% glycerol with 1% ethanol. Cells from cultures with an OD₆₀₀ of 1.0 (1×10^7 cells) were isolated at 4, 6, 8 and 18 h of induction and the protein was extracted. *SNCA* encoding IntTox α -syn was tagged with YFP and an antibody against GFP was used. The loading control protein used was *PGK1*. (A) shows the blotting images and (B) shows quantification of the bands. Image

quantification was performed using ImageJ. The experiment was repeated three times, and the bar graphs represent mean + SE. Protein expression at 8 h of induction in galactose was used as the reference value. N.S., not significantly different compared to protein levels at 8 h galactose.

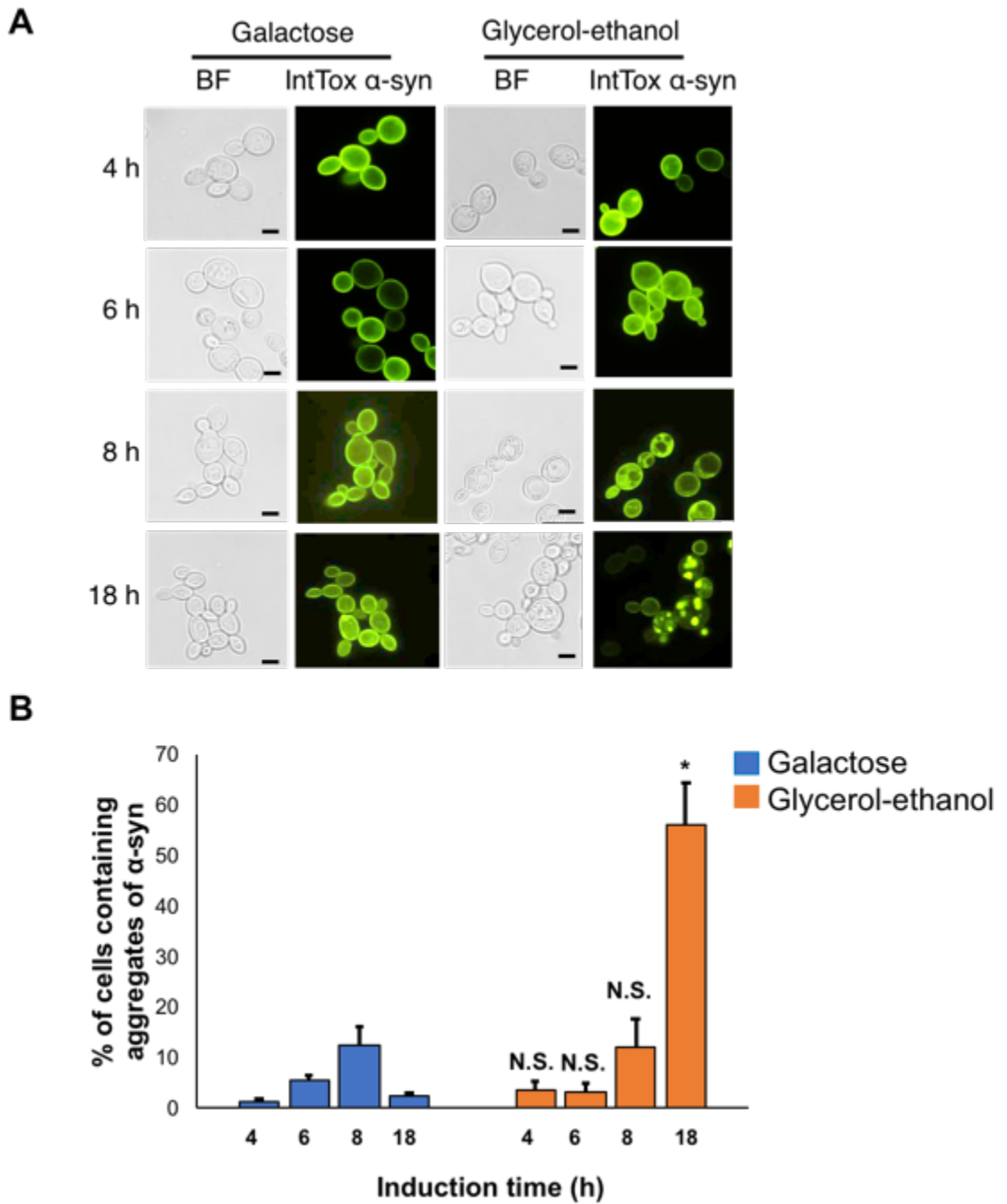


Figure 17. Aggregates of IntTox α -synuclein are elevated under glycerol-ethanol compared to galactose.

Single diploid yeast colonies containing both IntTox α -syn (W303 *MAT α* strain) and *GAL3_{A368V}* (W303 *MAT α* strain) were grown overnight in double selective 2% glucose media. The culture was washed twice with distilled water and diluted to an OD₆₀₀ of 1.0 and was grown in double selective 2% galactose and 3% glycerol with 1% ethanol media, and induced for 4, 6, 8 and 18 h. At each time point, the cells were isolated and 3 μ L of suspension was placed on a glass slide and aggregates were viewed under the YFP channel. Scale bar: 5 μ m (A). Quantification of the aggregates (B) were performed using ImageJ and verified by manual counting. The experiments were repeated three times and a minimum of 200 cells were counted for each condition and timepoint. Bars represent mean + SE. Repeated measures ANOVAs with a random subject effect was used to compare the percentage of cells with α -syn aggregates in galactose and glycerol-ethanol at each time points. BF, bright field. * $p < 0.05$ and hence, significantly different compared to galactose. N.S., not significant.

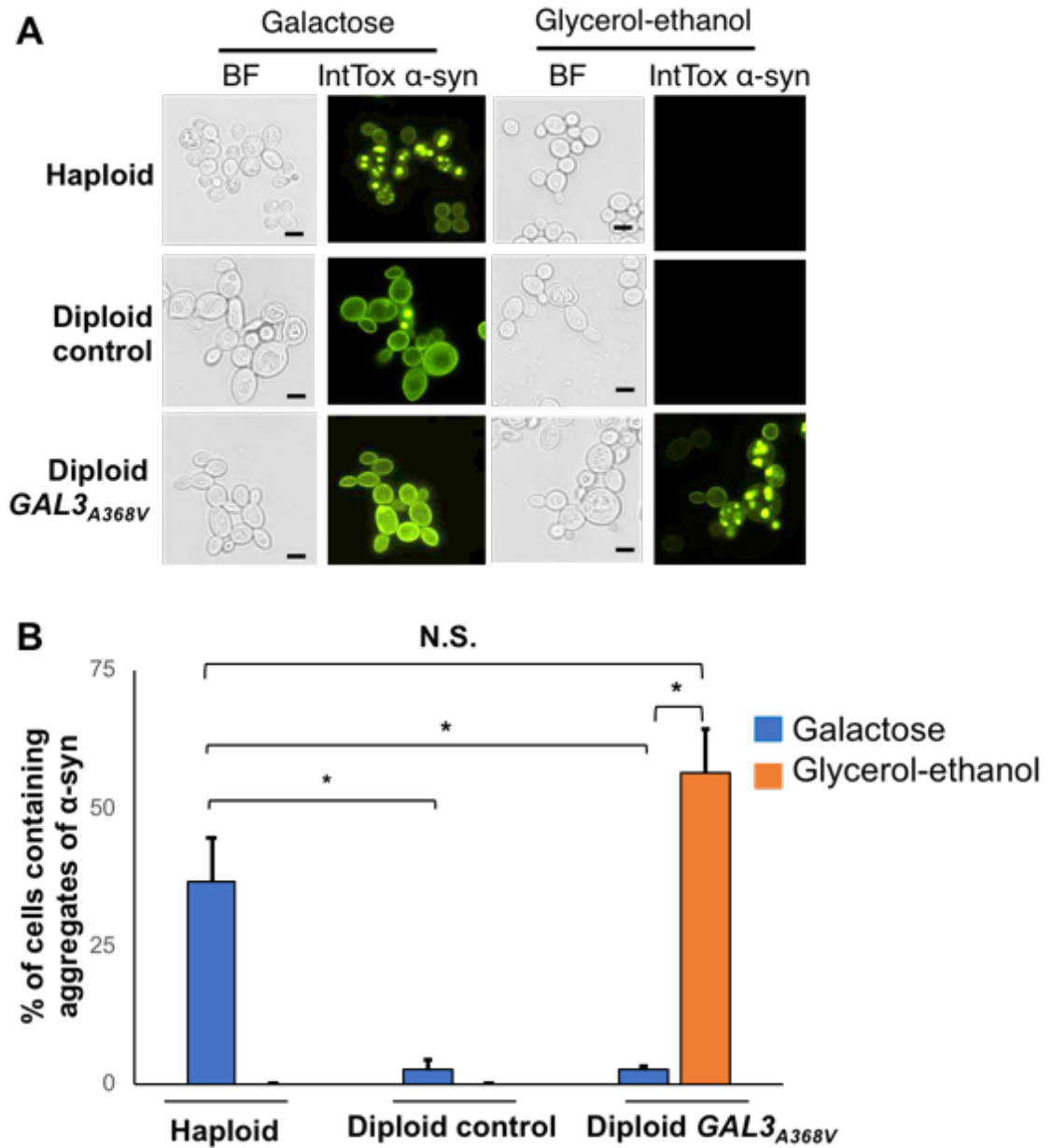


Figure 18. Aggregates of IntTox α -synuclein are elevated in haploid galactose and diploid glycerol-ethanol yeast strains.

Three yeast strains were used: IntTox α -syn without $GAL3_{A368V}$ (haploid), IntTox α -syn with empty vector (pRS303-GAL) (diploid control) and IntTox α -syn with $GAL3_{A368V}$ (diploid $GAL3_{A368V}$). Single haploid or diploid yeast colonies were grown overnight in

double selective 2% glucose media. The culture was washed twice with distilled water and diluted to an OD₆₀₀ of 1.0 and was grown in double selective 2% galactose and 3% glycerol with 1% ethanol media and induced for 18 h. Cells were isolated and 3 μ L of suspension was placed on a glass slide. Aggregates were viewed under the YFP channel. Scale bar: 5 μ m (A). Quantification of the aggregates (B) was performed using ImageJ and verified by manual counting. The experiments were repeated three times and a minimum of 200 cells were counted for each condition and timepoint. Bars represent mean + SE. Two-way ANOVA was used to compare the percentage of cells with α -syn aggregates in galactose and glycerol-ethanol conditions. The assumption of constant variance was violated, due to two of the groups having values of zero. Satterthwaite's approximation was used to adjust the degrees of freedom to account for this violation. Natural log transformation was used for the data before analysis. Since the natural log of zero is undefined, a value of 1 was added to all observations. All results are in terms of natural log (response value + 1). BF, bright field; * p < 0.05; N.S., not significant.

IntTox α-syn reduces both viability and respiratory competency only under glycerol-ethanol. We first sought to quantify the number of viable and respiratory-competent cells in each condition to better understand the increased toxicity in glycerol-ethanol. The experiment was performed as explained under Methods (Quantification of viable and respiratory-competent cells). Respiratory competency refers to cells having fully functional mitochondria and the capacity to grow in glycerol-ethanol condition. We expected that IntTox α-syn would induce dysfunction of the mitochondria irrespective of the growth condition. Since galactose is a fermentable carbon source that requires functional mitochondria for viability, we hypothesized that under galactose, viability would not be reduced, however, the respiratory competency would be.

Figure 19 A and B shows that the viability of the IntTox α-syn was not affected in galactose however, it was significantly ($p = 0.009$ for 6 h and $p = 0.04$ for 18 h) reduced in glycerol-ethanol in the presence of IntTox α-syn. Conversely to what we expected, respiratory competency was lower but was not significantly reduced by IntTox α-syn in galactose (**Figure 19 C**), however, was reduced in glycerol-ethanol (**Figure 19 D**). We analyzed these results for statistically significant interactions between gene and the time required before differences were observed between IntTox α-syn and the control; however, we did not observe any interactions, thereby ruling out potential skewed results. Hence, we concluded that IntTox α-syn affects viability and respiratory competency only under glycerol-ethanol.

Mitochondria show dense morphology under glycerol-ethanol and disrupted membrane potential signal under both galactose and glycerol-ethanol in the presence of α-syn. Using pMitoLoc, healthy mitochondria can be identified via the co-localization

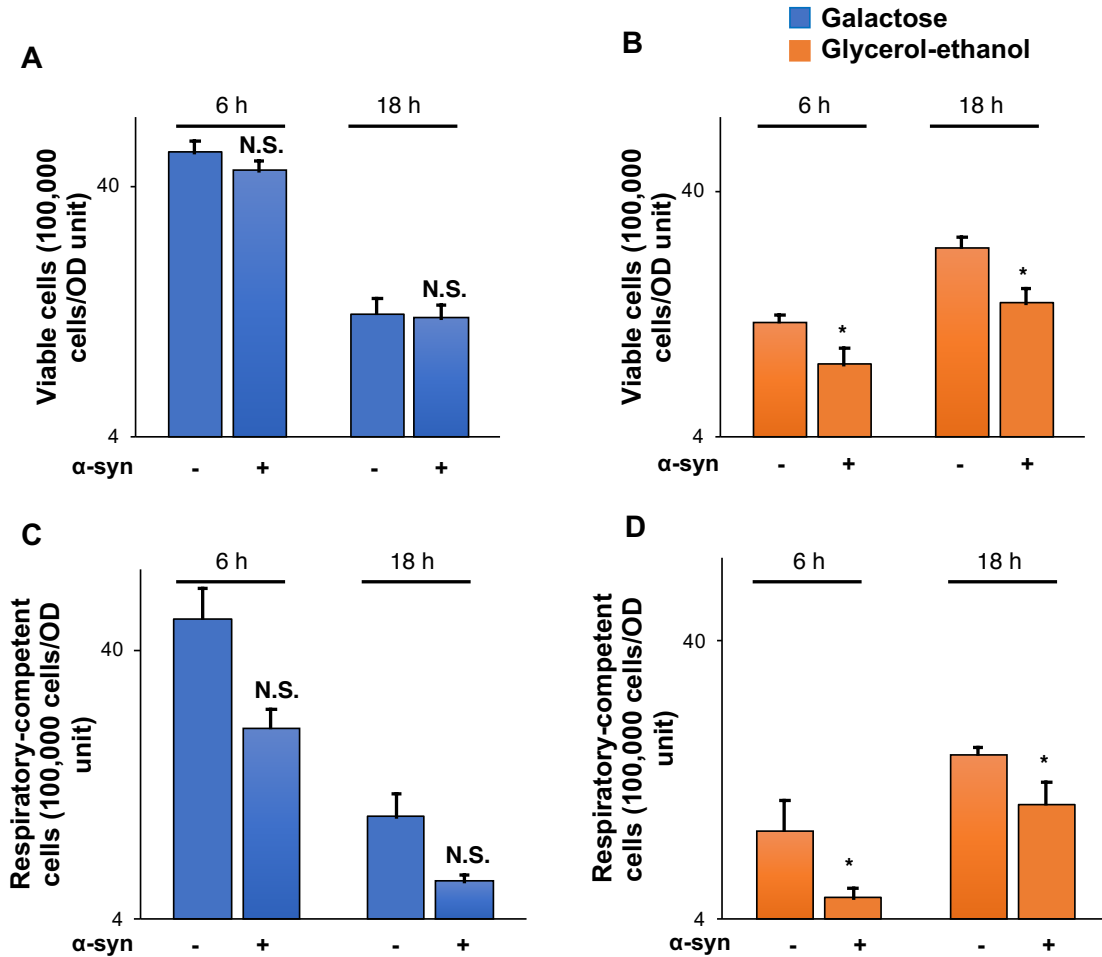


Figure 19. IntTox α -synuclein reduces the number of viable and respiratory-competent cells only under glycerol-ethanol.

Single diploid yeast colonies containing both control (pRS303-GAL) or IntTox α -syn (W303 *MAT α* strain) and *GAL3_{A368V}* (W303 *MAT α* strain) were grown overnight in double selective 2% glucose media. The culture was washed twice with distilled water and diluted to an OD₆₀₀ of 1.0 and was grown in double selective 2% galactose and 3% glycerol with 1% ethanol media, and induced for 6 and 18 h. At an OD₆₀₀ of 1.0 cells were harvested and diluted; for α -syn strain, 100 μ L each of 10⁻⁴ dilution and 10⁻⁵ dilution, and for the control strain, 100 μ L of the 10⁻⁵ dilution from both medias were

plated on YPD and YPGE agar plates to determine the numbers of viable (A) and respiratory-competent cells (B), respectively. Agar plates were incubated for 2 – 3 days and single colonies were counted. For α -syn strain, the dilution that provided colony counts closer to 100 was chosen. The colony counts for both strains were multiplied by the respective dilution factor and used for statistical analysis. Type III tests of fixed effects were used to analyze the difference between α -syn and the control at each timepoint. A natural log transformation was performed to correct for violation to the assumption of constant variance between groups. * $p < 0.05$; Y-axis, logarithmic scale; N.S., not significant; OD, optical density.

of teal and mCherry; whereas unhealthy mitochondria are identified as having reduced or no co-localization. Moreover, in unhealthy mitochondria mCherry will diffuse throughout the cytoplasm. The lower the co-localization, the lower was the membrane potential. This is due to the inability of preCOX4-mCherry to enter the mitochondria when the membrane potential is lower, causing it to instead disperse throughout the cytoplasm. As shown in **Figure 20**, IntTox α -syn induced the formation of dense mitochondrial structures rather than as thread-like elongated structures under glycerol-ethanol. This may be due to large IntTox α -syn aggregates in glycerol-ethanol and thus, the mitochondrial structures are more closely packed together, compared to galactose condition. We also observed the disrupted membrane potential signal, i.e. the reduced overlap of teal and red both under galactose and glycerol-ethanol. Further mitochondrial structure specific examination is required to confirm the results of disrupted membrane potential signal.

α -syn increases the percentage of cells that accumulate ROS under both conditions.

We examined ROS production at 3, 6, and 18 h of induction in both conditions. ROS has been shown to increase α -syn aggregation while α -syn increases ROS production. Hence, we hypothesized that under both conditions, increased ROS production would be observed, however, more so under glycerol-ethanol condition since in glycerol-ethanol oxidative phosphorylation, the major source of ROS production, would be elevated in this condition. Further, since IntTox α -syn is more toxic in glycerol-ethanol; the toxicity may be mediated via increased ROS production. We first performed quantitative assessment of ROS using a plate reader. We observed that IntTox α -syn increased ROS levels at 6 h ($p = 0.04$) and 18 h ($p < 0.001$) in galactose and at 18 h ($p = 0.002$) in glycerol-ethanol compared to galactose (**Figure 21**). Microscopic examination did not reveal increased

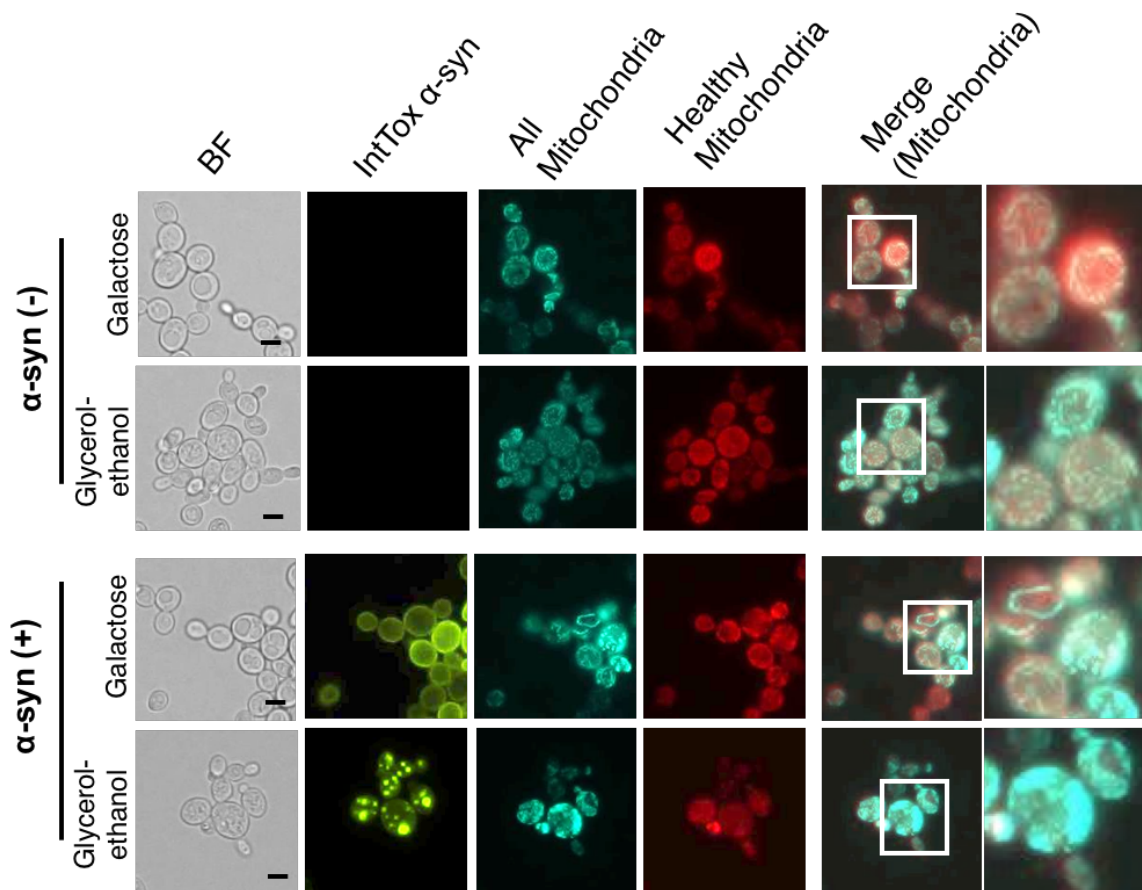


Figure 20. Mitochondria show dense morphology under glycerol-ethanol and disrupted membrane potential signal under both galactose and glycerol-ethanol in the presence of α -synuclein.

Single diploid yeast colonies containing both vector (pRS303-GAL) or IntTox α -syn (W303 *MAT α* strain) and *GAL3_{A368V}* (W303 *MAT α* strain) were grown overnight in double selective 2% glucose media. The vector and α -syn strain were transformed with pMitoLoc which contains two (preSU9-CFP and preCOX4-mCherry) tags with mitochondrial targeting sequences. Teal represents all mitochondria and red represents healthy mitochondria. The culture was washed twice with distilled water and diluted to an OD_{600} of 1.0 and was grown in double selective 2% galactose and 3% glycerol with 1%

ethanol media, and induced for 18 h. At each time point, the cells were isolated and 3 μ L of suspension was placed on a glass slide and aggregates were viewed under the YFP, CFP and Tx Red channels. *SNCA* encoding α -syn was tagged with YFP. CFP images were obtained by Z-stack. Images of mitochondria were merged using ImageJ. Scale bar: 5 μ m. BF, bright field.

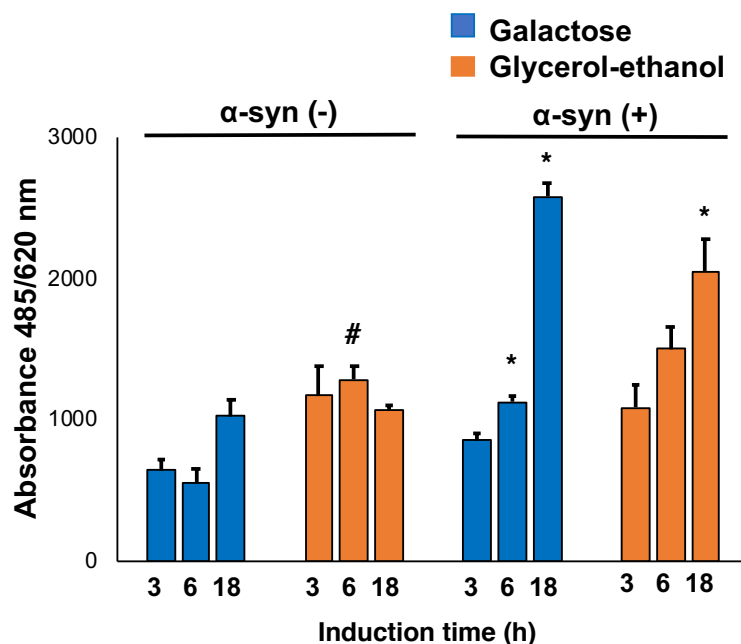


Figure 21. Quantitative assessment of reactive oxygen species under galactose and glycerol-ethanol conditions in the presence of α -synuclein.

Single diploid yeast colonies containing both vector (pRS303-GAL) or IntTox α -syn (W303 *MATa* strain) and *GAL3_{A368V}* (W303 *MATa* strain) were grown overnight in double selective 2% glucose media. The culture was washed twice with distilled water and diluted to an OD_{600} of 1.0 and was grown in double selective 2% galactose and 3% glycerol with 1% ethanol media, and induced for 3, 6 and 18 h. Cells were incubated with dihydroethidium (DHE) for 20 min in the dark and absorbance was measured at $\lambda_{ex} = 485$ nm and $\lambda_{em} = 620$ nm. The amount of ROS generated was calculated as the ratio of the absorbance to the OD_{600} . Repeated measures ANOVA with a random subject effect were run to analyze the difference between α -syn and the control. The experiment was repeated three times and the bars represent mean + SE. * $p < 0.05$ and hence significantly different compared to control. # $p < 0.05$ and hence significantly different compared to galactose.

ROS under the two conditions. However, upon closer examination many cells were stained with red fluorescence (**Figure 22 A**) in both conditions. We then examined the proportion of these bright red cells (**Figure 22 B**) and determined that there were more in both conditions in the presence of IntTox α -syn (both $p < 0.004$) with no apparent difference between the two conditions. The bright red fluorescent cells appeared dead under bright field microscopy. Hence, the higher ROS that was seen with the plate reader measurement was likely due to the higher red fluorescence emitted by the large number of cells that accumulate ROS. Taken together these results suggest that no significant increase in ROS production occurred, however, increased cell death due to accumulation of ROS was observed in both conditions.

Finally, we sought to examine if IntTox α -syn localizes to the mitochondrial matrix, thereby directly inhibiting its function under glycerol-ethanol. For this, we used a previously validated split GFP system, where the first ten GFP β -sheets (GFP₁₋₁₀) are tagged with the mitochondrial targeting sequence and the 11th β -sheet (GFP₁₁) is tagged with the gene of interest, in our case, *SNCA*. We did not see mitochondrial targeting of α -syn in either condition (**Figure 23**). However, we used CIT1, a mitochondrial matrix protein, as a positive control, which also did not show targeting to the matrix. Assuming the intervening stop codon prevented the transcription of the gene, we performed PCR analysis and Yeast Gap Repair to remove it. We also confirmed the in-frame sequence of *SNCA* in the GFP₁₁ construct. However, we were still unable to observe targeting with the positive control. Thus, although the construct required to perform the targeting experiment has been created, further experimental optimizations are required before the targeting of α -syn to mitochondrial matrix can be confirmed. Although we were unable

to directly detect mitochondrial targeting, we did observe dense mitochondrial structures under glycerol-ethanol and were, therefore, able to corroborate the findings of the pMitoLOC analysis.

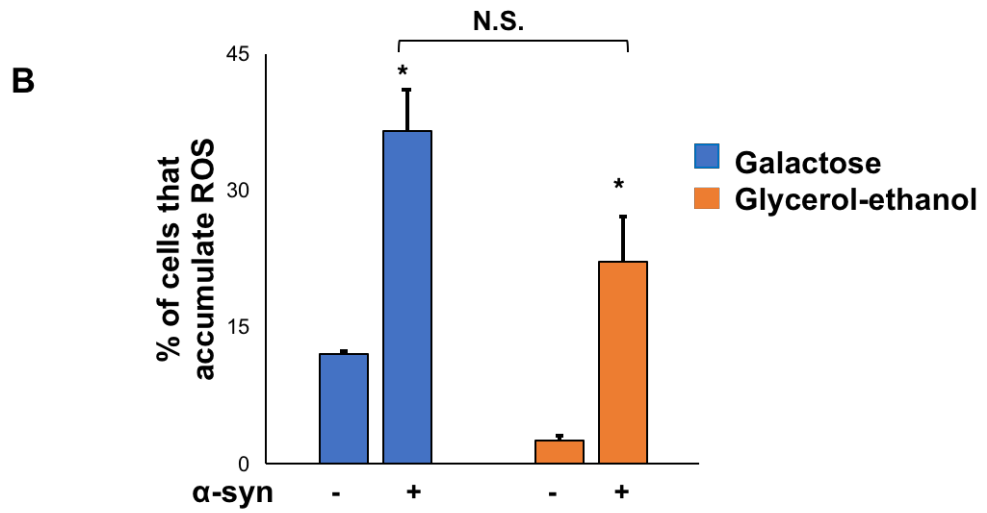
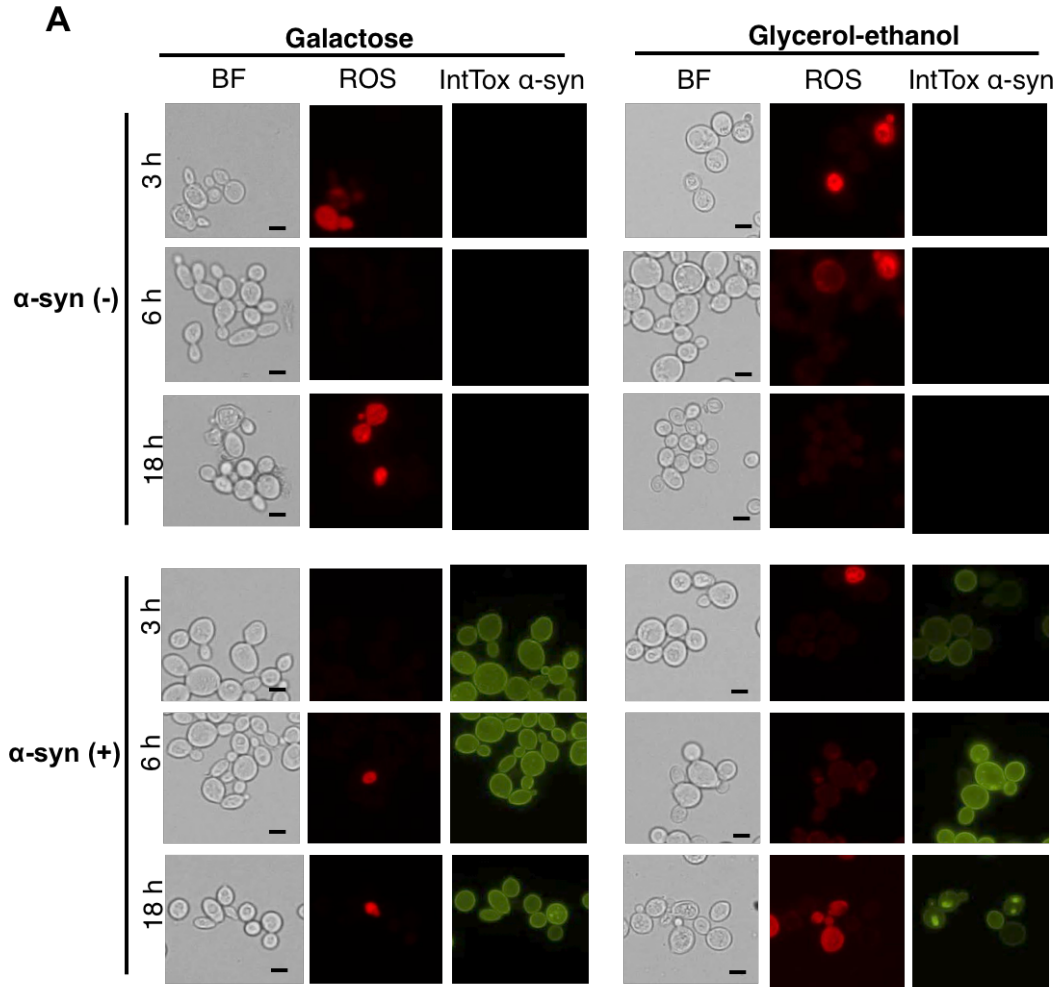


Figure 22. Number of cells that accumulate ROS are elevated under galactose and glycerol-ethanol conditions in the presence of α -synuclein.

The same sample of cells from Figure 22 was used for microscopic imaging. Three microliters of cells were placed on the glass slide and viewed under YFP (α -syn) and Tx Red (ROS) channels. ROS, when generated in the cells react with DHE and emit red color; the intensity of the red color indicates the amount of ROS. (A) ROS and α -syn in galactose and glycerol-ethanol at 3, 6 and 18 h of induction. (B) Quantification of the cells that accumulate ROS (bright red fluorescence in [A]) in two conditions at 18 h of induction. Proportion of cells that accumulate ROS were calculated as the ratio of the number of bright red fluorescent cells to the total number of cells. The experiments were repeated three times and the bars represent mean + SE. Two-way ANOVA was used to analyze the difference between α -syn and the control. Data had to be natural log transformed in order to adhere to the assumption of constant variance * $p < 0.05$ and hence significantly different compared to control. Scale bar: 5 μ m. BF, bright field; N.S., not significant; ROS, reactive oxygen species.

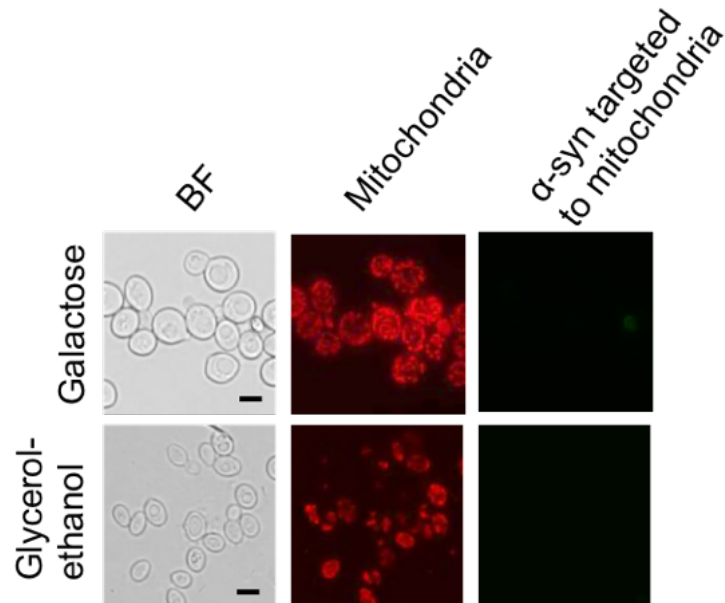


Figure 23. Targeting of α -synuclein to mitochondria was not successful.

SNCA (W303 *MAT α* strain) was tagged with GFP₁₁; this strain was also transformed GFP₁₋₁₀ with a mitochondrial targeting sequence tagged with mCherry. Single diploid yeast colonies containing both *SNCA* (GFP₁₁ tagged) and *GAL3_{A368V}* (W303 *MAT α* strain) were grown overnight in double selective 2% glucose media. The culture was washed twice with distilled water and diluted to an OD₆₀₀ of 1.0 and grown in double selective 2% galactose and 3% glycerol with 1% ethanol media, and induced for 18 h. Cells were isolated and 3 μ L of suspension was placed on a glass slide. Cells were viewed under GFP and Tx Red channels. Mitochondria appeared red (Tx Red channel) and α -syn, if targeted to mitochondria, should appear green (GFP channel) due to GFP fusion. Scale bar: 5 μ m. BF, bright field.

V. AIM 3: TO SCREEN AND CHARACTERIZE THE SUPPRESSORS OF INTTOX
 α -SYNUCLEIN TOXICITY UNDER GLYCEROL-ETHANOL

Rationale

Screening of overexpressed α -syn genes in yeast under galactose conditions has contributed to the elucidation of the pathophysiology, genetic interactions, and biological pathways underlying Parkinson's disease.^{39,42,64,65,100,101} In our study, we observed previously unknown phenotypes of α -syn under glycerol-ethanol. However, genetic screening to identify modifiers of α -syn has not yet been performed under glycerol-ethanol condition. Previous genetic screening techniques require first identifying yeast genes that can modify toxicity, and only after identifying its human homolog can the effects of the modifier be further analyzed. Since our lab has a collection of approximately 15,000 human genes cloned into yeast expression vectors, we designed a model for a human gene library and *GAL3_{A368V}*, effectively bypassing the need for cross-species comparisons and allowing for the direct screening of human gene modifiers of IntTox α -syn toxicity under glycerol-ethanol.

Experimental design

Human gene library and genetic screening by mating. To study human genes in yeast, our laboratory has successfully cloned 14,827 full-length sequences verified to be human gene clones into the Gateway yeast expression vector pRS416-GAL1-ccdB. Each

overexpressed human gene clone was transformed into the WT haploid strain W303 *MATa* containing α -syn. This yeast strain was mated with a strain containing *GAL3_{A368V}* (W303 *MAT α*). The diploid yeast was grown in selective media for 48 h before plating on glucose (negative control) and glycerol-ethanol plates (**Figure 24**). We did not perform screening in galactose condition as IntTox α -syn was not toxic under diploid galactose conditions.

Confirmation of genetic hits. Scoring of the genetic hits was performed by visually examining the phenotypes of the yeast strain in glycerol-ethanol agar plates (**Figure 25**). Four types of scoring were employed: trace, mild, moderate, and strong. We chose 184 hits and the original plasmid of these hits was revived from the bacterial glycerol stock. The process of plasmid isolation and individual transformation into yeast are described under Methods (Confirmation of genetic hits). Once the yeast strains were ready, the toxicity was re-evaluated by spotting of the diploid strains. This verification step allowed us to exclude false positives.

Results

3.1: To identify human gene suppressors of IntTox α -synuclein toxicity under glycerol-ethanol

Unique suppressors of IntTox α -syn are identified under a glycerol-ethanol. Based on an initial screening of 14,827 human genes, we identified 184 hits that suppressed the toxicity of α -syn under glycerol-ethanol conditions. After confirmation, 87 hits remained. The confirmed suppressors were compared with the list of suppressors of IntTox α -syn toxicity under haploid galactose conditions (previously performed in our lab). Of these 87 hits, only 44 were present in galactose screening. Of the 43 hits, eight of the genes had

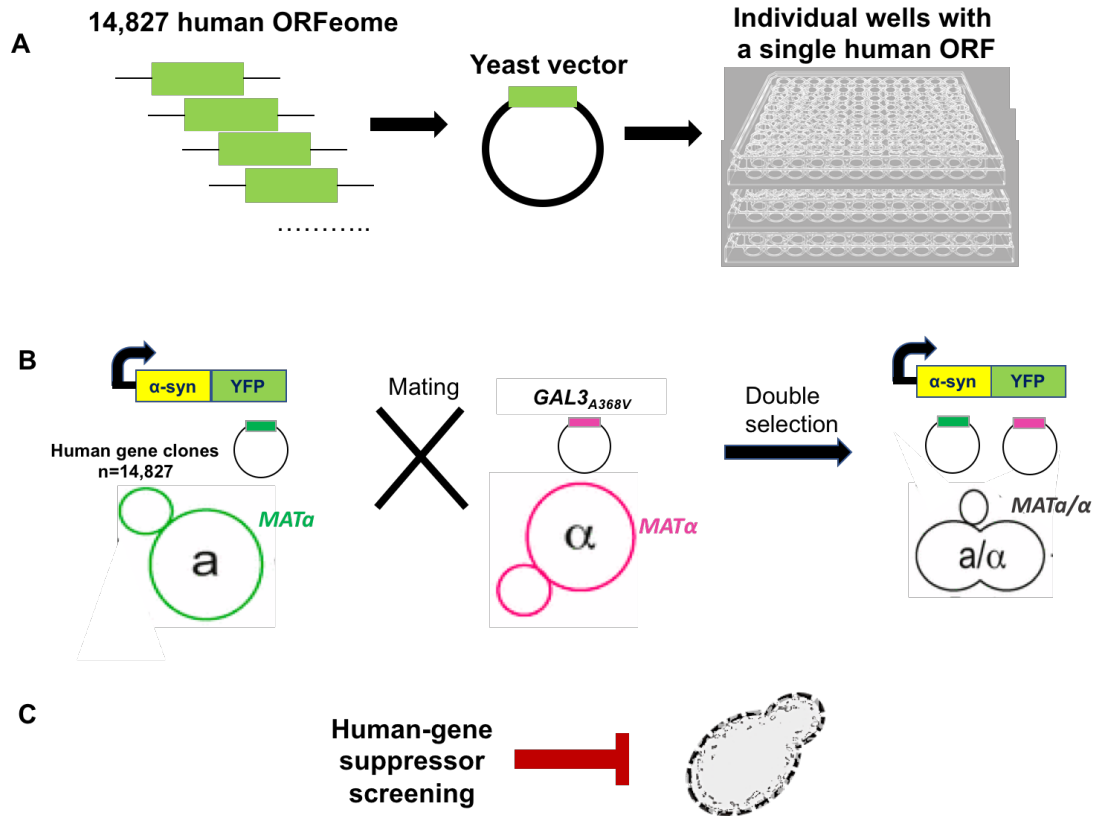


Figure 24. Schematic representation of the yeast overexpression screening to identify suppressors of IntTox α -synuclein toxicity under glycerol-ethanol.

(A) Human gene clones (14,827) were cloned into a yeast expression vector and individually transformed into a yeast strain. The yeast strains were then stored as glycerol stocks in individual wells of 96-well plates. (B) The human genes were transformed into a strain containing α -syn, which were then mated with a strain of the opposite mating type containing the *GAL3_{A368V}* allele. (C) The diploid yeast strain was selected and assessed for its ability to suppress α -syn toxicity.

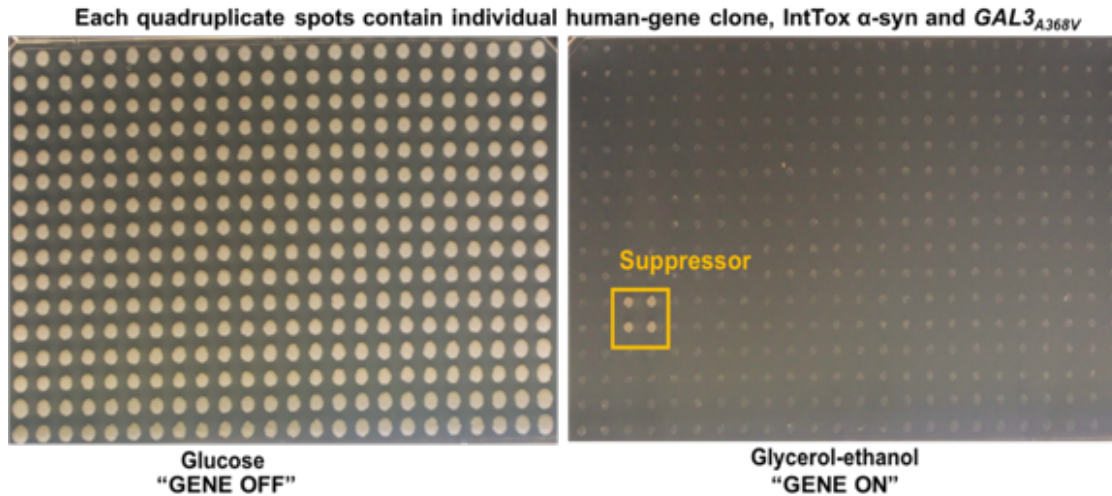


Figure 25. Sample image of spotting showing a suppressor of IntTox α -synuclein in glycerol-ethanol agar plate.

IntTox α -syn and human gene clone were transformed into the W303 *MAT α* strain.

GAL3_{A368V} was transformed into the W303 *MAT α* strain. Single colonies from both

strains were grown in 96-well plates. Each strain was transferred into a single 96-well

plate containing YPD media and grown overnight for mating. The mixture was then

transferred to another 96-well plate containing double selective 2% glucose media for

selection of diploid strains containing α -syn, human gene clone and *GAL3_{A368V}*. The

culture was grown for 48 h and then spotted onto 2% glucose and 3% glycerol with 1%

ethanol agar plates. The agar plates were incubated for 3–5 days, at which point the

images were obtained. The background growth in glycerol-ethanol shows the toxic

phenotype of α -syn. The yellow box highlights a suppressor. Each diploid strain was

spotted in quadruplicate, and each of the four dots represented a single human gene clone.

mitochondrial-related functions.

Gene ontology analysis of the hits in suppressor screening of IntTox α -syn under glycerol-ethanol. We used 87 hits from the glycerol-ethanol screening to perform the GO term enrichment analysis and identified groups of genes that are enriched based on molecular function, biological process and cellular compartment (**Table 4**). Based on molecular function, the analysis showed a 14.2-fold enrichment in genes with RNA polymerase II distal enhancer sequence-specific DNA binding, followed by an 8.9-fold enrichment with DNA-binding transcription activator activity, RNA polymerase II-specific, and 5.1-fold enrichment of RNA polymerase II regulatory region DNA binding. Based on biological process, the analysis showed a 22.1-fold enrichment of genes involved in embryonic skeletal system morphogenesis, 12.0-fold enrichment of anterior/posterior pattern specification and a 5.0-fold enrichment of positive regulation of transcription by RNA polymerase II. A cellular component-based analysis showed 2-fold enrichment of genes in the nucleoplasm while approximately 0.2-fold underrepresentation of genes in the integral component of the membrane and the organelle membrane was observed.

14-3-3 protein isotypes suppress IntTox α -syn toxicity under glycerol-ethanol condition. Of the eight hits that had mitochondrial-related functions, four of them were 14-3-3 isotypes (**Table 5**). There is a total of seven 14-3-3 protein isotypes, of which our library had six (β , θ , γ , ζ , σ , and η). The one isotype we did not have was 14-3-3 ϵ . Of the six isotypes, four (β , θ , γ , and ζ) suppressed the toxicity of IntTox α -syn (**Table 5**). We confirmed the end-read sequencing of all six 14-3-3 isotype clones.

Table 4. Gene ontology enrichment analysis of IntTox α -synuclein suppressor hits.

GO category	# genes in the library	# of hits	# of expected hits	Fold enrichment	over (+) or under (-) represented	<i>p</i> value
Molecular Function						
RNA polymerase II distal enhancer sequence-specific DNA binding	72	7	0.49	14.15	+	0.002
DNA-binding transcription activator activity, RNA polymerase II-specific	310	19	2.13	8.92	+	1.3E-09
RNA polymerase II regulatory region DNA binding	374	13	2.57	5.06	+	0.005
Biological Process						
Embryonic stem cell morphogenesis	66	10	0.45	22.06	+	6.42E-07
Anterior/posterior pattern specification	146	12	1	11.96	+	5.18E-06
Positive regulation of transcription by RNA polymerase II	819	28	5.63	4.98	+	5.95E-09
Cellular Component						
Nucleoplasm	2446	34	16.8	2.02	+	0.03
Integral component of membrane	3600	5	24.73	0.2	-	0.0003
Organelle membrane	2469	3	16.96	0.18	-	0.02

The enrichment analysis was performed using the online tool as described under **Methods (Gene Ontology enrichment analysis)**. The analysis list included all genes that were confirmed as suppressors (n = 87) of toxicity in glycerol-ethanol plates in

the large-scale screening analysis. The reference list included the list of genes from the human library (n = 12,890). Duplicate clones were removed prior to analysis. A Fischer's exact test was used and Bonferroni correction for multiple testing was selected. Only results with Bonferroni-corrected for $p < 0.05$ are displayed. The analysis was run based on molecular function (A) biological process (B) and cellular component (C). n represents the number of hits matching the criteria. Number (#) of hits represent the number of IntTox α -syn suppressors that map to this annotation data category. Fold enrichment (fifth column) is calculated by the online software based on the number of actual hits in comparison to the number of expected hits (fourth column). Over (+) or under (-) represented denotes if the specific category is higher or lower compared to expected values.

Table 5. 14-3-3 protein isotypes that suppressed the IntTox α -synuclein toxicity under glycerol-ethanol condition.

Gene name	Protein name	Significance¹⁰²
14-3-3 β	14-3-3 protein β/α	Present in tangles in Alzheimer's disease
14-3-3 θ	14-3-3 protein theta	Present in Lewy bodies in Parkinson's disease
14-3-3 γ	14-3-3 protein gamma	Present in Lewy bodies in Parkinson's disease
14-3-3 ζ	14-3-3 protein zeta/delta	Present in Lewy bodies in Parkinson's disease

There is a total of seven 14-3-3 protein isotypes. Of the seven, six were included in our human gene library. Of the six, four 14-3-3 proteins suppressed the α -syn toxicity under glycerol-ethanol condition.

3.2: To characterize the 14-3-3 isotype suppressors of IntTox α -synuclein toxicity
14-3-3 isotypes suppress the toxicity but do not reduce aggregate formation of IntTox α -syn under glycerol-ethanol. We used all six 14-3-3 isotypes (4 suppressors and two non-suppressors) to perform a spotting assay. **Figure 26** shows that only four of the six isotypes (β , θ , γ , and ζ) can suppress the toxicity of IntTox α -syn toxicity under glycerol-ethanol. Galactose was used as a control where no toxicity with IntTox α -syn was observed. As shown in Aim 2, IntTox α -syn shows toxicity in galactose in a haploid yeast strain. Hence, we performed spotting assays in the haploid condition without *GAL3_{A368V}*. Interestingly, the 14-3-3 suppressor isotypes did not suppress the toxicity in galactose (**Figure 27**). Whether the suppressor isotypes instead enhance the toxicity of IntTox α -syn in galactose condition requires further investigation.

Next, we quantified the proportion of cells containing α -syn aggregates in the presence of 14-3-3 isotypes (**Figure 28 A and B**). 14-3-3 θ , 14-3-3 γ , and 14-3-3 ζ did not reduce the percentage of cells with aggregates; while 14-3-3 β increased ($p = 0.02$) the proportion of cells with aggregates. Further, the non-suppressor isotypes, 14-3-3 σ , and 14-3-3 η did not increase the aggregates. We also observed that the protein expression level of α -syn was not affected by the 14-3-3 suppressor subtypes (**Figure 29 A and B**).
14-3-3 isotypes do not increase the viability and respiratory competency of cells. We predicted that the suppressors may increase the amount of viable and respiratory-competent cells. However, the 14-3-3 isotypes did not significantly impact the viability, or respiratory competency, of cells (**Figure 30 A and B**).

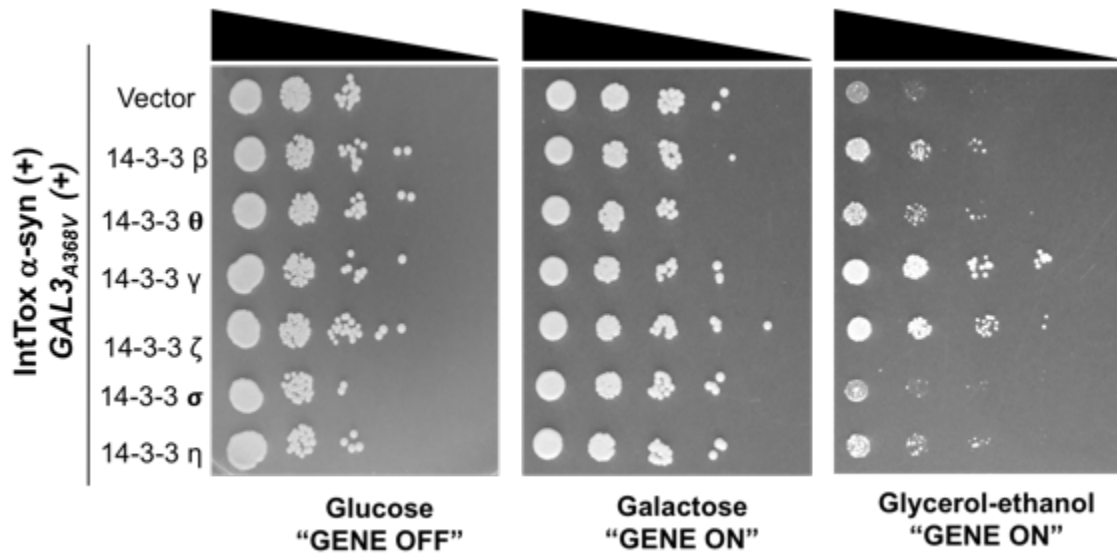


Figure 26. Four 14-3-3 isotypes suppress the toxicity of IntTox α -synuclein in glycerol-ethanol.

The W303 *MAT α* strain containing IntTox α -syn was transformed with an empty vector (pRS416-GAL) or 14-3-3 isotypes. Single diploid yeast colonies containing both IntTox α -syn (with 14-3-3 isotypes) and *GAL3*^{A368V} (W303 *MAT α* strain) were grown overnight in double selective 2% glucose media. The culture was washed twice with distilled water and diluted to an OD₆₀₀ of 1.0 and was spotted (left-most column). The diluted culture was further serially diluted 10-fold and spotted four times. The dilution was repeated until the last column on the right. The dilution is indicated by the tapering triangle bar on the top. Cells were then spotted onto solid double selective agar plates containing 2% glucose (negative control), 2% galactose (positive control), or 3% glycerol and 1% ethanol, and incubated for 2–5 days.

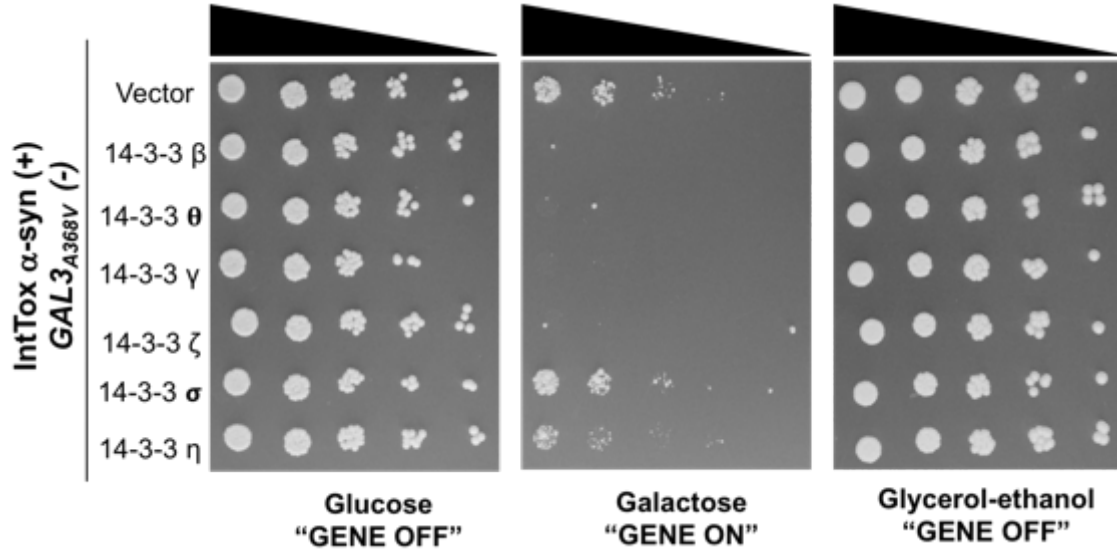
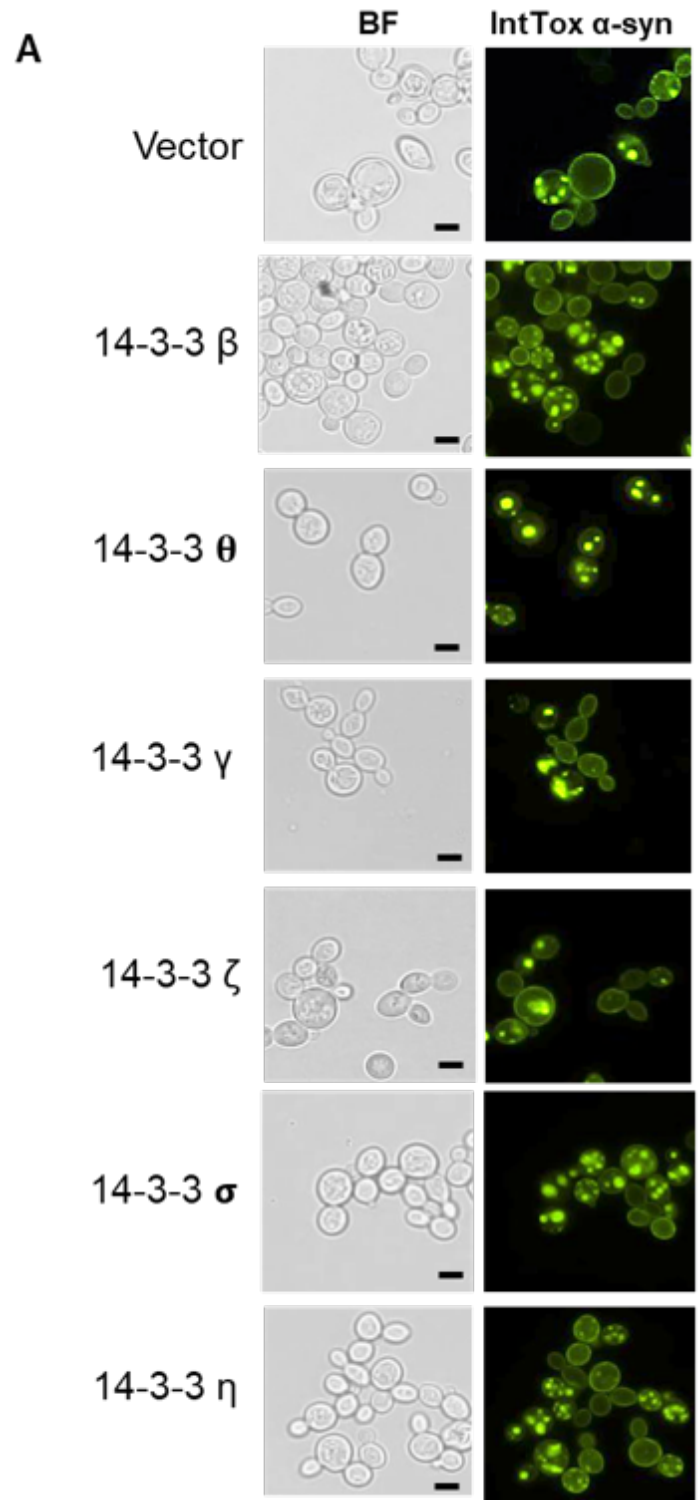


Figure 27. Four 14-3-3 isotypes do not suppress the toxicity of IntTox α -synuclein in galactose.

The W303 *MATa* strain containing IntTox α -syn was transformed with an empty vector (pRS416-GAL) or 14-3-3 isotypes. Single haploid yeast colonies containing both IntTox α -syn (with 14-3-3 isotypes) were grown overnight in double selective 2% glucose media. The culture was washed twice with distilled water and diluted to an OD₆₀₀ of 1.0 and was spotted (left-most column). The diluted culture was further serially diluted 10-fold and spotted four times; the dilution was repeated until the last column on the right. The dilution is indicated by the tapering triangle bar on the top. Cells were then spotted onto solid double selective agar plates containing 2% glucose (negative control), 2% galactose (positive control), or 3% glycerol and 1% ethanol, and incubated for 2–5 days.



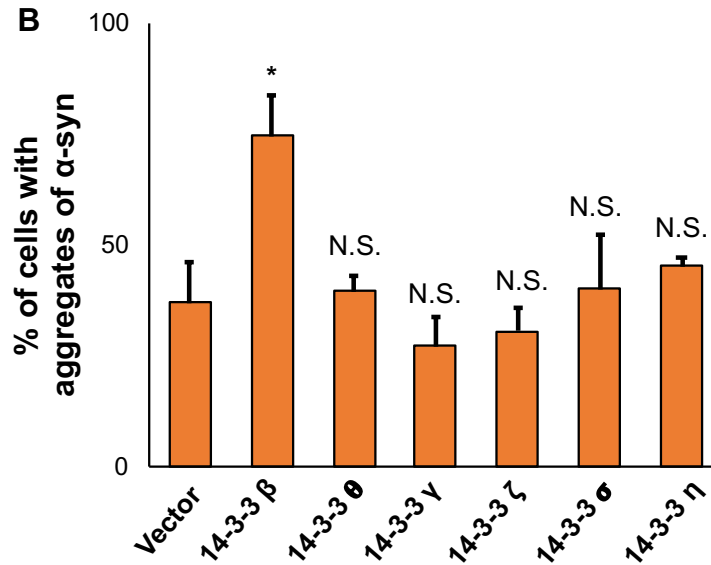


Figure 28. 14-3-3 β increases IntTox α -synuclein aggregates in glycerol-ethanol.

IntTox α -syn was transformed with an empty vector (pRS416-GAL) or 14-3-3 isotypes.

Single diploid yeast colonies containing both IntTox α -syn (W303 *MAT α* strain) and *GAL3_{A368V}* (W303 *MAT α* strain) were grown overnight in double selective 2% glucose media. The culture was washed twice with distilled water and diluted to an OD₆₀₀ of 1.0 and was grown in double selective 3% glycerol with 1% ethanol media and induced for 18 h. Cells were isolated and 3 μ L of suspension was placed on a glass slide and aggregates were viewed under the YFP channel. Scale bar: 5 μ m. BF, bright field (A).

Quantification of the aggregates (B) was performed using ImageJ and verified by manual counting. The experiments were repeated three times and a minimum of 200 cells were counted for each isotype. Bars represent mean + SE. Dunnett's test was performed to compare each 14-3-3 isotype to the vector. * $p < 0.05$ and hence significantly different compared to the vector. N.S., not significantly different compared to the vector.

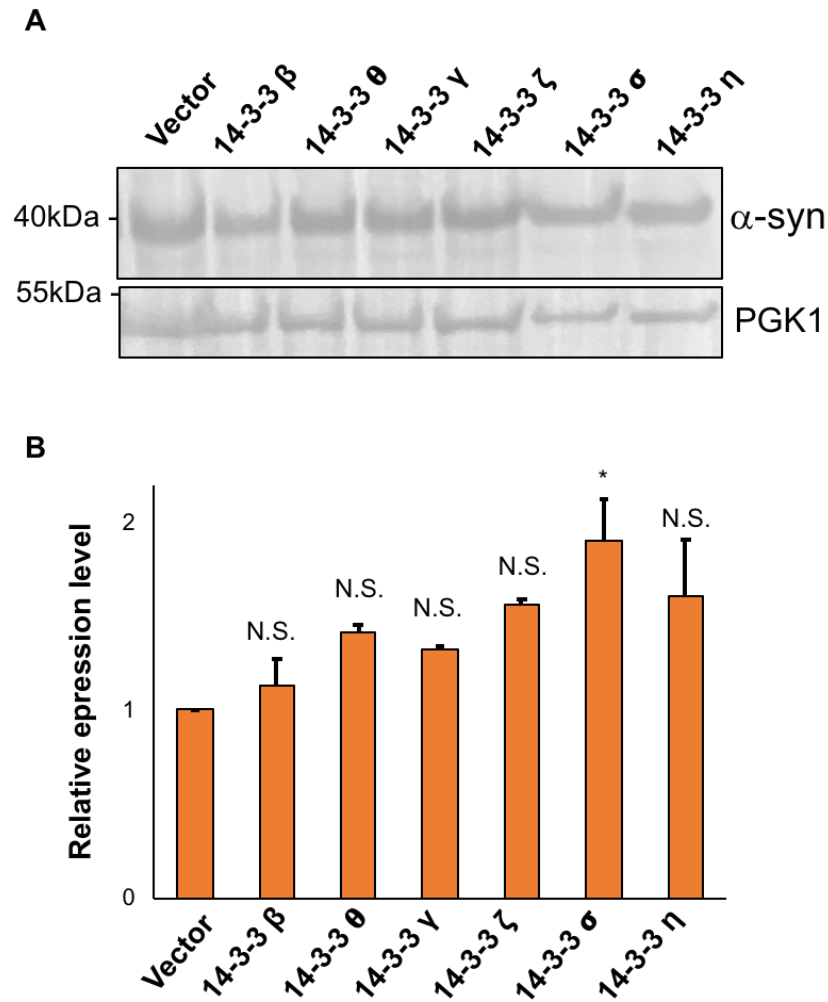


Figure 29. 14-3-3 suppressor isotypes do not reduce IntTox α -synuclein protein expression in glycerol-ethanol.

Single diploid yeast colonies containing both IntTox α -syn (W303 *MATa* strain) and *GAL3_{A368V}* (W303 *MAT α* strain) were grown overnight in double selective 2% glucose media. IntTox α -syn was transformed with an empty vector (pRS416-GAL) or 14-3-3 isotypes. The culture was washed twice with distilled water and diluted to an OD₆₀₀ of 1.0 and was grown in double selective 3% glycerol with 1% ethanol media and induced for 18 h. Cell cultures at an OD₆₀₀ of 1.0 (1×10^7 cells) were isolated and the protein was extracted. *SNCA* encoding IntTox α -syn was tagged with YFP and an antibody against

GFP was used. The loading control protein used was PGK1. (A) shows the blotting images and (B) shows quantification of the bands. Image quantification was performed using ImageJ. The experiment was repeated three times, and the bar graphs represent mean + SE. Protein expression in the presence of vector was used as the reference value. Dunnett's test was performed to compare each 14-3-3 isotype to the vector. $*p < 0.05$ and hence significantly different compared to the vector. N.S., not significantly different compared to the vector.

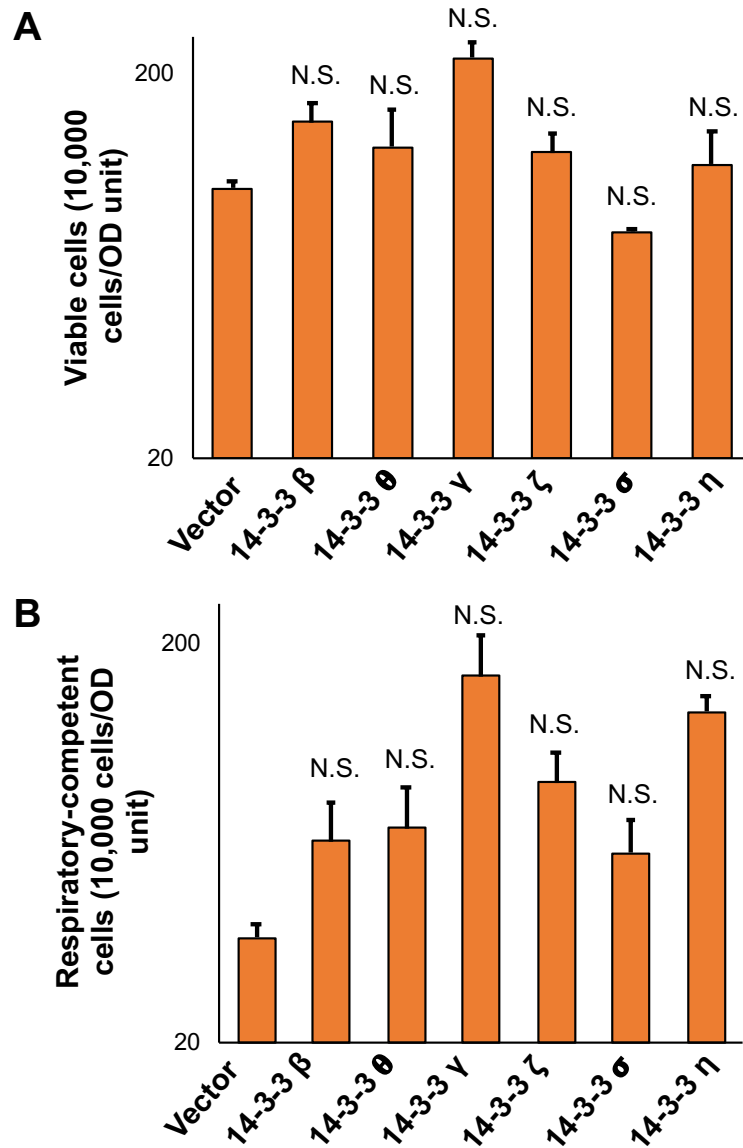


Figure 30. 14-3-3 suppressor isotypes do not increase viability or respiratory competency in glycerol-ethanol.

Single diploid yeast colonies containing both IntTox α -syn (W303 *MAT α* strain) and *GAL3_{A368V}* (W303 *MAT α* strain) were grown overnight in double selective 2% glucose media. IntTox α -syn has been transformed with an empty vector (pRS416-GAL) or 14-3-3 isotypes. The culture was washed twice with distilled water and diluted to an OD₆₀₀ of 1.0 and was grown in double selective 3% glycerol with 1% ethanol media and induced

for 18 h. Cells at an OD₆₀₀ of 1.0 were harvested and diluted; 100 μL each of 10⁻⁴ dilution and 10⁻⁵ dilution were plated on YPD and YPGE agar plates to determine the number of viable (A) and respiratory-competent cells (B), respectively. Agar plates were incubated for 2–3 days and single colonies were counted. Colony counts from the dilution that were nearest to 100 were chosen. The colony counts were multiplied by the respective dilution factor and used for statistical analysis. Dunnett's test was performed to compare each 14-3-3 isotype to the vector. N.S., not significantly different compared to the vector. Y-axis, logarithmic scale; OD, optical density.

14-3-3 isotypes do not modify the mitochondrial structure or the disrupted membrane potential signal. We next transformed the 14-3-3 plasmids into the yeast strains containing pMitoLoc and examined the mitochondrial structure and membrane potential. When we examined the mitochondria, we did not see a reduction in the dense mitochondrial structures (**Figure 31**). Moreover, the 14-3-3 subtypes did not modify the disrupted membrane potential. When we examined the IntTox α -syn aggregates, we noticed that there were fewer than in the previous experiments (**Figure 27**). Hence, we compared the proportion of aggregates between the two experiments and found that there was a 12–71 percent difference between the two experiments. The highest difference in the percentage of aggregates occurred with the empty vector (41% decrease) and 14-3-3 β (71% decrease).

14-3-3 isotypes do not decrease the ROS production and 14-3-3 β decreases the percentage of cells that accumulate ROS. Upon examining mitochondrial ROS with a plate reader, the 14-3-3 suppressors did not significantly reduce ROS production (**Figure 32**). Further, under microscopic examination, no visible increase or decrease in ROS was noted (**Figure 33 A**). All 14-3-3 suppressor isotypes had lower percentage of cells that accumulates ROS, although only 14-3-3 β was significant ($p = 0.04$) (**Figure 33 B**).

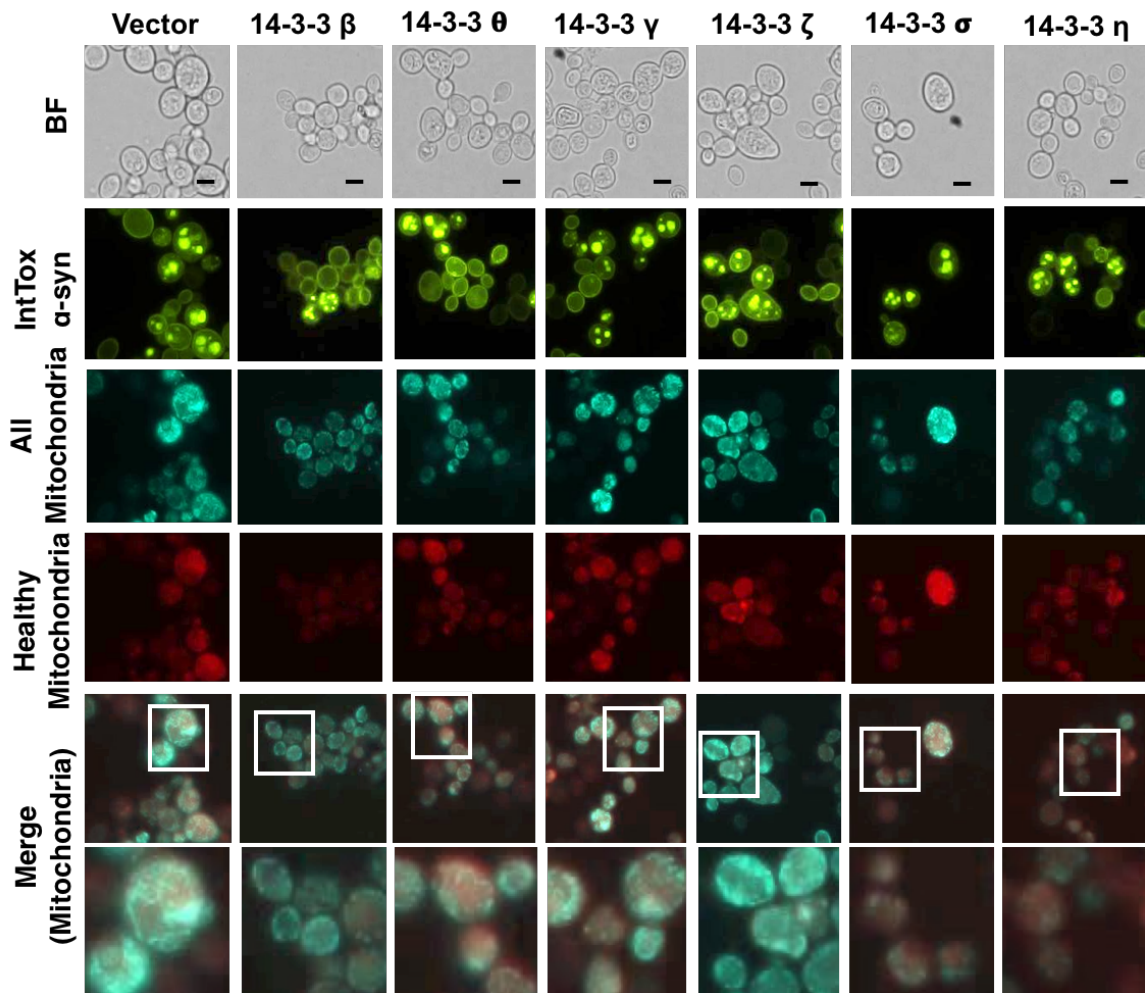


Figure 31. 14-3-3 isotypes do not modify the mitochondrial structure or the disrupted membrane potential signal.

The IntTox α -syn strain were transformed with pMitoLoc which has two (TFP and mCherry) tags with mitochondrial targeting sequence. Teal (TFP) represents all mitochondria; red (mCherry) represents only healthy mitochondria. Single diploid yeast colonies containing both IntTox α -syn (W303 *MATa* strain) and *GAL3_{A368V}* (W303 *MATa* strain) were grown overnight in double selective 2% glucose media. IntTox α -syn has been transformed with an empty vector (pRS416-GAL) or 14-3-3 isotypes. The culture was washed twice with distilled water and diluted to an OD₆₀₀ of 1.0 and grown in double

selective 3% glycerol with 1% ethanol media and induced for 18 h. Cells were isolated and 3 μ L of suspensions were placed on a glass slide and viewed under the YFP, CFP and Tx Red channels. *SNCA* encoding α -syn wasa tagged with YFP. CFP images were obtained by Z-stack. Images of mitochondria were merged using ImageJ. Scale bar: 5 μ m. BF, bright field.

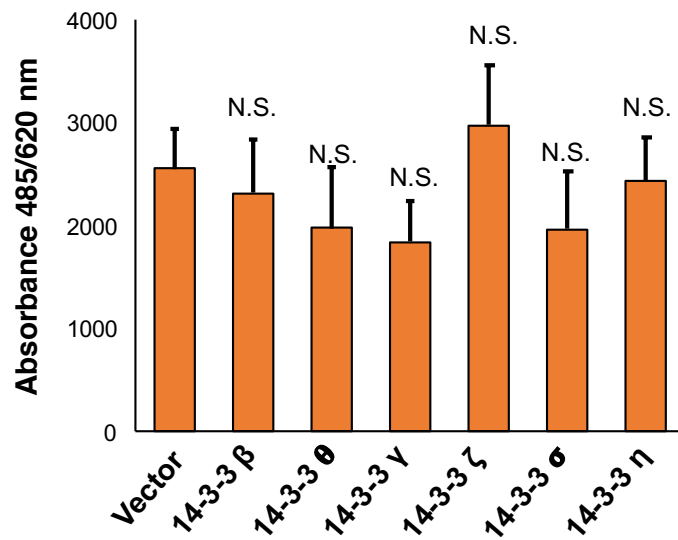
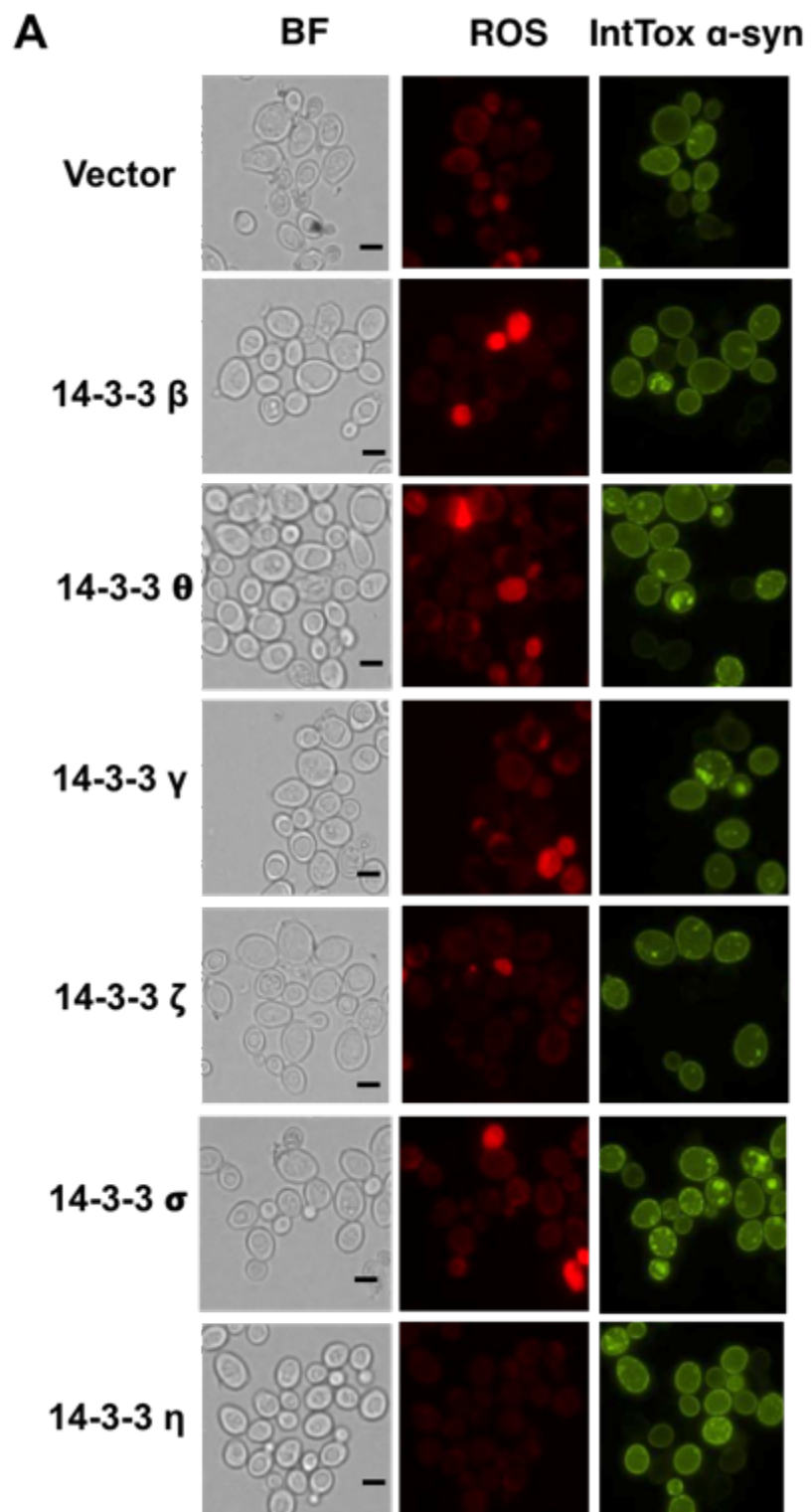


Figure 32. 14-3-3 isotypes do not decrease ROS production.

Single diploid yeast colonies containing both IntTox α -syn (W303 *MAT α* strain) and *GAL3_{A368V}* (W303 *MAT α* strain) were grown overnight in double selective 2% glucose media. IntTox α -syn was transformed with an empty vector (pRS416-GAL) or 14-3-3 isotypes. The culture was washed twice with distilled water and diluted to an OD₆₀₀ of 1.0 and grown in double selective 3% glycerol with 1% ethanol media and induced for 18 h. Cells were incubated with DHE for 20 min in the dark and absorbance was measured at λ_{ex} = 485 nm and λ_{em} = 620 nm. The amount of ROS generated was calculated as the ratio of the absorbance to the OD₆₀₀. Dunnett's test was performed to compare each 14-3-3 isotype to the vector. N.S., not significantly different compared to the vector.



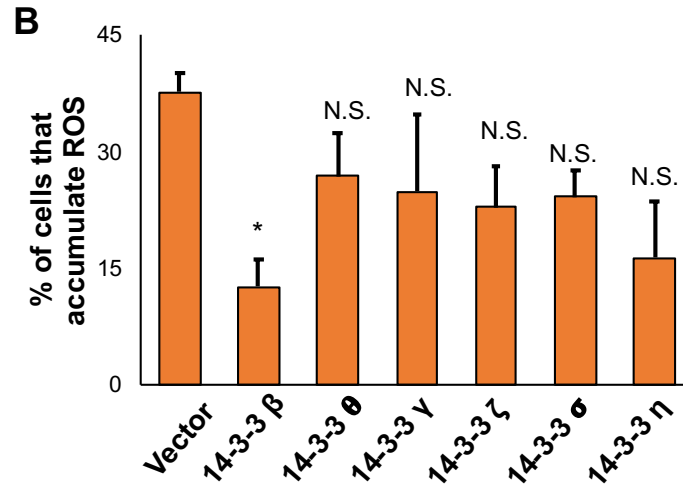


Figure 33. 14-3-3 β decreases the percentage of cells that accumulate ROS.

The same sample of cells from Figure 32 was used for microscopic imaging. Three microliters of the cells were placed on the glass slide and viewed under the YFP (α -syn) and Tx Red (ROS) channels. ROS, when generated in the cells reacts with DHE and emits a red color; the intensity of the red color indicates the amount of ROS. (A) ROS and α -syn in glycerol-ethanol at 18 h of induction. (B) Quantification of the cells that accumulate ROS (bright red fluorescence in [A]). Percentage of cells that accumulate ROS was calculated as the ratio of the number of bright red fluorescent cells to the total number of cells. The experiments were repeated three times and the bars represent mean + SE. Dunnett's test was performed to compare each 14-3-3 isotype to the vector. * $p < 0.05$ and hence significantly different compared to vector. N.S., not significantly different compared to the vector. Scale bar: 5 μ m. BF, bright field; ROS, reactive oxygen species.

VI. DISCUSSION

In Aim 1, we chose three *GAL3* alleles - *GAL3_{F237Y}*, *GAL3_{A368V}* and *GAL3_{S509P}* and tested their ability to induce the *GALI* promoter under non-galactose conditions. We used β -galactosidase assay to test the level of promoter induction. We also corroborated the findings from the β -galactosidase assay using a yeast spotting assay. We found that all three *GAL3* alleles induced the *GALI* promoter in glycerol-ethanol condition (**Figure 3**), however, the combination of these alleles did not induce the promoter (**Figure 4**) as the combinations failed to enable transition to a 'closed active' Gal3p conformation (**Figure 5**). Based on α -syn as the model in the spotting assay, we chose to use *GAL3_{A368V}* for further experiments. Yet, when *GAL3_{A368V}* was assessed in other non-galactose conditions, including caloric restriction and nitrogen starvation conditions, we found that it did not induce the *GALI* promoter in the presence of glucose (**Figure 6**). This finding was verified by spotting assay using α -syn, FUS, TDP-43 and HTT103Q (**Figure 7**). However, when glucose content was reduced from 0.5% to 0.1% and when the glucose was replaced with raffinose, we saw rapid induction of the *GALI* promoter (**Figure 8**). Under calorie restriction (0.1% glucose), raffinose and nitrogen starvation (2% raffinose), IntTox and HiTox α -syn overexpression caused differential toxicity and aggregate formation. Specifically, IntTox α -syn showed toxicity, however, did not exhibit aggregate formation in raffinose conditions (**Figure 9 and 10**); while HiTox α -syn did not induce toxicity yet showed aggregate formation under calorie restriction (**Figure 9**

and 11). This is the first study showing the uncoupling of toxicity and aggregate formation of α -syn. Results from Aim 1, therefore, show that *GAL3_{A368V}* can be used to study genes in any non-galactose condition lacking glucose.

We chose three *GAL3* alleles from a previous publication⁷⁵ where a haploid condition was utilized and the WT *GAL3* was deleted. To this end, we first examined the *GAL3* alleles in a diploid condition and then in the presence of WT *GAL3*. Our lab had previously validated genetic screening in diploid conditions⁹⁸ and thus performing a screening with deletion of WT *GAL3* from about 15,000 yeast strains containing human genes seemed impractical. For the first time, we have shown that *GAL3* alleles can be constitutively active and induce the *GALI* promoter in diploid conditions in the presence of two WT *GAL3* (from the two haploid strains). Once we understood that *GAL3_{A368V}* activity need not be restricted to glycerol-ethanol but rather to any non-galactose conditions, we extended our analysis to other conditions including, calorie restriction and nitrogen starvation. We also found that *GAL3* alleles are unable to induce the *GALI* promoter in the presence of low glucose concentrations (0.5%). This is likely attributable to the significant suppressive function of glucose on the *GALI* promoter.⁷⁷ Glucose represses *GALI* expression by three primary mechanisms.⁷⁶ Firstly, glucose acts on the upstream activating sequence and reduces Gal4p (transcriptional activator) while increasing Gal80p (repressor) expression. Secondly, Mig1p, a transcriptional repressor binds to the upstream repression sequence and represses *GALI* expression in the presence of glucose. Thirdly, glucose inhibits the transcription of *GAL2* encoded galactose permease and reduces the level of functional inducer in the cell. Thus, *GAL3_{A368V}* was unable to circumvent this multi-tactical repression mechanism by glucose.

Additionally, we found that the combination of *GAL3* alleles did not significantly increase *GALI* promoter strength. Structural analysis of Gal3p showed that the mutations, in combination, prevented the transition to the ‘closed active’ conformation of Gal3p. F237 of Gal3p sits in a hydrophobic pocket that is comprised of F247, M403, L65, F414, F418, and I245. A closed conformation will force the F237 from the hydrophobic pocket to a more hydrophilic site. Similarly, substituting phenylalanine for tyrosine in F237Y (i.e. a hydroxyl group) has the same result, effectively drawing the peptide out. The position in which the F237 extends from the pocket is where S509 is located. Alternatively, substituting serine for proline (S509P) prevents F237Y from popping out of the hydrophobic pocket and, thus, the combination of alleles cancels the transition to a closed conformation.⁷³

Finally, the most interesting finding of this Aim was the discrepancy between toxicity and aggregate formation observed with IntTox and HiTox α -syn overexpression in non-galactose conditions. Previously, all studies involving α -syn report the presence of cellular toxicity or neurodegeneration with the presence of α -syn inclusions.¹⁰³ However, here we are the first to comprehensively demonstrate that α -syn can augment or attenuate toxicity irrespective of the presence of inclusions, depending on the growth conditions. Although understanding this discrepancy requires further investigation, we hypothesize potential causes for these observations. Under caloric restriction conditions, the lifespan of yeast cells becomes extended and subsequently the decline of UPR is abrogated.¹⁰⁴ In addition, calorie restriction maintains autophagy (the cell’s recycling machinery) in homeostasis by reducing Sir2 activity.⁹⁴ Thus, it may be that under calorie restriction, the cell’s protective mechanisms (UPR and autophagy) neutralize the presence of aggregates

and reduce cellular toxicity. In case of raffinose condition, no aggregates were observed although toxicity was apparent with IntTox α -syn. This may have been caused by raffinose activating alternate signaling pathways that reduce ROS production and/or cytochrome c release.¹⁰⁵ Further experiments testing the level of ROS and cytochrome c can help explain if these mechanisms are responsible for the absence of aggregates despite the presence of toxicity. Reduction of ROS and cytochrome c will result in reduction of mitochondrial stress. Reduced mitochondrial stress means functional mitochondria and we know that α -syn requires a functional mitochondria in yeast to produce toxicity.⁴⁴ Thus, the protective signaling mechanisms activated under raffinose likely reduces the mitochondrial stress to a level that can prevent aggregate formation but not to a level that can suppress toxicity caused by IntTox α -syn overexpression.

In Aim 2, we saw that IntTox α -syn was toxic under glycerol-ethanol but not under galactose in diploid yeast strains (**Figure 13**). Although we did not observe an increase in α -syn protein expression (**Figure 16**) in the glycerol-ethanol condition that would explain the higher toxicity, we did see an increase in the proportion of cells with α -syn aggregates under glycerol-ethanol (**Figure 17**) compared to galactose conditions, that may provide a partial explanation for the observed toxicity. IntTox α -syn did not affect the respiratory competency in galactose but rather affected it only under glycerol-ethanol (**Figure 19**). We also observed dense mitochondrial structures predominantly under glycerol-ethanol condition (**Figure 20**). Based on quantitative and microscopic assessment, we concluded that increased ROS reading with IntTox α -syn overexpression is due to increased percentage of cells that accumulate high-level of ROS (**Figure 21 and 22**). From Aim 2, it can be concluded that the increased toxicity of IntTox α -syn in

glycerol-ethanol condition compared to galactose is due to increased aggregate formation, decreased number of viable and respiratory-competent cells and the presence of dense mitochondrial structures. The other parameters including protein expression level, membrane potential, ROS production and presence of cells that accumulate ROS did not differ significantly between the two conditions and thus, cannot explain the increased toxicity in the glycerol-ethanol condition.

Under glycerol-ethanol, we saw that the toxicity of all genes – *SNCA* (IntTox and HiTox), *FUS*, and *TDP-43* – increased. α -syn affects the mitochondria in multiple ways and reduces the respiratory cellular activity. Hsp60, a mitochondrial chaperone, mediates *FUS* entry into the mitochondria and in transgenic flies, and thus, downregulation of Hsp60 rescues mitochondrial defects and neurodegenerative phenotypes caused by *FUS* overexpression.¹⁰⁶ *TDP-43* preferentially binds mitochondrial mRNAs of complex I subunits ND3 and ND6 eventually causing complex I disassembly.¹⁰⁷ In a transgenic *TDP-43* mutant mouse model, disrupting the mitochondrial localization of *TDP-43* results in abrogation of mitochondrial dysfunction and neuronal loss. Thus, it is possible that under glycerol-ethanol condition, there is an increase in toxicity of all genes that affect the mitochondria.

We observed both toxicity and aggregates with IntTox α -syn in diploid glycerol-ethanol and haploid galactose strains. Further, the level of toxicity between the two strains as determined via spotting and liquid growth assays, was similar. However, when we compare the percentage of aggregates between the two strains, we see fewer in haploid galactose conditions (37%) compared to glycerol-ethanol (56%). It is, therefore, important to note that these two conditions cannot be directly compared and are not

interchangeable with differing underlying mechanisms of toxicity associated with each. Further, we observed that when IntTox α -syn is induced in haploid and diploid conditions, toxicity is completely absent in diploid. A proteome quantification study using stable-isotope labeling of amino acids in haploid and diploid yeast cell cultures showed unaltered expression levels of approximately 4,500 proteins between haploid and diploid wild-type yeast.¹⁰⁸ Only a few proteins involved in pheromone signaling and cell wall structure were upregulated in haploid yeast. We do not, however, understand whether these subtle changes in protein levels are sufficient to suppress the toxic phenotype of α -syn. A direct comparison of mitochondrial structure and mitochondria-related functions including ROS production, cytochrome c release, apoptosis, and mitochondrial membrane potential between haploid and diploid condition in the presence of *GAL3*_{A368V} and α -syn might help explain the differences in toxicity between the two strains.

Under galactose condition, in contrast to what we hypothesized, we did not observe reduced respiratory competency with α -syn overexpression. This result, along with an absence in mitochondrial structure alterations in galactose conditions denotes that α -syn does not affect the mitochondrial function under galactose to the same extent as in glycerol-ethanol. If the mitochondria are not functioning at their full capacity, as in the case of galactose, α -syn does not seem to affect the mitochondrial function.

Alternatively, in glycerol-ethanol, when cell survival is dependent on mitochondrial function, α -syn reduces mitochondrial function as well as respiratory competency. The N-terminal amphipathic domain of α -syn has been reported to be associated with alterations in mitochondrial morphology and the activation of mitochondrial permeability

transition pores.¹⁰⁹ This was associated with a decrease in mitochondrial cardiolipin content. Glycerol-ethanol may induce changes in mitochondrial structures and thus becomes vulnerable to the action of α -syn.

Despite previous reports showing higher ROS production by α -syn under galactose conditions,^{69,110} in our study, α -syn did not increase ROS production in the two conditions. These previous studies measured ROS using quantitative techniques and as such, the cells that accumulate ROS with red fluorescence may have been included in the measurements and overlooked. Had we not performed the microscopic examination, we too would have concluded that ROS production was indeed higher in the presence of α -syn. Hence, plate reader measurements must be re-evaluated by excluding the fluorescence emitted by the cells that accumulate ROS. Also, the reason as to why ROS production was not increased by α -syn in our study remains unclear. The DHE dye that we used primarily identifies cellular and not mitochondrial superoxide.¹¹¹ The by-products of this reaction include a ethidium (nonspecific redox product) and 2-hydroxyethidium (adduct of superoxide).¹¹² The wavelengths of these two by-products overlap and thus, provide inconsistent results in a regular plate reader and in microscopic images. The use of high-pressure liquid chromatography may serve to circumvent this problem. Although we do not fully know which ROS species becomes induced by α -syn, hydrogen peroxide rather than superoxide appears to dominate.¹¹³ Techniques to identify different types of ROS would assist in better addressing these questions.

We measured the number of cells that accumulate ROS and found that they increased in the presence of α -syn in both conditions although, there was no difference between the two conditions. To identify the specific apoptotic stage of cells, further

testing using Annexin V/propidium iodide (PI) co-staining is useful. This stain quantifies externalization of phosphatidylserine, an early apoptotic event, and membrane permeabilization, indicative for necrotic death. It also allows for the discrimination between early apoptotic (Annexin V positive, PI negative), late apoptotic (Annexin V positive, PI positive), and necrotic (Annexin V negative, PI positive) cells. Staining at different time points during growth in the two conditions and their correlation with the presence of aggregates can help predict the sequence of the two events.

YCAI is the yeast orthologue of mammalian caspase; the deletion of *YCAI* abolishes the ROS accumulation induced by α -syn, suggesting that caspase is the key mediator in ROS production. We can, therefore, determine if deletion of *YCAI* prevents or reduces apoptosis in the glycerol-ethanol condition. Alternatively, pan-caspase inhibitor Q-VD-OPh¹¹⁴ can be used to examine the role of caspase in apoptotic cell death induced by α -syn in glycerol-ethanol. Nevertheless, the amount (< 25%) of apoptosis alone cannot explain the increased toxicity in the glycerol-ethanol condition. Hence, it can be concluded that mitochondrial function plays a dominant role in inducing apoptosis and toxicity in glycerol-ethanol.

In Aim 3, using yeast mating technique validated in our lab,⁹⁸ we screened 14,827 human gene clones (corresponding to 12,890 genes) to identify suppressors of IntTox α -syn in glycerol-ethanol. There were 184 hits in the screen, however, after performing a confirmation step, only 87 remained. When this list was compared with the hits obtained from the haploid galactose condition performed in our lab, we found that 43 of the 87 hits were present only under glycerol-ethanol. Further, GO enrichment analysis of IntTox α -syn suppressor hits showed significant overexpression of genes related to the function of

RNA polymerase II (**Table 4**). Any process that activates or increases the frequency, rate or extent of transcription from an RNA polymerase II promoter were overrepresented in suppressors of IntTox α -syn. Genes associated with anterior-posterior pattern specification were also overrepresented. Anterior-posterior pattern specification is a process in which specific areas of cell differentiation are determined along the anterior-posterior axis during neuronal development. Additionally, homeobox proteins dominated both RNA polymerase II and anterior-posterior pattern specification groups. Genes that belong to nucleoplasm were overrepresented whereas genes that belonged to organelle membrane were underrepresented among the confirmed suppressors.

Interestingly, among the 43 hits, four of the 14-3-3 isotypes (β , θ , γ , and ζ) emerged as suppressors of IntTox α -syn only in glycerol-ethanol and not in galactose condition (**Table 5 and Figure 26 and 27**). Whether 14-3-3 isotypes enhanced the toxicity of IntTox α -syn in galactose must be confirmed in subsequent analyses. Nevertheless, 14-3-3 β increased the number of IntTox α -syn aggregates (**Figure 28**) although this result was not consistent across other experiments. 14-3-3 suppressor isotypes neither reduced protein expression levels (**Figure 29**) of IntTox α -syn nor increased viability and respiratory competency in glycerol-ethanol (**Figure 30**). Moreover, no changes in mitochondria was observed (**Figure 31**), and ROS production was not decreased (**Figure 32**) by the 14-3-3 suppressors. However, 14-3-3 β was found to decrease the proportion of cells that accumulate ROS (**Figure 33**). This Aim unraveled some unique patterns of suppressors – the involvement of RNA polymerase II, anterior-posterior axis morphogenesis and nucleus. Although we were unable to characterize how

the four 14-3-3 proteins suppressed IntTox α -syn toxicity in glycerol-ethanol, we were able to rule out certain mechanisms.

The overrepresentation of genes involved in RNA polymerase II function and anterior-posterior axis specification highlights the fact that modification at the transcriptional level and early neuronal development play key roles in suppressing the toxicity of IntTox α -syn in glycerol-ethanol. Further, these groups were dominated by homeobox proteins. Homeobox genes are a group of approximately 250 genes each containing a 60-amino acid homeodomain that is responsible for DNA binding and regulation of hindbrain morphogenesis and axial skeleton patterning by acting as transcriptional regulators.¹¹⁵ Two of the homeobox protein suppressors, *LHX4* and *OTX1*, have been shown to be present in dopaminergic neuron progenitor cells in the midbrain and to regulate their development.^{116,117} Homeobox proteins, *EN-1* and *EN-2*, in addition to regulating transcription also regulate mRNA translation. Specifically, in two (mutant α -syn and MPTP toxin-induced) Parkinson's disease model, *EN-1* and *EN-2* were shown to regulate Ndufs1 and Ndufs3 translation, two mitochondrial complex I proteins, and prevented dopaminergic neuron death *in vivo*.¹¹⁸ Thus, homeobox genes are dynamic in that they not only regulate gene transcription but are also able to regulate translation of mitochondrial proteins in dopaminergic neurons. Although it is unlikely that homeobox proteins regulate the expression of the *GALI* promoter driven *SNCA* in yeast, the protein levels of α -syn need to be examined to rule out this possibility. Alternatively, the suppressor genes could alter the expression of other yeast genes, alleviating the toxicity of α -syn.

Four isotypes of 14-3-3 protein was found to suppress the toxicity of IntTox α -syn in glycerol-ethanol. 14-3-3 proteins have 40% homology to α -syn, colocalize with α -syn and accumulate in Lewy bodies in Parkinson's disease brains.¹¹⁹ 14-3-3 proteins play key roles in neuronal cell division and differentiation through phosphorylation of mitogen-activated protein kinase kinase by activating gene transcription.¹²⁰ Specifically, 14-3-3 η binds with aggregate prone oligomers of α -syn; while overexpression of α -syn sequesters and downregulates 14-3-3 η .¹²¹ When 14-3-3 γ , 14-3-3 θ , and 14-3-3 ϵ were overexpressed in neuroglioma cells, a reduction in the number of aggregates was observed.¹²² We did not observe such a reduction in the number of aggregates with any of the 14-3-3 suppressor isotypes. In fact, we saw an increase in the amount of aggregates with 14-3-3 β . We also saw a variation in the percentage of aggregates between experiments. We are unsure of the cause of such variations between experiments. It might be worth integrating one or more copies of the 14-3-3 genes in the yeast genome to re-examine their effect on α -syn aggregation.

Next, 14-3-3 proteins exhibit anti-apoptotic functions by binding to, and sequestering, pro-apoptotic Bad.^{123,124} In our study, we saw that 14-3-3 β reduced the proportion of cells that accumulate ROS. Hence, the suppression of toxicity may be partially explained by the anti-apoptotic effect of 14-3-3. This must be validated as yeast does not contain the mammalian anti-apoptotic machinery. Specifically, *YCA1*, an orthologue of caspase in yeast, can be deleted and the suppressive effect retested with 14-3-3 β . Alternatively, a pan-caspase inhibitor, Q-VD-OPh,¹¹⁴ can be used to test the role of apoptotic inhibition in the suppressive function of 14-3-3 β .

Finally, we did not see any changes in mitochondrial structure, membrane potential, ROS production, viability or respiratory competency with 14-3-3 suppressor proteins; thus, an alternate explanation for the suppressive effect must exist and may rely on that information. As mentioned before, 14-3-3 η , 14-3-3 γ , 14-3-3 θ , and 14-3-3 ϵ have been shown, in *in vitro* and other models, to sequester α -syn and reduce the formation of aggregates.^{120,121} It is interesting to see similar findings of α -syn toxicity suppression in a simple eukaryotic cell, yeast. Although we do not know the exact mechanisms underlying the suppressor effect of 14-3-3 isotypes in yeast, we speculate that a direct interaction between the 14-3-3 isotypes and α -syn could be involved. The binary interaction can be tested using yeast-two-hybrid assay. Alternatively, other conserved functions of 14-3-3 in yeast might be at play. Such functions might be affected by carbon source, since the suppressor effect was not observed on galactose. It would be interesting to determine if 14-3-3 was able to suppress the toxicity on raffinose condition to better understand if the α -syn aggregation foci are involved. Finally, the proposed mechanisms need to differentiate the suppressors from the non-suppressors that were identified.

VII. CONCLUSION

Three *GAL3* alleles - *GAL3_{F237Y}*, *GAL3_{A368V}* and *GAL3_{S509P}* - induced *GALI* promoter in glycerol-ethanol condition, however, the combination of the alleles did not induce the promoter. *GAL3_{A368V}* did not induce *GALI* promoter in the presence of glucose. IntTox α -syn induced toxicity in raffinose without aggregate formation. HiTox α -syn failed to induce toxicity yet formed aggregates under caloric restriction. IntTox α -syn was toxic under glycerol-ethanol yet not under galactose. IntTox α -syn protein levels were not increased but the aggregates were increased in glycerol-ethanol compared to galactose. Respiratory competency was reduced, while cell population that accumulated ROS was increased by IntTox α -syn in glycerol-ethanol. By screening 14,827 human gene clones, we identified 87 hits as suppressors of IntTox α -syn toxicity. GO enrichment analysis of the suppressor hits showed significant overexpression of genes related to the function of RNA polymerase II, anterior/posterior pattern specification and nucleoplasm. These three categories were enriched with genes of the homeobox proteins pointing toward transcriptional regulation playing a vital role in suppressing toxicity of IntTox α -syn in glycerol-ethanol. Four of the 14-3-3 isotypes (β , θ , γ , and ζ) emerged as the suppressors of IntTox α -syn only under glycerol-ethanol. 14-3-3 β increased the number of aggregates of IntTox α -syn. 14-3-3 suppressor isotypes neither reduced protein expression levels of IntTox α -syn nor increased viability and respiratory competency in glycerol-ethanol.

Mitochondrial structure was unchanged, and ROS production was not decreased by the 14-3-3 suppressors. 14-3-3 β decreased the percentage of cells that accumulated ROS.

Our study obliterates the limitation of performing screening only under galactose condition. Future studies should focus on pinpointing the difference in transcription and translation between galactose and glycerol-ethanol conditions since the parameters tested did not provide a clear answer. Although yeast is a single eukaryotic cell with no neurons, it still possesses the conserved cellular biology that underpins Parkinson's disease pathology. Therapeutic targets identified in prior α -syn yeast screening analyses have been validated in higher organisms highlighting the relevance of this system in studying Parkinson's disease. Although there are aspects of this disease which are beyond the scope of yeast, with the advancement of system and computational biology, large-scale yeast genetic data on α -syn and Parkinson's disease can be efficiently analyzed and translated to humans.

VIII. REFERENCES

1. Poewe W, Seppi K, Tanner CM, et al. Parkinson disease. *Nat Rev Dis Prim.* 2017;3:1-21.
2. Van Den Eeden SK. Incidence of Parkinson's disease: variation by age, gender, and race/ethnicity. *Am J Epidemiol.* 2003;157:1015-1022.
3. Savica R, Grossardt BR, Bower JH, et al. Incidence and pathology of synucleinopathies and tauopathies related to parkinsonism. *JAMA Neurol.* 2013;70:859-866.
4. Dorsey ER, Constantinescu R, Thompson JP, et al. Projected number of people with Parkinson disease in the most populous nations, 2005 through 2030. *Neurology.* 2007;68:384-386.
5. Pinter B, Diem-Zangerl A, Wenning GK, et al. Mortality in Parkinson's disease: A 38-year follow-up study. *Mov Disord.* 2015;30:266-269.
6. Kalia L V., Lang AE. Parkinson's disease. *Lancet.* 2015;386(9996):896-912.
7. Dickson DW, Braak H, Duda JE, et al. Neuropathological assessment of Parkinson's disease: refining the diagnostic criteria. *Lancet Neurol.* 2009.
8. Shulman JM, De Jager PL, Feany MB. Parkinson's disease: genetics and pathogenesis. *Annu Rev Pathol Mech Dis.* 2011;6:193-222.
9. Nussbaum RL, Polymeropoulos MH. Genetics of Parkinson's disease. *Cold Spring Harb Perspect Med.* 1997;6:1687-1691.
10. Polymeropoulos MH, Lavedan C, Leroy E, et al. Mutation in the α -synuclein gene

- identified in families with Parkinson's disease. *Science*. 1997;276:2045-2047.
11. Fuchs J, Nilsson C, Kachergus J, et al. Phenotypic variation in a large Swedish pedigree due to SNCA duplication and triplication. *Neurology*. 2007;68:916-922.
 12. Klein C, Schlossmacher MG. The genetics of Parkinson disease: implications for neurological care. *Nat Clin Pract Neurol*. 2006;2:136-146.
 13. Maroteaux L, Campanelli J, Scheller R. Synuclein: a neuron-specific protein localized to the nucleus and presynaptic nerve terminal. *J Neurosci*. 2018;8:2804-2815.
 14. Conway KA, Lee SJ, Rochet JC, et al. Acceleration of oligomerization, not fibrillization, is a shared property of both α -synuclein mutations linked to early-onset Parkinson's disease: Implications for pathogenesis and therapy. *Proc Natl Acad Sci U S A*. 2000;18;97(2):571-6.
 15. Fares MB, Ait-Bouziad N, Dikiy I, et al. The novel Parkinson's disease linked mutation G51D attenuates in vitro aggregation and membrane binding of α -synuclein, and enhances its secretion and nuclear localization in cells. *Hum Mol Genet*. 2014;23(17):4491-509.
 16. Hughes AJ, Daniel SE, Kilford L, et al. Accuracy of clinical diagnosis of idiopathic Parkinson's disease: a clinico-pathological study of 100 cases. *J Neurol Neurosurg Psychiatry*. 1992;55:181-184.
 17. Burré J, Sharma M, Tsetsenis T, et al. α -Synuclein promotes SNARE-complex assembly in vivo and in vitro. *Science* 2010;329(5999):1663-7.
 18. Colla E, Jensen PH, Pletnikova O, et al. Accumulation of toxic α -synuclein oligomer within endoplasmic reticulum occurs in α -synucleinopathy in vivo. *J*

- Neurosci.* 2012;32(10):3301-5.
19. Diao J, Burré J, Vivona S, et al. Native α -synuclein induces clustering of synaptic-vesicle mimics via binding to phospholipids and synaptobrevin-2/VAMP2. *Elife.* 2013;2:e00592..
 20. Chen RHC, Wislet-Gendebien S, Samuel F, et al. α -Synuclein membrane association is regulated by the Rab3a recycling machinery and presynaptic activity. *J Biol Chem.* 2013;288:7438-7449.
 21. Kanthasamy A. α -Synuclein negatively regulates PKC δ expression to suppress apoptosis in dopaminergic neurons by reducing p300 HAT activity. *Apoptosis.* 2011;231:2035-2051.
 22. Martinez J, Moeller I, Erdjument-Bromage H, et al. Parkinson's disease-associated α -synuclein is a calmodulin substrate. *J Biol Chem.* 2003;278:17379-17387.
 23. Peng XM. α -Synuclein activation of protein phosphatase 2A reduces tyrosine hydroxylase phosphorylation in dopaminergic cells. *J Cell Sci.* 2005.
 24. Dauer W, Przedborski S. Parkinson's disease: mechanisms and models. *Neuron.* 2003;39:889-909.
 25. Buell AK, Galvagnion C, Gaspar R, et al. Solution conditions determine the relative importance of nucleation and growth processes in α -synuclein aggregation. *Proc Natl Acad Sci U S A.* 2014;111(21):7671-6.
 26. Vilar M, Chou HT, Lühns T, et al. The fold of α -synuclein fibrils. *Proc Natl Acad Sci U S A.* 2008;105(25):8637-42.
 27. Soto C. Unfolding the role of protein misfolding in neurodegenerative diseases. *Nat Rev Neurosci.* 2003;4(1):49-60.

28. Flagmeier P, Meisl G, Vendruscolo M, et al. Mutations associated with familial Parkinson's disease alter the initiation and amplification steps of α -synuclein aggregation. *Proc Natl Acad Sci U S A*. 2016;113(37):10328-10333.
29. Stefani M. Protein misfolding and aggregation: new examples in medicine and biology of the dark side of the protein world. *Biochim Biophys Acta*. 2004;1739:5-25.
30. Hoseki J, Ushioda R, Nagata K. Mechanism and components of endoplasmic reticulum-associated degradation. *J Biochem*. 2010;147(1):19-25.
31. Gauss R, Jarosch E, Sommer T, et al. A complex of Yos9p and the HRD ligase integrates endoplasmic reticulum quality control into the degradation machinery. *Nat Cell Biol*. 2006;8(8):849-54.
32. Anelli T, Sitia R. Protein quality control in the early secretory pathway. *EMBO J*. 2008; 27(2): 315–327.
33. Wolf DH. From lysosome to proteasome: The power of yeast in the dissection of proteinase function in cellular regulation and waste disposal. *Cell Mol Life Sci*. 2004; 61(13):1601-14.
34. Römisch K. Cdc48p is UBX-linked to ER ubiquitin ligases. *Trends Biochem Sci*. 2006; 31(1):24-5.
35. Kim HM, Yu Y, Cheng Y. Structure characterization of the 26S proteasome. *Biochim Biophys Acta - Gene Regul Mech*. 2011;1809(2):67-79.
36. Walter P, Ron D. The unfolded protein response: From stress pathway to homeostatic regulation. *Science* 2011;334(6059):1081-6.
37. Haynes CM, Titus EA, Cooper AA. Degradation of misfolded proteins prevents

- ER-derived oxidative stress and cell death. *Mol Cell*. 2004 ;15(5):767-76.
38. Conn KJ, Gao W, McKee A, et al. Identification of the protein disulfide isomerase family member PDIp in experimental Parkinson's disease and Lewy body pathology. *Brain Res*. 2004 ;1022(1-2):164-72.
 39. Cooper AA, Gitler AD, Cashikar A, et al. α -Synuclein blocks ER-Golgi traffic and Rab1 rescues neuron loss in Parkinson's models. *Science*. 2006;313:324-328.
 40. Colla E, Coune P, Liu Y, et al. Endoplasmic reticulum stress is important for the manifestations of α -synucleinopathy in vivo. *J Neurosci*. 2012;32(10):3306-20.
 41. Song J, Kim BC, Nguyen DTT, et al. Levodopa (L-DOPA) attenuates endoplasmic reticulum stress response and cell death signaling through DRD2 in SH-SY5Y neuronal cells under α -synuclein-induced toxicity. *Neuroscience*. 2017 ;358:336-348.
 42. Gitler AD, Chesi A, Geddie ML, et al. α -Synuclein is part of a diverse and highly conserved interaction network that includes PARK9 and manganese toxicity. *Nat Genet*. 2009;41:308-315.
 43. Herker E, Jungwirth H, Lehmann KA, et al. Chronological aging leads to apoptosis in yeast. *J Cell Biol*. 2004 ;164(4):501-7.
 44. Büttner S, Bitto A, Ring J, et al. Functional mitochondria are required for α -synuclein toxicity in aging yeast. *J Biol Chem*. 2008;283(12):7554-7560.
 45. Bose A, Beal MF. Mitochondrial dysfunction in Parkinson's disease. *J Neurochem*. 2016;139:216-231.
 46. Nakamura K. α -Synuclein and mitochondria: partners in crime? *Neurotherapeutics*. 2013;10:391-399.

47. Haelterman NA, Yoon WH, Sandoval H, et al. A mitocentric view of Parkinson's disease. *Annu Rev Neurosci.* 2014;37:137-159.
48. Nakamura K, Nemani VM, Azarbal F, et al. Direct membrane association drives mitochondrial fission by the Parkinson disease-associated protein α -synuclein. *J Biol Chem.* 2011;286:20710-20726.
49. Siddiqui A, Chinta SJ, Mallajosyula JK, et al. Selective binding of nuclear α -synuclein to the PGC1 α promoter under conditions of oxidative stress may contribute to losses in mitochondrial function: implications for Parkinson's disease. *Free Radic Biol Med.* 2012;53:993-1003.
50. Devi L, Raghavendran V, Prabhu BM, et al. Mitochondrial import and accumulation of α -synuclein impair complex I in human dopaminergic neuronal cultures and Parkinson disease brain. *J Biol Chem.* 2008;283:9089-9100.
51. Loeb V, Yakunin E, Saada A, et al. The transgenic overexpression of α -synuclein and not its related pathology associates with complex I inhibition. *J Biol Chem.* 2010;285:7334-7343.
52. Chinta SJ, Mallajosyula JK, Rane A, et al. Mitochondrial α -synuclein accumulation impairs complex I function in dopaminergic neurons and results in increased mitophagy in vivo. *Neurosci Lett.* 2010;486:235-239.
53. Liu G, Zhang C, Yin J, et al. α -Synuclein is differentially expressed in mitochondria from different rat brain regions and dose-dependently down-regulates complex I activity. *Neurosci Lett.* 2009;454:187-192.
54. Smith WW, Jiang H, Pei Z, et al. Endoplasmic reticulum stress and mitochondrial cell death pathways mediate A53T mutant α -synuclein-induced toxicity. *Hum*

- Mol Genet.* 2005;14:3801-3811.
55. Parihar MS, Parihar A, Fujita M, et al. Alpha-synuclein overexpression and aggregation exacerbates impairment of mitochondrial functions by augmenting oxidative stress in human neuroblastoma cells. *Int J Biochem Cell Biol.* 2009;41:2015-2024.
 56. Junn E, Mouradian MM. Human α -Synuclein over-expression increases intracellular reactive oxygen species levels and susceptibility to dopamine. *Neurosci Lett.* 2002;320:146-150.
 57. Nakamura K, Nemani VM, Wallender EK, et al. Optical Reporters for the Conformation of α -Synuclein Reveal a Specific Interaction with Mitochondria. *J Neurosci.* 2008;28(47):12305-12317.
 58. Nicklas WJ, Vyas I, Heikkila RE. Inhibition of NADH-linked oxidation in brain mitochondria by 1-methyl-4-phenyl-pyridine, a metabolite of the neurotoxin, 1-methyl-4-phenyl-1,2,5,6-tetrahydropyridine. *Life Sci.* 1985;36:2503-2508.
 59. Betarbet R, Sherer TB, MacKenzie G, et al. Chronic systemic pesticide exposure reproduces features of Parkinson's disease. *Nat Neurosci.* 2000;3:1301-1306.
 60. Bonifati V, Rizzu P, Squitieri F, et al. DJ-1 (PARK7), a novel gene for autosomal recessive, early onset parkinsonism. *Neurol Sci.* 2003;24:159-160.
 61. Gautier CA, Kitada T, Shen J. Loss of PINK1 causes mitochondrial functional defects and increased sensitivity to oxidative stress. *Proc Natl Acad Sci U S A.* 2008;105:11364-11369.
 62. Casarejos MJ, Menéndez J, Solano RM, et al. Susceptibility to rotenone is increased in neurons from parkin null mice and is reduced by minocycline. *J*

- Neurochem.* 2006;97:934-946.
63. Ekstrand MI, Terzioglu M, Galter D, et al. Progressive parkinsonism in mice with respiratory-chain-deficient dopamine neurons. *Proc Natl Acad Sci U S A.* 2007;104:1325-1330.
 64. Willingham S, Outeiro TF, DeVit MJ, et al. Yeast genes that enhance the toxicity of a mutant Huntingtin fragment or α -synuclein. *Science.* 2003;302:1769-1772.
 65. Khurana V, Lindquist S. Modelling neurodegeneration in *Saccharomyces cerevisiae*: why cook with baker's yeast? *Nat Rev Neurosci.* 2010;11:436-449.
 66. Valastyan JS, Termine DJ, Lindquist S. Splice isoform and pharmacological studies reveal that sterol depletion relocalizes α -synuclein and enhances its toxicity. *Proc Natl Acad Sci.* 2014;111(8):3014-3019.
 67. Botstein D, Chervitz SA, Cherry JM. Yeast as a model organism. *Science.* 1997;277:1259-1260.
 68. Malhotra V, Emr SD. Rothman and Schekman SNAREd by Lasker for trafficking. *Cell.* 2002;111:1-3.
 69. Tardiff DF, Jui NT, Khurana V, et al. Yeast reveal a "druggable" Rsp5/Nedd4 network that ameliorates α -Synuclein toxicity in neurons. *Science.* 2013;342:979-983.
 70. Rodrigues F, Ludovico P, Leão C. Sugar metabolism in yeasts: an overview of aerobic and anaerobic glucose catabolism. In: *Biodiversity and Ecophysiology of Yeasts. The Yeast Handbook.* Peter G, Rosa C, eds. Springer, Berlin, Heidelberg. 2006:101-121.
 71. Beauvoit B, Rigoulet M, Bunoust O, et al. Interactions between glucose

- metabolism and oxidative phosphorylations on respiratory-competent *Saccharomyces cerevisiae* cells. *Eur J Biochem.* 1993;214:163-172.
72. Malecki M, Bitton DA, Rodríguez-López M, et al. Functional and regulatory profiling of energy metabolism in fission yeast. *Genome Biol.* 2016;17:1-18.
 73. Lavy T, Kumar PR, He H, et al. The Gal3p transducer of the GAL regulon interacts with the Gal80p repressor in its ligand-induced closed conformation. *Genes Dev.* 2012;26:294-303.
 74. Egriboz O, Goswami S, Tao X, et al. Self-association of the Gal4 inhibitor protein Gal80 is impaired by Gal3: evidence for a new mechanism in the GAL gene switch. *Mol Cell Biol.* 2013;33:3667-3674.
 75. Blank TE, Woods MP, Lebo CM, et al. Novel Gal3 proteins showing altered Gal80p binding cause constitutive transcription of Gal4p-activated genes in *Saccharomyces cerevisiae*. *Mol Cell Biol.* 1997;17:2566-2575.
 76. Johnston M, Flick JS, Pexton T. Multiple mechanisms provide rapid and stringent glucose repression of GAL gene expression in *Saccharomyces cerevisiae*. *Mol Cell Biol.* 1994;14(6):3834-3841.
 77. Flick JS, Johnston M. Two Systems of Glucose Repression of the GAL] Promoter in *Saccharomyces cerevisiae*. *Microbiology.* 1990;10(9):4757-4769.
 78. Alberti S, Gitler AD, Lindquist S. A suite of Gateway® cloning vectors for high-throughput genetic analysis in *Saccharomyces cerevisiae*. *Yeast.* 2007;24:913-919.
 79. Chen DC, Yang BC, Kuo TT. One-step transformation of yeast in stationary phase. *Curr Genet.* 1992;21:83-84.
 80. Schirmer EC. Dominant gain-of-function mutations in Hsp104p reveal crucial

- roles for the middle region. *Mol Biol Cell*. 2004;15:2061-2072.
81. Kushnirov V V. Rapid and reliable protein extraction from yeast. *Yeast*. 2000;16(9):857-60.
 82. Vowinckel J, Hartl J, Butler R, et al. MitoLoc: a method for the simultaneous quantification of mitochondrial network morphology and membrane potential in single cells. *Mitochondrion*. 2015;24:77-86.
 83. Neklesa TK, Davis RW. Superoxide anions regulate TORC1 and its ability to bind Fpr1:rapamycin complex. *Proc Natl Acad Sci U S A*. 2008;105:15166-15171.
 84. Tarpey MM, Fridovich I. Methods of detection of vascular reactive species: nitric oxide, superoxide, hydrogen peroxide, and peroxynitrite. *Circ Res*. 2001;89:224-236.
 85. Weir M, Keeney JB. PCR mutagenesis and gap repair in yeast. *Methods Mol Biol*. 2014;1205:29-35.
 86. Fleming MS, Gitler AD. High-throughput yeast plasmid overexpression screen. *J Vis Exp*. 2011. Jul 27;(53). pii: 2836.
 87. Mi H, Muruganujan A, Casagrande JT, Thomas PD. Large-scale gene function analysis with the panther classification system. *Nat Protoc*. 2013 ;8(8):1551-66.
 88. Tardiff DF, Tucci ML, Caldwell KA, et al. Different 8-hydroxyquinolines protect models of TDP-43 protein, α -synuclein, and polyglutamine proteotoxicity through distinct mechanisms. *J Biol Chem*. 2012;287:4107-4120.
 89. Ju S, Tardiff DF, Han H, et al. A yeast model of FUS/TLS-dependent cytotoxicity. *PLoS Biol*. 2011; ;9(4):e1001052.
 90. Kayatekin C, Matlack KES, Hesse WR, et al. Prion-like proteins sequester and

- suppress the toxicity of huntingtin exon 1. *Proc Natl Acad Sci.* 2014;111(33):12085-12090.
91. Graff J, Kahn M, Samiei A, et al. A dietary regimen of caloric restriction or pharmacological activation of SIRT1 to delay the onset of neurodegeneration. *J Neurosci.* 2013;33:8951-8960.
 92. Ntsapi C, Loos B. Caloric restriction and the precision-control of autophagy: a strategy for delaying neurodegenerative disease progression. *Exp Gerontol.* 2016;83:97-111.
 93. Dehay B, Bove J, Rodriguez-Muela N, et al. Pathogenic lysosomal depletion in Parkinson's disease. *J Neurosci.* 2010;30:12535-12544.
 94. Guedes A, Ludovico P, Sampaio-Marques B. Caloric restriction alleviates alpha-synuclein toxicity in aged yeast cells by controlling the opposite roles of Tor1 and Sir2 on autophagy. *Mech Ageing Dev.* 2017;161:270-276.
 95. Hetz C, Thielen P, Matus S, et al. XBP-1 deficiency in the nervous system protects against amyotrophic lateral sclerosis by increasing autophagy. *Genes Dev.* 2009;23:2294-2306.
 96. Petroi D, Popova B, Taheri-Talesh N, et al. Aggregate clearance of α -synuclein in *Saccharomyces cerevisiae* depends more on autophagosome and vacuole function than on the proteasome. *J Biol Chem.* 2012;287:27567-27579.
 97. Marshall RS, McLoughlin F, Vierstra RD. Autophagic turnover of inactive 26S proteasomes in yeast is directed by the ubiquitin receptor Cue5 and the Hsp42 chaperone. *Cell Rep.* 2016;16:1717-1732.
 98. Hayden E, Chen S, Chumley A, et al. Mating-based overexpression library

- screening in yeast. *J Vis Exp*. 2018;(137).
99. Ruan L, Zhou C, Jin E, et al. Cytosolic proteostasis through importing of misfolded proteins into mitochondria. *Nature*. 2017;543(7645):443-446.
 100. Tardiff DF, Khurana V, Chung CY, et al. From yeast to patient neurons and back again: A powerful new discovery platform. *Mov Disord*. 2014;29(10):1231-1240.
 101. Su LJ, Auluck PK, Outeiro TF, et al. Compounds from an unbiased chemical screen reverse both ER-to-Golgi trafficking defects and mitochondrial dysfunction in Parkinson's disease models. *Dis Model Mech*. 2010;3(3-4):194-208.
 102. Berg D, Holzman C, Riess O. 14-3-3 Proteins in the Nervous System. *Nat Rev Neurosci*. 2003;4(9):752-762.
 103. Outeiro TF, Putcha P, Tetzlaff JE, et al. Formation of toxic oligomeric α -synuclein species in living cells. *PLoS One*. 2008; 3(4):e1867.
 104. Sampaio-Marques B, Pereira H, Santos AR, et al. Caloric restriction rescues yeast cells from alpha-synuclein toxicity through autophagic control of proteostasis. *Aging (Albany NY)*. 2018;10(12):3821-3833.
 105. Guaragnella N, Ždravlević M, Lattanzio P, et al. Yeast growth in raffinose results in resistance to acetic-acid induced programmed cell death mostly due to the activation of the mitochondrial retrograde pathway. *Biochim Biophys Acta - Mol Cell Res*. 2013 ;1833(12):2765-2774.
 106. Deng J, Yang M, Chen Y, et al. FUS interacts with HSP60 to promote mitochondrial damage. *PLoS Genet*. 2015 ;11(9):e10053571.
 107. Wang W, Wang L, Lu J, et al. The inhibition of TDP-43 mitochondrial localization blocks its neuronal toxicity. *Nat Med*. 2016;22:869-878.

108. de Godoy LMF, Olsen J V, Cox J, et al. Comprehensive mass-spectrometry-based proteome quantification of haploid versus diploid yeast. *Nature*. 2008;30;455(7217):1251-4.
109. Shen J, Du T, Wang X, et al. α -synuclein amino terminus regulates mitochondrial membrane permeability. *Brain Res*. 2014 ;1591:14-26.
110. Flower TR, Chesnokova LS, Froelich CA, et al. Heat shock prevents alpha-synuclein-induced apoptosis in a yeast model of Parkinson's disease. *J Mol Biol*. 2005;351:1081-1100.
111. Benov L, Szejnberg L, Fridovich I. Critical evaluation of the use of hydroethidine as a measure of superoxide anion radical. *Free Radic Biol Med*. 1998 ;25(7):826-31.
112. Zielonka J, Kalyanaraman B. Hydroethidine- and MitoSOX-derived red fluorescence is not a reliable indicator of intracellular superoxide formation: Another inconvenient truth. *Free Radic Biol Med*. 2010 ;48(8):983-1001.
113. Thomas MP, Chartrand K, Reynolds A, et al. Ion channel blockade attenuates aggregated alpha synuclein induction of microglial reactive oxygen species: Relevance for the pathogenesis of Parkinson's disease. *J Neurochem*. 2007;100(2):503-19.
114. Keoni CLI, Brown TL. Inhibition of apoptosis and efficacy of pan caspase inhibitor, Q-VD-Oph, in models of human disease. *J Cell Death*. 2015 ;8:1-7..
115. Mark M, Rijli FM, Chambon P. Homeobox genes in embryogenesis and pathogenesis. *Pediatr Res*. 1997 ;42(4):421-9.
116. Andersson E, Tryggvason U, Deng Q, et al. Identification of intrinsic determinants

- of midbrain dopamine neurons. *Cell*. 2006 ;124(2):393-405.
117. Puelles E, Annino A, Tuorto F, et al. Otx2 regulates the extent, identity and fate of neuronal progenitor domains in the ventral midbrain. *Development*. 2004;131(9):2037-48.
 118. Alvarez-Fischer D, Fuchs J, Castagner F, et al. Engrailed protects mouse midbrain dopaminergic neurons against mitochondrial complex I insults. *Nat Neurosci*. 2011;14(10):1260-6.
 119. Kawamoto Y, Akiguchi I, Nakamura S, et al. 14-3-3 Proteins in Lewy bodies in Parkinson disease and diffuse Lewy body disease brains. *J Neuropathol Exp Neurol*. 2002;61:245-253.
 120. Kiryu S, Morita N, Ohno K, et al. Regulation of mRNA expression involved in Ras and PKA signal pathways during rat hypoglossal nerve regeneration. *Mol Brain Res*. 1995;29:147-156.
 121. Plotegher N, Kumar D, Tessari I, et al. The chaperone-like protein 14-3-3 η interacts with human α -synuclein aggregation intermediates rerouting the amyloidogenic pathway and reducing α -synuclein cellular toxicity. *Hum Mol Genet*. 2014;23:5615-5629.
 122. Yacoubian TA, Slone SR, Harrington AJ, et al. Differential neuroprotective effects of 14-3-3 proteins in models of Parkinson's disease. *Cell Death Dis*. 2010;1:e2.
 123. Zha J, Harada H, Yang E, et al. Serine phosphorylation of death agonist BAD in response to survival factor results in binding to 14-3-3 not BCL-X(L). *Cell*. 1996;87:619-628.
 124. Muslin AJ, Xing H. 14-3-3 proteins: regulation of subcellular localization by

molecular interference. *Cell Signal.* 2000;12:703-709.